

APPENDIX 2

Three reports on the performance of the JEFF-3.1 neutron general purpose library are included below. They were all prepared by S. Van der Marck, NRG Petten in October 2005, see JEF/DOC-1105-1107 in the JEFF working paper list above. The three reports are entitled:

- *β_{eff} calculations using JEFF-3.1 nuclear data,*
- *Shielding benchmark calculations with MCNP-4c3 using JEFF-3.1 nuclear data,*
- *Criticality Safety benchmark calculations with MCNP-4c3 using JEFF-3.1 nuclear data.*

**β_{eff} calculations using JEFF-3.1
nuclear data**

S.C. van der Marck

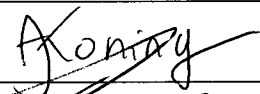
Petten, October 7, 2005

21616/05.69454/P FAI/SVDM/MB

author : S.C. van der Marck



reviewed : A.J. Koning



16 page(s)

approved : R.P.C. Schram

beta.tex



© NRG 2005

Subject to agreement with the client, the information contained in this report may not be disclosed to any third party and NRG is not liable for any damage arising out of the use of such information.

Abstract

Calculations were performed with MCNP-4C3 to validate the delayed neutron data of the new JEFF-3.1 nuclear data library.

Keywords

MCNP-4C3

JEFF-3.1

nuclear data

effective delayed neutron fraction

Contents

1	Introduction	5
2	Benchmark systems	6
3	Results	9
	References	11
Appendix A	JEFF-3.1 results for β_{eff} and β_0 in 8 groups	13

1. Introduction

Recently the new nuclear data library JEFF-3.1 has been made available by the NEA. The delayed neutron data in this library is new. For the first time, 8 time groups have been used to represent these data, instead of the customary 6 time groups [1].

To validate the results that can be obtained with the new delayed neutron data, we have calculated β_{eff} for many systems for which measurements have been reported in the open literature. The results of these calculations are reported here.

The results in this report have been obtained using MCNP-4C3 [2], extended with a method to calculate β_{eff} [3]. The standard versions of MCNP-4C3, MCNP-5, and MCNPX can all work with delayed neutron data in 8 time groups. However, because these codes do not calculate a value for β_{eff} , we included our own β_{eff} method into MCNP-4C3. This method has been used earlier to calculate β_{eff} for other nuclear data libraries, viz. JEFF-3.0, ENDF/B-VI.8, and JENDL-3.3 [4].

2. Benchmark systems

We have searched in the literature for measurements of the effective delayed neutron fraction, the result of which is listed below. We will use these experiments as benchmarks for the calculation of β_{eff} on the basis of JEFF-3.1 nuclear data. For some systems we have found experimental values for the parameter α , which is linked to β_{eff} through $\alpha = [k(1 - \beta_{\text{eff}}) - 1]/l$, where l is the prompt neutron life time. All systems described below are at delayed criticality, so that the parameter we can compare with is the value $\alpha_{\text{dc}} = \alpha(k = 1) = -\beta_{\text{eff}}/l$.

When not stated explicitly, the MCNP [2] model for the experiment was taken, without modifications, from the ICSBEP data [5]. Where possible, the ICSBEP identification is given in brackets after the benchmark name.

- **Godiva** (heu-met-fast-001)
A bare sphere of highly enriched (94 wt%) uranium.
- **Jezebel** (pu-met-fast-001)
A bare sphere of plutonium (95 at% Pu-239).
- **Skidoo** (u233-met-fast-001)
A bare sphere of uranium, of which 98 at% U-233.
- **Topsy** (Flattop 25, heu-met-fast-028)
A highly enriched (93 wt%) uranium sphere surrounded by a thick reflector of normal uranium. Experimental results are given in Ref. [6].
- **Popsy** (Flattop-Pu, pu-met-fast-006)
A plutonium (94 wt% Pu-239) sphere surrounded by a thick reflector of normal uranium. Experimental results are given in Ref. [6].
- **Flattop 23** (u233-met-fast-006)
A uranium (98 at% U-233) sphere surrounded by a thick reflector of normal uranium. Experimental results are given in Ref. [6].
- **Big Ten** (ieu-met-fast-007)
A large, mixed-uranium-metal cylindrical core with 10% average U-235 enrichment, surrounded by a thick reflector of depleted uranium [7].
- **ZPR** (heu-met-inter-001, ieu-met-fast-010, mix-met-fast-011 case 1, pu-met-inter-002)
Four cores in the Zero Power Reactor at ANL. The first one is a highly enriched uranium/iron benchmark, reflected by steel. The second is a heterogeneous cylindrical core of uranium (average enrichment 9%). The third has plutonium/uranium/zirconium fuel, reflected by graphite. The last core had heterogeneous plutonium metal fuel with carbon/stainless steel dilutions, and a steel reflector. Measured values for β_{eff} are given in e.g. Ref. [8].
- **SNEAK** (cores 7A, 7B, 9C1, and 9C2)
Measurements of β_{eff} in four unmoderated PuO₂-UO₂ cores, surrounded by a depleted uranium reflector [9]. One core, 9C1, had only uranium as fuel. The 9C2 core was diluted with sodium. MCNP models were built based on the R-Z model descriptions in Ref. [9].
- **Masurca** (cores R2 and ZONA2)
Measurements of β_{eff} by several international groups in two unmoderated cores, viz. R2 and ZONA2 [10]. Core R2 had of $\sim 30\%$ enriched uranium as fuel, whereas ZONA2 had both plutonium and depleted uranium. Both cores were surrounded by a 50-50 UO₂-Na mixture blanket, and by steel shielding. MCNP models were built based on the R-Z model descriptions

in Ref. [10].

- **FCA** (cores XIX-1, XIX-2, and XIX-3)
Measurements of β_{eff} by several international groups in three unmoderated cores in the Fast Critical Assembly [10]. One core had highly enriched uranium, one had plutonium and natural uranium, and the third one had plutonium as fuel. The cores were surrounded by two blanket regions, one with depleted uranium oxide and sodium, and another one with only depleted uranium metal. MCNP models were built based on the R-Z model descriptions in Ref. [10].
- **TCA** (related to leu-comp-therm-006)
A light water moderated low-enriched UO_2 core in the Tank-type Critical Assembly. From the description of this experiment in Ref. [11] it is clear that this experiment is closely related to benchmark leu-comp-therm-006 [5]. We have taken the MCNP input decks given in Ref. [5], and changed the loading pattern, the water height and lattice pitch.
- **IPEN/MB-01** (related to leu-comp-therm-077)
Measurement of β_{eff} in the research reactor IPEN/MB-01, with a core consisting of 28×26 UO_2 (4.3% enriched) fuel rods inside a light water filled tank [12]. An MCNP input deck was made available by the authors of Ref. [12].
- **Winco slab tanks** (related to heu-sol-therm-038 case 5)
Measurement of α in the Westinghouse Idaho Nuclear Company Slab Tank Assembly. The experiment consisted of two thin coaxial slab tanks with 93% enriched uranyl nitrate solution. From the description of this experiment in Ref.[13] it is clear that this experiment is closely related to heu-sol-therm-038, case 5 [5]. We have taken the MCNP input deck given in Ref. [5], and removed the stainless steel absorber between the two slab tanks.
- **Stacy** (leu-sol-therm-004, -007, -016, -021)
Measurements of β_{eff}/l in uranyl nitrate solution (10 % enrichment) in several cores in the STACY facility. From the description of these experiments in Ref. [14], one can identify several experiments that have been included in the criticality benchmark collection [5].
- **Sheba** (core II)
Measurement of β_{eff}/l in a critical assembly vessel, filled with 5% enriched uranyl fluoride, UO_2F_2 , the Solution High-Energy Burst Assembly [15]. The vessel had a cylindrical shape, and there was no reflector. An MCNP model was built from scratch.
- **SHE-8**
Measurement of β_{eff}/l in a split table type critical assembly called Semi-Homogeneous Assembly [16]. The core was shaped in a hexagonal prism, with graphite matrix tubes and graphite rods. There was no axial reflector. The central region in core 8 consisted of 73 fuel rods with 2.9% enriched UO_2 dispersed in graphite. An MCNP model was built from scratch.
- **Proteus** (core 5)
Measurement of β_{eff}/l in a graphite reflected pebble bed reactor, containing uranium-carbon fuel pebbles (16.7% enrichment) and graphite moderator pebbles. As the reactor was operated below 1 kW, no coolant was needed. An MCNP model was made available by the authors of Ref. [17].

For Godiva, Jezebel, and Skidoo, both Keepin [18] and Paxton [6] give experimental values for β_{eff} . Although these values are not identical, the differences are small and have no significant impact on the conclusions drawn in this paper. Therefore we will use the numbers given by Keepin, because this is the commonly used reference.

For Big Ten, an experimental value $\alpha = -(1.17 \pm 0.01) \times 10^5 \text{ s}^{-1}$ is given by Paxton [6]. Based on a

calculation of $\beta_{\text{eff}} = 720$ pcm, he estimates the prompt neutron life time to be 6.15×10^{-8} s, which is consistent with our calculation of 6.15×10^{-8} s within a fraction of a percent. Therefore we feel it is justified in this case to compare with the value of $\beta_{\text{eff}} = 720$ pcm as if it were determined by experiment.

For the Stacy, Winco, SHE-8, Sheba-II, and Proteus experiments, we will compare with the α values given in the respective references, because that is the measured quantity. Also, for the Winco experiment, there is some uncertainty in deriving a value for β_{eff} from the measured α . The comparison in the next section is done by dividing the calculated β_{eff} by the prompt neutron fission life time. This life time is calculated by MCNP by default, and is given in the output as the 'fission lifespan' (see the discussion of life time estimation in section 2.VIII.B of the manual [2]).

3. Results

The results for the Sheba-II, SHE-8, TCA and Winco experiments should be viewed with some caution, since the preparation of the MCNP models for these experiments involved interpretation on our part, based on the references given earlier. However, since the computational results for these cases are close to the experimental values, we judge the models to be appropriate for calculating β_{eff} and α .

	Experiment	Calculation		C/E (JEFF-3.1)
		JEFF-3.0	JEFF-3.1	
TCA	771±17	817±9	793.4±1.4	1.029±0.002
IPEN	742±7	788±4	771.7±4.1	1.040±0.005
Masurca_R2	721±11	735±7	728.9±6.9	1.011±0.009
Masurca_Z2	349±6	358±5	356.2±4.6	1.021±0.013
FCA-XIX-1	742±24	767±8	749.7±7.5	1.010±0.010
FCA-XIX-2	364±9	387±5	383.7±4.9	1.054±0.013
FCA-XIX-3	251±4	255±4	250.3±4.1	0.997±0.016
Sneak-9C1	758±24	757±7	743.8±7.0	0.981±0.009
Sneak-7A	395±12	381±5	377.3±4.8	0.955±0.013
Sneak-7B	429±13	447±5	434.2±5.0	1.012±0.012
Sneak-9C2	426±19	395±5	388.0±4.9	0.911±0.013
Zpr-Heu	667±15	696±9	685.8±8.8	1.028±0.013
Zpr-U9	725±17	769±9	747.7±8.3	1.031±0.011
Zpr-Mox	381±9	373±6	369.8±5.1	0.971±0.014
Zpr-Pu	222±5	243±5	241.3±5.2	1.087±0.022
BigTen	720±7	765±7	735.3±6.4	1.021±0.009
Godiva	659±10	677±8	669.4±4.0	1.016±0.006
Topsy	665±13	666±8	659.5±3.9	0.992±0.006
Jezebel	194±10	200±5	201.8±2.2	1.040±0.011
Popsy	276±7	283±5	282.5±2.5	1.024±0.009
Skidoo	290±10	284±5	309.1±2.7	1.066±0.009
Flattop	360±9	343±6	361.9±2.8	1.005±0.008

Table 3.1 The experimental and calculated β_{eff} (in pcm). The uncertainty for C/E includes only the statistical uncertainty of the calculation. This corresponds to the error bar in Fig. 3.1. The experimental uncertainty range is shown with dashed lines in Fig. 3.1.

Concerning the Winco slab tank experiment, another remark is in order. Our calculation of β_{eff} yields a value of 845 ± 4 pcm, contradicting the value 1500 ± 120 calculated in Ref. [13], based on the experimental α -value and other experimental information, not involving the prompt neutron fission life time. However, in Ref. [13] it is noted that its calculated value is higher than the expected value of roughly 900 pcm, the reason for which was not well understood. Our value for α is close to the experimental value.

	Experiment	Calculation		C/E
		JEFF-3.0	JEFF-3.1	
Proteus	3.60±0.02	3.82±0.05	3.70±0.02	1.028±0.005
SHE-8	6.53±0.34	6.36±0.08	6.21±0.15	0.951±0.024
Sheba-II	200.3±3.6		203.79±1.38	1.017±0.007
Stacy-029	122.7±4.1	122.2±2.6	120.76±0.75	0.984±0.006
Stacy-033	116.7±3.9	129.5±2.4	114.11±0.72	0.978±0.006
Stacy-046	106.2±3.7	109.3±2.2	104.77±0.66	0.987±0.006
Stacy-030	126.8±2.9	129.8±2.7	129.17±0.81	1.019±0.006
Stacy-125	152.8±2.6	162.3±2.4	156.38±1.00	1.023±0.006
Stacy-215	109.2±1.8	114.6±2.3	109.28±0.68	1.001±0.006
Winco	1109.3±0.3	1169.±13.	1134.98±5.54	1.023±0.005

Table 3.2 The experimental and calculated α (in s^{-1}). The uncertainty for C/E includes only the statistical uncertainty of the calculation. This corresponds to the error bar in Fig. 3.1. The experimental uncertainty range is shown with dashed lines in Fig. 3.1.

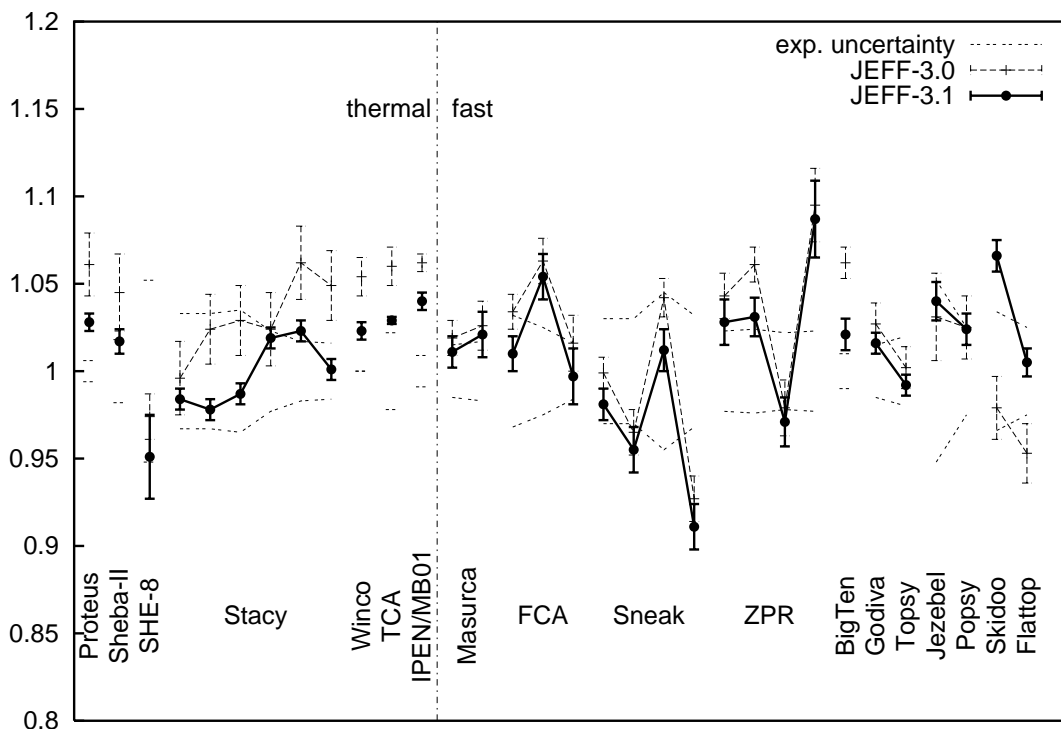


Figure 3.1 C/E for β_{eff} (or β_{eff}/l , see text) for many benchmark systems. The systems are roughly ordered with respect to the average energy at which fission takes place, from low energy (left) to high (right).

References

- [1] J.L. Rowlands, *Delayed neutron data in 8 time groups*, JEFDOC-976 (2003) J.L. Rowlands, *Delayed neutron yield and relative abundance data for some minor isotopes, missing from current compilations*, JEFDOC-1073 (2005)
- [2] J.F. Briesmeister (Ed.), *MCNP - A General Monte Carlo N-Particle Transport Code, Version 4C*, Technical Report LA-13709-M, Los Alamos National Laboratory, USA (2000); J.S. Hendricks, *MCNP4C3*, Report X-5:RN(U)-JSH-01-17, Los Alamos National Laboratory, USA (2001)
- [3] S.C. van der Marck and R. Klein Meulekamp, *Calculation of the effective delayed neutron fraction by Monte Carlo*, Proc. Physor-2004, Chicago, USA (2004);
R. Klein Meulekamp and S.C. van der Marck, *Calculation of the effective delayed neutron fraction by Monte Carlo*, to be published in Nucl. Sci. Eng. (2006)
- [4] S.C. van der Marck, R. Klein Meulekamp, A. Hogenbirk, and A.J. Koning, *Benchmark results for delayed neutron data*, Proc. ND-2004, Santa Fe, USA (2004) pp. 531–534
- [5] J. Blair Briggs (Ed.), *International Handbook of Evaluated Criticality Safety Benchmark Experiments*, NEA/NSC/DOC(95)03/I, Nuclear Energy Agency, Paris (September 2003 Edition)
- [6] H.C. Paxton, *Fast Critical Experiments*, Progress in Nuclear Energy **7** (1981) 151–174
- [7] L.J. Sapir, H.H. Helmick, and J.D. Orndoff, *Big Ten, a 10% Enriched Uranium Critical Assembly: Kinetic Studies*, Trans. Am. Nucl. Soc. **15**, 1 (1972) 312
- [8] E. Fort, V. Zammit-Averlant, M. Salvatores, and A. Filip, *Recommended values of the delayed neutron yield for U-235, U-238, and Pu-239*, JEFDOC-820
- [9] E.A. Fischer, *Integral measurements of the effective delayed neutron fractions in the fast critical assembly SNEAK*, Nucl. Sci. Eng. **62** (1977) 105–116
- [10] S. Okajima, T. Sakurai, J.F. Lebrat, V.Z. Averlant, and M. Martini, *Summary on International Benchmark Experiments for Effective Delayed Neutron Fraction*, Progress in Nuclear Energy, **41** (2002) 285–301
- [11] K. Nakajima, *Re-evaluation of the Effective Delayed Neutron Fraction Measured by the Substitution Technique for a Light Water Moderated Low-Enriched Uranium Core*, J. Nucl. Sci. Technol. **38** (2001) 1120–1125
- [12] A. dos Santos, R. Diniz, L.C.C.B. Fanaro, R. Jerez, G.S. de Andrade e Silva, and M. Yamaguchi, *The experimental determination of the effective delayed neutron parameters of the IPEN/MB-01 reactor*, Proc. Physor-2004, Chicago
- [13] G.D. Spriggs, *A Measurement of the Effective Delayed Neutron Fraction of the Westinghouse Idaho Nuclear Company Slab Tank Assembly using Rossi- α Techniques*, Nucl. Sci. Eng. **115** (1993) 76–80
- [14] K. Tonoike, Y. Miyoshi, T. Kikuchi, and T. Yamamoto, *Kinetic Parameter β_{eff}/l Measurement on Low Enriched Uranyl Nitrate Solution with Single Unit Cores (600 ϕ , 280T, 800 ϕ) of STACY*, J. Nucl. Sci. Technol. **39** (2002) 1227–1236
- [15] K.B. Butterfield, *The SHEBA experiment*, Trans. Am. Nucl. Soc. **74** (1994) 199–200;
R. Sanchez and P. Jaegers, *Prompt neutron decay constants in SHEBA*, Trans. Am. Nucl. Soc. **76** (1997) 363–364
- [16] M. Takano, M. Hirano, R. Shindo, and T. Doi, *Analysis of SHE critical experiments by neutronic design codes for experimental Very High Temperature Reactor*, J. Nucl. Sci. Technol. **22** (1985) 358–370;

- Y. Kaneko, F. Akino, and T. Yamane, *Evaluation of delayed neutron data for thermal fission of U-235 based on integral experiments at Semi-Homogeneous Experiment*, J. Nucl. Sci. Techn. **25** (1988) 673–681
- [17] T. Williams, M. Rosselet, and W. Scherer (Eds.), *Critical Experiments and Reactor Physics Calculations for Low-Enriched High Temperature Gas Cooled Reactors*, IAEA Tecdoc 1249 (advance electronic version, 2001)
- [18] G.R. Keepin, *Physics of Nuclear Kinetics*, Addison-Wesley, Reading, USA, 1965

APPENDIX A. JEFF-3.1 results for β_{eff} and β_0 in 8 groups

In the JEFF-3.1 nuclear data library the delayed neutron data have been represented using 8 time groups. Since this is the first time this representation has been used, it is deemed useful to list the results of our calculations per time group, for reference.

group g	Godiva		Jezebel		Skidoo	
	$\beta_{\text{eff},g}$	$\beta_{0,g}$	$\beta_{\text{eff},g}$	$\beta_{0,g}$	$\beta_{\text{eff},g}$	$\beta_{0,g}$
1	24.2±0.8	20.9±0.5	6.5±0.4	6.4±0.3	26.6±0.8	22.4±0.5
2	95.4±1.5	93.0±1.0	45.4±1.0	47.2±0.7	46.1±1.0	44.1±0.7
3	69.4±1.3	61.5±0.8	18.6±0.7	19.2±0.4	44.4±1.0	38.0±0.6
4	132.6±1.8	124.6±1.1	30.9±0.8	31.3±0.6	62.3±1.2	56.4±0.8
5	208.9±2.2	198.5±1.4	68.9±1.3	71.0±0.8	93.6±1.5	86.1±0.9
6	62.7±1.2	59.5±0.8	8.4±0.4	8.5±0.3	12.0±0.5	10.9±0.3
7	59.3±1.2	55.5±0.7	19.2±0.7	20.1±0.5	19.4±0.7	17.0±0.4
8	17.0±0.7	16.0±0.4	3.8±0.3	3.7±0.2	4.8±0.4	3.9±0.2

Table A.1 The partial β_{eff} and β_0 for Godiva, Jezebel and Skidoo (in pcm).

group g	Topsy		Popsy		Flatop-23	
	$\beta_{\text{eff},g}$	$\beta_{0,g}$	$\beta_{\text{eff},g}$	$\beta_{0,g}$	$\beta_{\text{eff},g}$	$\beta_{0,g}$
1	21.1±0.7	20.8±0.5	6.1±0.4	9.0±0.3	21.3±0.7	20.6±0.5
2	85.5±1.4	107.6±1.0	47.3±1.0	76.9±0.9	47.5±1.0	73.2±0.9
3	60.1±1.2	61.2±0.8	19.9±0.7	31.0±0.6	39.4±1.0	44.4±0.7
4	125.8±1.7	147.7±1.2	40.6±0.9	79.9±0.9	66.4±1.2	99.3±1.0
5	202.7±2.2	249.9±1.6	90.6±1.4	170.7±1.3	107.8±1.5	175.1±1.3
6	75.3±1.3	107.9±1.0	30.5±0.8	81.5±0.9	33.9±0.8	79.7±0.9
7	64.2±1.2	84.3±0.9	33.1±0.8	65.8±0.8	31.0±0.8	60.5±0.8
8	24.8±0.7	40.4±0.6	14.3±0.5	37.7±0.6	14.7±0.6	36.9±0.6

Table A.2 The partial β_{eff} and β_0 for Topsy, Popsy, and Flatop-23 (in pcm).

group g	$\beta_{\text{eff},g}$	$\beta_{0,g}$
1	15.4±0.9	20.1±0.7
2	97.8±2.3	120.5±1.8
3	52.0±1.7	63.2±1.3
4	125.7±2.6	155.7±2.1
5	221.7±3.5	279.1±2.8
6	101.4±2.3	130.7±1.9
7	77.8±2.1	98.6±1.7
8	43.3±1.6	54.6±1.2

Table A.3 The partial β_{eff} and β_0 for Big Ten (in pcm).

<i>g</i>	Pu		Mox		HEU		U9	
	$\beta_{\text{eff},g}$	$\beta_{0,g}$	$\beta_{\text{eff},g}$	$\beta_{0,g}$	$\beta_{\text{eff},g}$	$\beta_{0,g}$	$\beta_{\text{eff},g}$	$\beta_{0,g}$
1	8.2±1.0	7.7±0.6	7.9±0.7	9.0±0.5	25.9±1.7	21.7±1.0	15.7±1.2	19.5±0.9
2	52.5±2.4	50.2±1.5	63.2±2.1	62.4±1.3	98.2±3.4	98.7±2.1	98.1±3.0	118.0±2.3
3	22.3±1.6	21.8±1.0	30.6±1.4	29.6±0.9	69.9±2.8	65.0±1.7	53.6±2.3	65.8±1.7
4	34.9±2.0	33.4±1.2	59.3±2.0	58.5±1.3	136.6±3.9	133.3±2.4	124.7±3.3	158.7±2.7
5	86.3±3.1	83.1±1.9	118.3±2.8	119.2±1.8	213.9±4.9	207.2±3.0	226.4±4.5	277.7±3.5
6	7.9±0.9	8.9±0.6	37.9±1.7	35.3±1.0	65.6±2.8	62.0±1.7	105.3±3.1	128.8±2.4
7	25.2±1.7	21.4±1.0	39.4±1.7	36.7±1.0	57.5±2.6	56.6±1.6	80.5±2.7	96.8±2.1
8	3.9±0.7	3.9±0.4	13.3±1.0	13.9±0.6	18.4±1.5	16.1±0.8	43.5±2.0	52.3±1.5

Table A.4 The partial β_{eff} and β_0 for ZPR-Pu, ZPR-Mox, ZPR-HEU, and ZPR-U9 (in pcm).

group <i>g</i>	TCA		IPEN/MB-01	
	$\beta_{\text{eff},g}$	$\beta_{0,g}$	$\beta_{\text{eff},g}$	$\beta_{0,g}$
1	24.3±0.2	21.4±0.1	26.3±0.8	22.9±0.5
2	115.1±0.5	106.0±0.3	111.3±1.6	103.7±1.0
3	68.7±0.4	61.0±0.2	70.1±1.2	61.5±0.8
4	150.5±0.6	136.9±0.4	148.4±1.8	136.2±1.2
5	256.0±0.8	234.3±0.5	250.0±2.3	229.0±1.5
6	83.6±0.4	75.6±0.3	76.5±1.3	69.7±0.9
7	69.7±0.4	63.3±0.3	66.5±1.2	60.8±0.8
8	25.6±0.2	23.5±0.2	22.5±0.7	21.1±0.5

Table A.5 The partial β_{eff} and β_0 for TCA and IPEN/MB-01 (in pcm).

group <i>g</i>	R2		ZONA2	
	$\beta_{\text{eff},g}$	$\beta_{0,g}$	$\beta_{\text{eff},g}$	$\beta_{0,g}$
1	21.9±1.2	21.3±0.8	6.5±0.6	8.3±0.5
2	102.1±2.6	110.1±1.8	57.9±1.8	71.6±1.4
3	63.5±2.1	64.8±1.3	21.8±1.1	27.9±0.9
4	132.6±2.9	142.2±2.0	50.1±1.7	62.9±1.3
5	222.7±3.8	241.6±2.6	114.9±2.6	146.6±2.0
6	87.8±2.4	96.8±1.6	44.0±1.6	60.7±1.3
7	69.8±2.1	75.7±1.5	40.3±1.5	55.8±1.2
8	28.4±1.4	33.5±1.0	20.8±1.2	25.9±0.8

Table A.6 The partial β_{eff} and β_0 for Masurca-R2 and Masurca-ZONA2 (in pcm).

group g	FCA-XIX-1		FCA-XIX-2		FCA-XIX-3	
	$\beta_{\text{eff},g}$	$\beta_{0,g}$	$\beta_{\text{eff},g}$	$\beta_{0,g}$	$\beta_{\text{eff},g}$	$\beta_{0,g}$
1	24.4±1.4	20.9±0.8	7.2±0.7	8.2±0.5	6.0±0.6	8.1±0.5
2	106.4±2.9	101.9±1.7	60.2±1.9	69.8±1.4	50.0±1.8	56.7±1.3
3	75.0±2.3	68.2±1.4	26.5±1.3	30.9±0.9	22.3±1.3	24.4±0.8
4	147.5±3.3	136.7±2.0	59.5±2.0	68.9±1.4	39.9±1.6	47.3±1.1
5	234.2±4.2	227.4±2.5	122.5±2.8	146.8±2.0	82.8±2.4	99.4±1.7
6	73.5±2.4	77.5±1.5	45.7±1.7	56.6±1.3	16.7±1.0	26.3±0.9
7	68.1±2.3	67.5±1.4	42.1±1.6	52.6±1.2	26.4±1.3	31.9±0.9
8	20.6±1.2	23.4±0.8	19.9±1.1	26.5±0.9	6.3±0.6	10.4±0.5

Table A.7 The partial β_{eff} and β_0 for FCA-XIX-1, FCA-XIX-2, and FCA-XIX-3 (in pcm).

g	7A		7B		9C2		9C1	
	$\beta_{\text{eff},g}$	$\beta_{0,g}$	$\beta_{\text{eff},g}$	$\beta_{0,g}$	$\beta_{\text{eff},g}$	$\beta_{0,g}$	$\beta_{\text{eff},g}$	$\beta_{0,g}$
1	6.5±0.6	8.8±0.5	7.6±0.6	10.9±0.5	6.9±0.7	9.4±0.5	20.8±1.2	22.3±0.8
2	59.6±1.9	75.4±1.4	64.6±1.9	80.8±1.5	60.7±1.9	77.7±1.5	101.7±2.6	110.5±1.8
3	23.7±1.2	31.9±0.9	25.8±1.2	33.1±1.0	26.3±1.3	32.3±0.9	62.8±2.1	62.3±1.3
4	56.7±1.9	76.9±1.5	63.6±2.0	82.7±1.5	56.4±1.9	77.1±1.5	133.7±2.9	147.6±2.0
5	120.4±2.7	166.1±2.2	136.4±2.8	178.0±2.2	123.9±2.8	165.7±2.1	225.6±3.8	251.6±2.6
6	47.0±1.7	71.8±1.4	60.5±1.9	81.3±1.5	49.3±1.8	71.0±1.4	93.8±2.5	105.9±1.7
7	41.8±1.6	57.6±1.3	49.4±1.7	65.2±1.3	42.8±1.6	60.3±1.3	73.4±2.2	82.3±1.5
8	21.6±1.1	33.2±1.0	26.4±1.2	36.1±1.0	21.6±1.2	32.2±0.9	31.9±1.4	39.3±1.0

Table A.8 The partial β_{eff} and β_0 for Sneak-7A, Sneak-7B, Sneak-9C2, and Sneak-9C1 (in pcm).

group g	029		033		046	
	$\beta_{\text{eff},g}$	$\beta_{0,g}$	$\beta_{\text{eff},g}$	$\beta_{0,g}$	$\beta_{\text{eff},g}$	$\beta_{0,g}$
1	25.4±0.9	22.1±0.5	24.5±0.8	21.7±0.5	24.5±0.8	22.5±0.5
2	113.5±1.8	102.8±1.0	111.3±1.8	104.0±1.0	107.1±1.7	102.3±1.0
3	68.7±1.4	61.3±0.8	64.6±1.4	60.0±0.8	66.1±1.4	61.0±0.8
4	143.6±2.0	130.8±1.2	143.6±2.0	131.0±1.2	141.7±2.0	131.5±1.2
5	241.2±2.7	220.0±1.5	243.7±2.7	221.5±1.5	237.0±2.6	219.8±1.5
6	70.2±1.4	61.4±0.8	66.3±1.4	61.4±0.8	65.6±1.3	60.9±0.8
7	61.7±1.3	54.9±0.7	59.7±1.3	54.8±0.7	59.2±1.3	53.9±0.7
8	17.4±0.7	16.4±0.4	17.7±0.7	16.3±0.4	17.3±0.7	15.8±0.4

Table A.9 The partial β_{eff} and β_0 for Stacy runs 029, 033, and 046 (in pcm).

group g	030		125		215	
	$\beta_{\text{eff},g}$	$\beta_{0,g}$	$\beta_{\text{eff},g}$	$\beta_{0,g}$	$\beta_{\text{eff},g}$	$\beta_{0,g}$
1	25.0±0.9	22.5±0.5	25.9±0.9	22.2±0.5	24.4±0.9	21.9±0.5
2	116.4±1.8	103.3±1.0	114.7±1.9	101.8±1.0	109.4±1.8	101.7±1.0
3	69.9±1.4	61.5±0.8	71.6±1.5	62.5±0.8	67.7±1.4	62.1±0.8
4	145.8±2.1	130.5±1.2	149.7±2.1	131.7±1.2	141.7±2.0	130.9±1.2
5	248.6±2.7	221.2±1.5	251.3±2.8	220.2±1.5	240.5±2.6	218.5±1.5
6	67.2±1.4	61.4±0.8	68.7±1.5	61.8±0.8	66.4±1.4	60.4±0.8
7	59.8±1.3	54.5±0.7	64.5±1.4	55.7±0.8	57.2±1.3	53.4±0.7
8	17.7±0.7	15.5±0.4	19.0±0.8	16.5±0.4	18.2±0.7	16.2±0.4

Table A.10 The partial β_{eff} and β_0 for Stacy runs 030, 125, and 215 (in pcm).

group g	Winco		Sheba-II	
	$\beta_{\text{eff},g}$	$\beta_{0,g}$	$\beta_{\text{eff},g}$	$\beta_{0,g}$
1	29.9±0.8	21.8±0.3	24.9±0.9	21.3±0.5
2	124.5±1.6	101.3±0.7	117.4±2.1	102.2±1.1
3	82.1±1.3	61.1±0.6	72.7±1.6	62.5±0.8
4	169.2±1.9	130.6±0.8	151.8±2.3	133.2±1.2
5	273.1±2.3	215.8±1.0	262.0±3.1	227.8±1.6
6	78.0±1.3	60.6±0.6	72.5±1.6	64.3±0.8
7	68.7±1.2	54.2±0.5	62.4±1.5	56.7±0.8
8	19.7±0.6	15.8±0.3	19.2±0.8	17.6±0.4

Table A.11 The partial β_{eff} and β_0 for the Winco slab tanks and Sheba-II (in pcm).

group g	Proteus		SHE-8	
	$\beta_{\text{eff},g}$	$\beta_{0,g}$	$\beta_{\text{eff},g}$	$\beta_{0,g}$
1	23.2±0.7	22.0±0.5	22.9±3.0	20.8±1.5
2	109.0±1.5	102.5±1.0	106.1±6.3	104.6±3.4
3	67.1±1.2	61.4±0.8	74.0±5.8	62.1±2.6
4	140.7±1.7	132.3±1.2	140.7±7.6	129.4±3.8
5	231.3±2.2	217.5±1.5	249.1±10.1	220.1±5.0
6	64.5±1.2	59.8±0.8	61.9±5.0	59.3±2.6
7	57.1±1.1	54.4±0.7	55.6±4.6	55.3±2.5
8	15.9±0.6	15.4±0.4	15.8±2.4	16.6±1.4



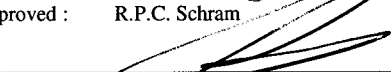
Table A.12 The partial β_{eff} and β_0 for Proteus and SHE-8 (in pcm).

Shielding benchmark calculations with MCNP-4C3 using JEFF-3.1 nuclear data

S.C. van der Marck

Petten, October, 2005

21616/05.69455/P

author :	S.C. van der Marck		reviewed :	A.J. Koning	
52 page(s)			approved :	R.P.C. Schram	
shield.tex					

© NRG 2005

Subject to agreement with the client, the information contained in this report may not be disclosed to any third party and NRG is not liable for any damage arising out of the use of such information.

Abstract

Shielding benchmark calculations were performed with MCNP-4C3 using the new JEFF-3.1 nuclear data library. The benchmarks used were Oktavian (for Al, Co, Cr, Cu, LiF, Mn, Mo, Si, Ti, W, Zr), FNS (for Be, C, Fe, and Pb), LLNL Pulsed Spheres (for concrete), and NIST Water Spheres (for water and Cd). The results of these calculations are reported as graphs of the neutron spectra, and in some cases also the photon spectrum, as well as in graphs and tables of calculated over experimental values of the neutron spectra.

Keywords

MCNP-4C3

JEFF-3.1

nuclear data

shielding benchmarks

Contents

1	Introduction	5
2	Brief description of the shielding benchmarks	6
2.1	Oktavian	6
2.2	FNS	7
2.3	LLNL Pulsed Spheres	8
2.4	NIST Water Spheres	9
3	Results	10
3.1	Oktavian	10
3.1.1	Oktavian, Al	10
3.1.2	Oktavian, Co	11
3.1.3	Oktavian, Cr	12
3.1.4	Oktavian, Cu	13
3.1.5	Oktavian, LiF	14
3.1.6	Oktavian, Mn	15
3.1.7	Oktavian, Mo	16
3.1.8	Oktavian, Si	17
3.1.9	Oktavian, Ti	18
3.1.10	Oktavian, W	19
3.1.11	Oktavian, Zr	20
3.2	FNS	21
3.2.1	Computational methods	21
3.2.2	FNS, Be, 5 cm	21
3.2.3	FNS, Be, 15 cm	23
3.2.4	FNS, C, 5 cm	25
3.2.5	FNS, C, 20 cm	27
3.2.6	FNS, C, 40 cm	29
3.2.7	FNS, N, 20 cm	31
3.2.8	FNS, O, 20 cm	33
3.2.9	FNS, Fe, 5 cm	35
3.2.10	FNS, Fe, 20 cm	37
3.2.11	FNS, Fe, 40 cm	39
3.2.12	FNS, Fe, 60 cm	41
3.2.13	FNS, Pb, 5 cm	43
3.2.14	FNS, Pb, 20 cm	45
3.2.15	FNS, Pb, 40 cm	47
3.3	LLNL Pulsed Spheres	49
3.3.1	LLNL Pulsed Spheres, Concrete, 21 cm	49
3.3.2	LLNL Pulsed Spheres, Concrete, 35.5 cm	49
3.4	NIST Water Spheres	50
4	Summary	51

1. Introduction

In May 2005 a new version of the JEFF general purpose nuclear data library was released: JEFF-3.1. Over the last several years there has been a concerted effort by many people in several countries to bring the quality of this nuclear data library to a new, higher level.

In this report, the results of many shielding benchmark runs are presented.

All results reported in this report were obtained by use of the Monte Carlo neutronics code MCNP, version 4C3 [1].

2. Brief description of the shielding benchmarks

2.1 Oktavian

The Oktavian benchmark specifications are given on the IAEA web site [3]. The measured quantity

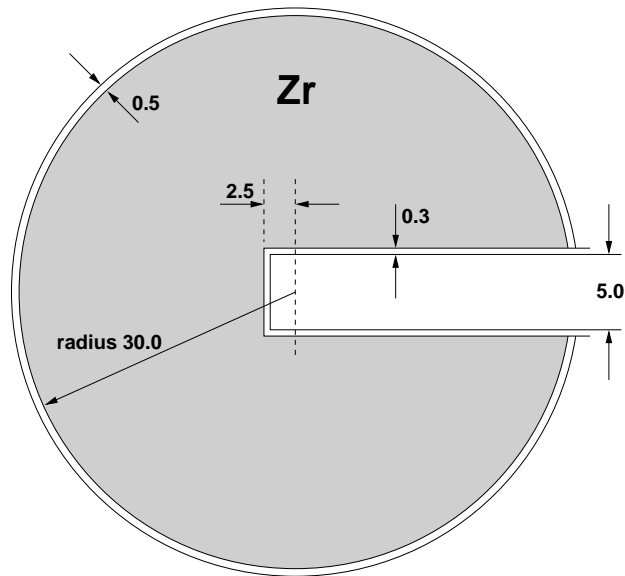


Figure 2.1 Schematic drawing of the Oktavian geometry for the Zr benchmark (not to scale). All dimensions are in cm.

was the leakage current spectrum from the outer surface of a spherical pile of a material. At the center of a pile a 14 MeV D-T neutron source was located. The leakage spectrum is given in units of neutrons per MeV per source neutron.

The materials for which benchmark calculations have been performed are list in Table 2.1. A schematic drawing of one of the models is given in Fig. 2.1 (see Ref. [4]).

material		outer diameter
aluminum	Al	40 cm
cobalt	Co	40 cm
chromium	Cr	40 cm
copper	Cu	61 cm
lithium fluoride	LiF	61 cm
molybdenum	Mo	61 cm
manganese	Mn	61 cm
silicon	Si	60 cm
titanium	Ti	40 cm
tungsten	W	40 cm
zirconium	Zr	61 cm

Table 2.1 The materials used in the Oktavian shielding benchmarks

2.2 FNS

The FNS Time-of-Flight benchmark specifications are given on the IAEA web site [5]. The neu-

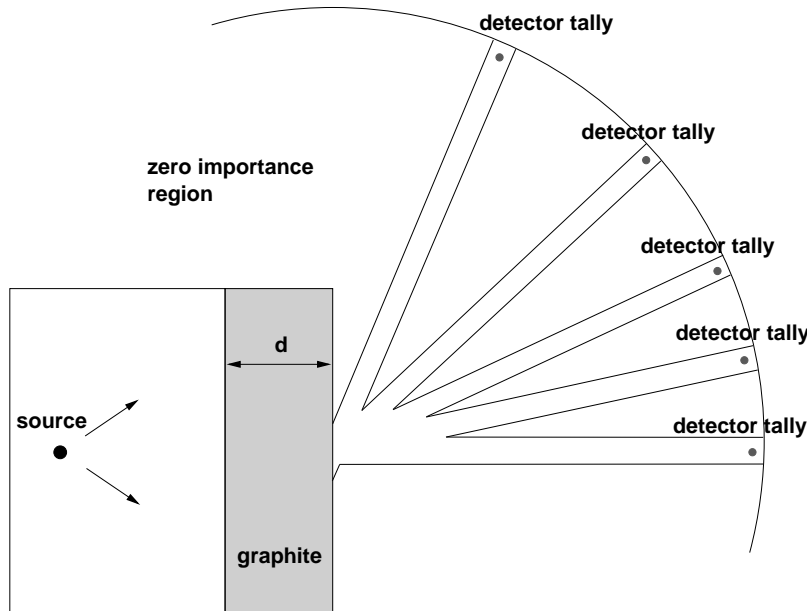


Figure 2.2 Schematic drawing of the MCNP model for the FNS benchmark for graphite (not to scale).

tron spectrum emerging from slabs of material of varying thickness, was measured at five different angles. The slabs were placed at 20 cm distance from a 14 MeV D-T neutron source. The materials for which benchmark calculations have been performed are listed in Table 2.2. A schematic drawing of the MCNP model for this benchmark is given in Fig. 2.2 [6].

material		slab thickness	angles
beryllium	Be	5 cm	0°, 24.9°, 42.8°, 66.8°
		15 cm	0°, 12.2°, 24.9°, 42.8°, 66.8°
graphite	C	5 cm	0°, 24.9°, 42.8°, 66.8°
		20 cm	0°, 12.2°, 24.9°, 42.8°, 66.8°
		40 cm	0°, 12.2°, 24.9°, 42.8°, 66.8°
nitrogen	N	20 cm	0°, 12.2°, 24.9°, 42.8°, 66.8°
oxygen	O	20 cm	0°, 12.2°, 24.9°, 42.8°, 66.8°
iron	Fe	5 cm	0°, 24.9°, 42.8°, 66.8°
		20 cm	0°, 12.2°, 24.9°, 42.8°, 66.8°
		40 cm	0°, 12.2°, 24.9°, 42.8°, 66.8°
		60 cm	0°, 12.2°, 24.9°, 42.8°
lead	Pb	5 cm	0°, 24.9°, 42.8°, 66.8°
		20 cm	0°, 12.2°, 24.9°, 42.8°, 66.8°
		40 cm	0°, 12.2°, 24.9°, 42.8°, 66.8°

Table 2.2 The materials used in the FNS shielding benchmarks

2.3 LLNL Pulsed Spheres

The description of the experiments performed in the Livermore Pulsed Sphere Program is given in Ref. [7]. Time-of-flight measurements were performed for neutrons passing through spherical shells of varying thickness, containing different materials. The source was a 14 MeV D-T neutron source.

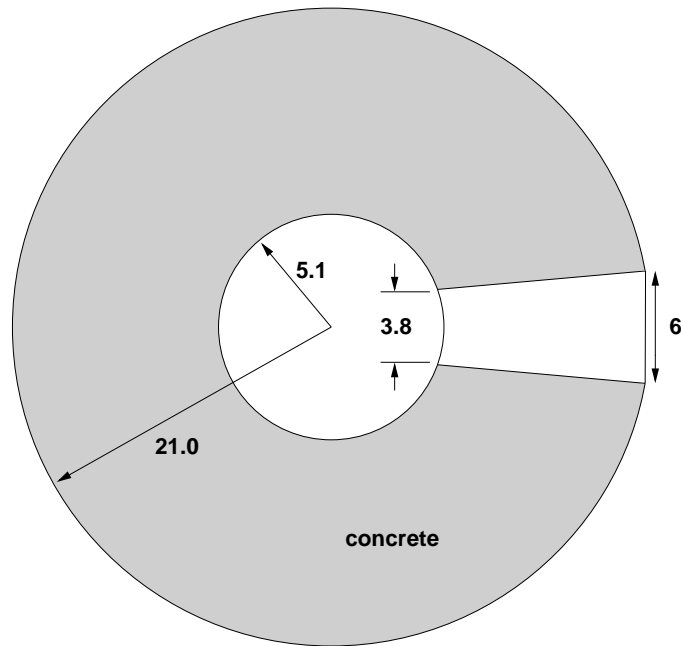


Figure 2.3 Schematic drawing of the MCNP model for the LLNL benchmark for concrete (not to scale). All dimensions are in cm.

Calculations were performed for two cases with concrete, one with inner radius of 5.1 cm, outer radius 21.0 cm (see Fig. 2.3), and the other with the same inner radius, but an outer radius of 35.5 cm. The composition of the concrete is given in Table 2.3; the density of the concrete was 2.35 g/cm³. The MCNP model used in the present work was taken over from Ref. [8].

Material	at%
O	55.7
H	15.1
Si	14.9
Ca	3.6
Al	3.2
C	3.1
Mg	1.8
Na	1.3
other	< 1.0 each

Table 2.3 The composition of the concrete used in the LLNL Pulsed Sphere experiments.

2.4 NIST Water Spheres

A description of the experiments performed at NIST with water and cadmium shielding is given in Ref. [10]. A Cf source was placed at the center of the experiment, and fission foils were placed at two, diametrically opposed positions. Between the source and the fission foils were several combinations of shielding materials, see Table 2.4. The fission foils used were ^{235}U , ^{239}Pu , ^{238}U , ^{237}Np .

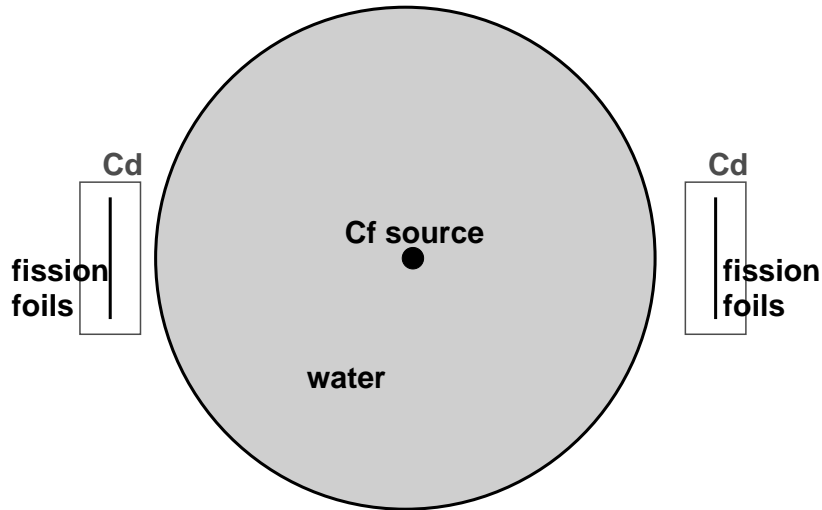


Figure 2.4 Schematic drawing of the MCNP model for the NIST benchmark (not to scale).

radius (inch)	material
1.5	—
2.0	—
1.5	Cd
2.0	Cd
1.5	H ₂ O
2.0	H ₂ O
2.5	H ₂ O
1.5	H ₂ O+Cd
2.0	H ₂ O+Cd
2.5	H ₂ O+Cd

Table 2.4 The radius and material combinations for which experiments have been performed.

3. Results

In this section we report on the results of our calculations. These results are reported as graphs of the neutron spectra, and in some cases also the photon spectrum, as well as in graphs and tables of calculated over experimental values of the neutron spectra.

3.1 Oktavian

3.1.1 Oktavian, Al

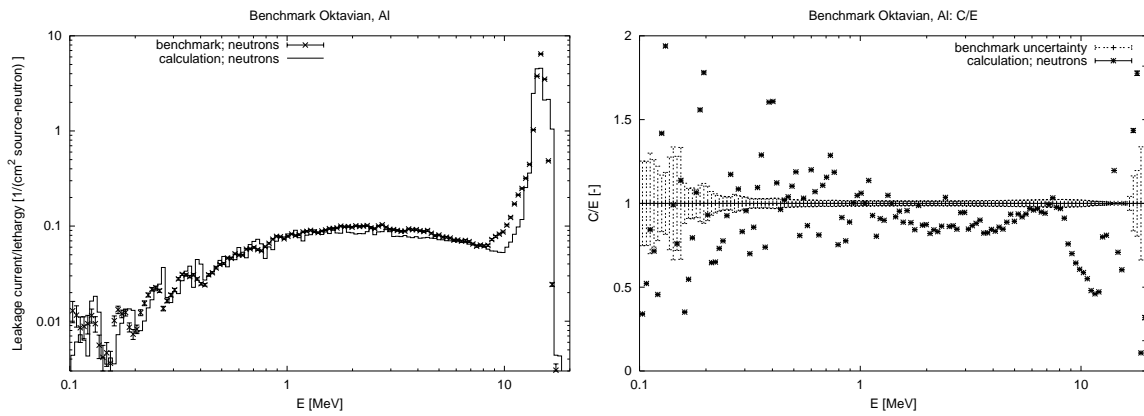


Figure 3.1 The result for the neutron leakage spectrum for the Oktavian Al benchmark.

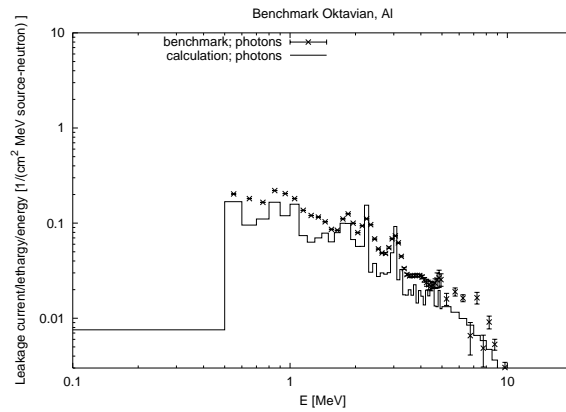


Figure 3.2 The result for the photon leakage spectrum for the Oktavian Al benchmark.

	energy range		C/E
Al	0.1–	1.0	1.01 ± 0.01
Al	1.0–	5.0	0.90 ± 0.01
Al	5.0–	10.0	0.90 ± 0.01
Al	10.0–	20.0	1.06 ± 0.01

Table 3.1 C/E values for the neutron spectrum of the Oktavian Al benchmark.

3.1.2 Oktavian, Co

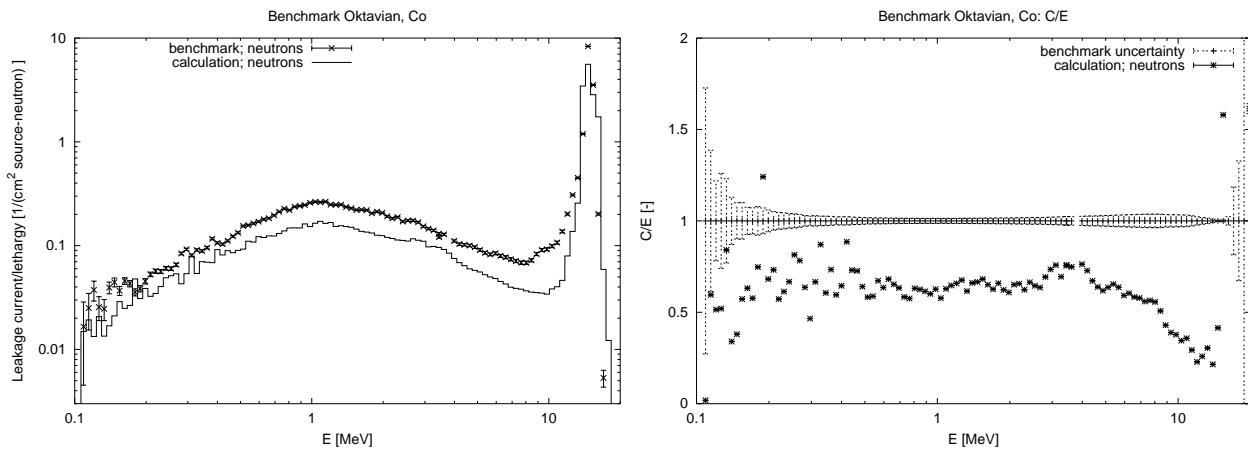


Figure 3.3 The result for the neutron leakage spectrum for the Oktavian Co benchmark.

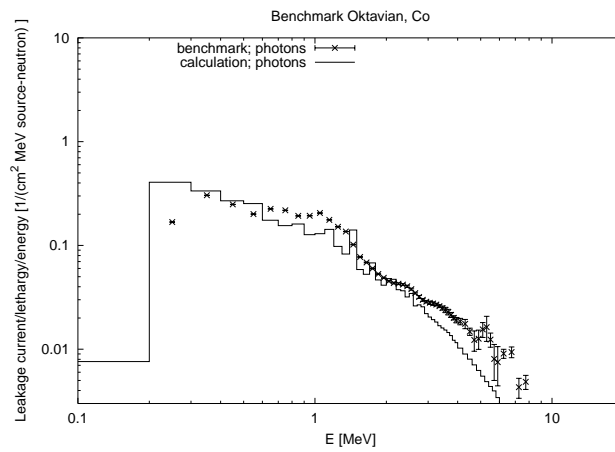


Figure 3.4 The result for the photon leakage spectrum for the Oktavian Co benchmark.

	energy range		C/E
Co	0.1–	1.0	0.64 ± 0.01
Co	1.0–	5.0	0.66 ± 0.01
Co	5.0–	10.0	0.54 ± 0.01
Co	10.0–	20.0	0.98 ± 0.01

Table 3.2 C/E values for the neutron spectrum of the Oktavian Co benchmark.

3.1.3 Oktavian, Cr

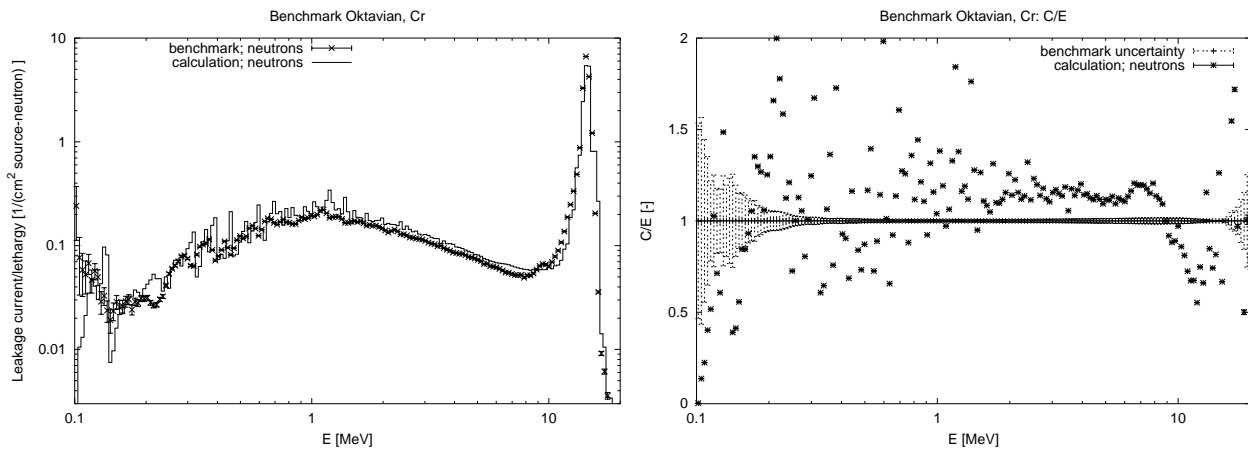


Figure 3.5 The result for the neutron leakage spectrum for the Oktavian Cr benchmark.

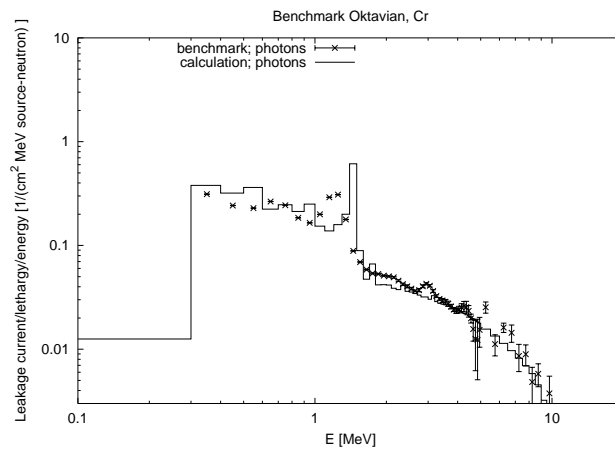


Figure 3.6 The result for the photon leakage spectrum for the Oktavian Cr benchmark.

	energy range		C/E
Cr	0.1–	1.0	1.09 ± 0.02
Cr	1.0–	5.0	1.19 ± 0.01
Cr	5.0–	10.0	1.10 ± 0.01
Cr	10.0–	20.0	0.95 ± 0.01

Table 3.3 C/E values for the neutron spectrum of the Oktavian Cr benchmark.

3.1.4 Oktavian, Cu

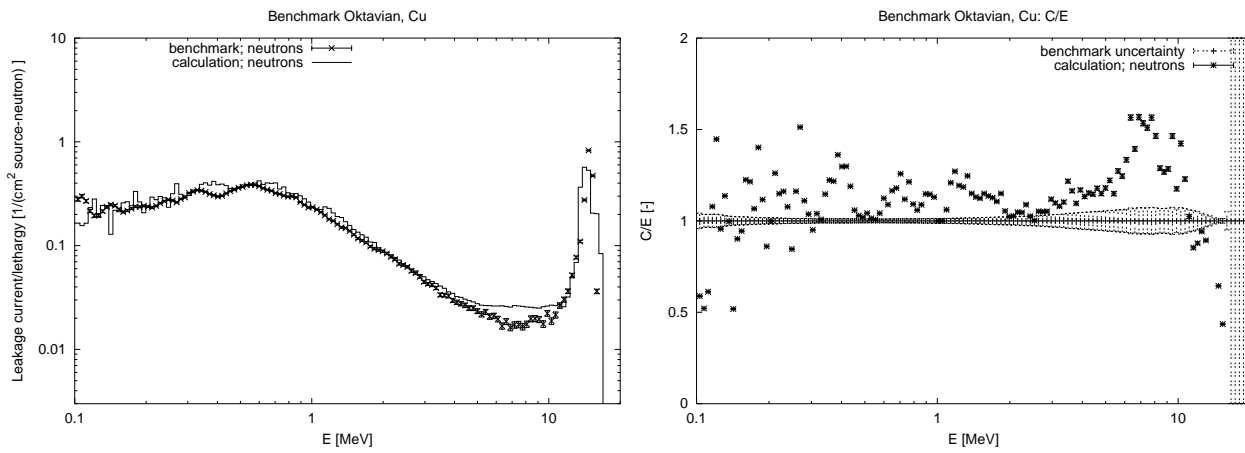


Figure 3.7 The result for the neutron leakage spectrum for the Oktavian Cu benchmark.

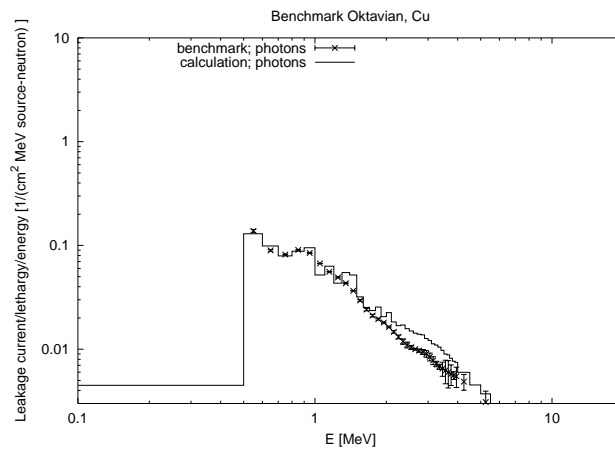


Figure 3.8 The result for the photon leakage spectrum for the Oktavian Cu benchmark.

	energy range		C/E
Cu	0.0–	0.1	0.27 ± 0.05
Cu	0.1–	1.0	1.07 ± 0.01
Cu	1.0–	5.0	1.11 ± 0.01
Cu	5.0–	10.0	1.36 ± 0.02
Cu	10.0–	20.0	1.12 ± 0.01

Table 3.4 C/E values for the neutron spectrum of the Oktavian Cu benchmark.

3.1.5 Oktavian, LiF

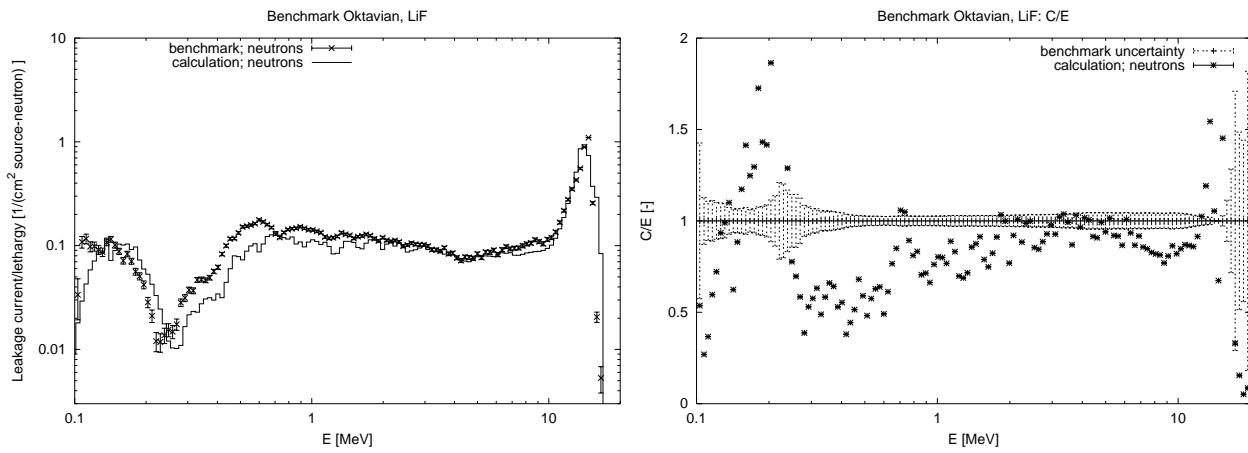


Figure 3.9 The result for the neutron leakage spectrum for the Oktavian LiF benchmark.

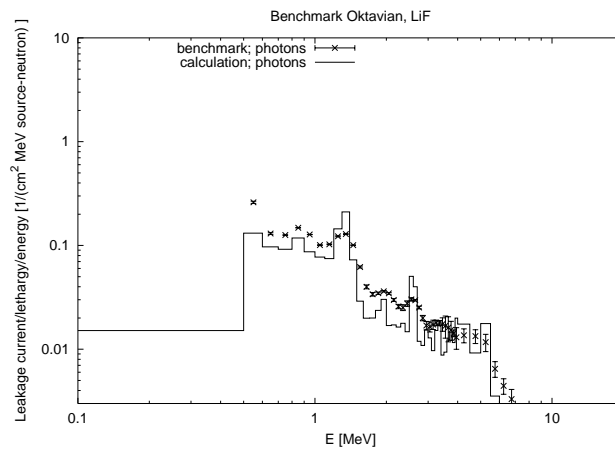


Figure 3.10 The result for the photon leakage spectrum for the Oktavian LiF benchmark.

	energy range		C/E
LiF	0.1–	1.0	0.76 ± 0.01
LiF	1.0–	5.0	0.89 ± 0.01
LiF	5.0–	10.0	0.88 ± 0.01
LiF	10.0–	20.0	1.09 ± 0.01

Table 3.5 C/E values for the neutron spectrum of the Oktavian LiF benchmark.

3.1.6 Oktavian, Mn

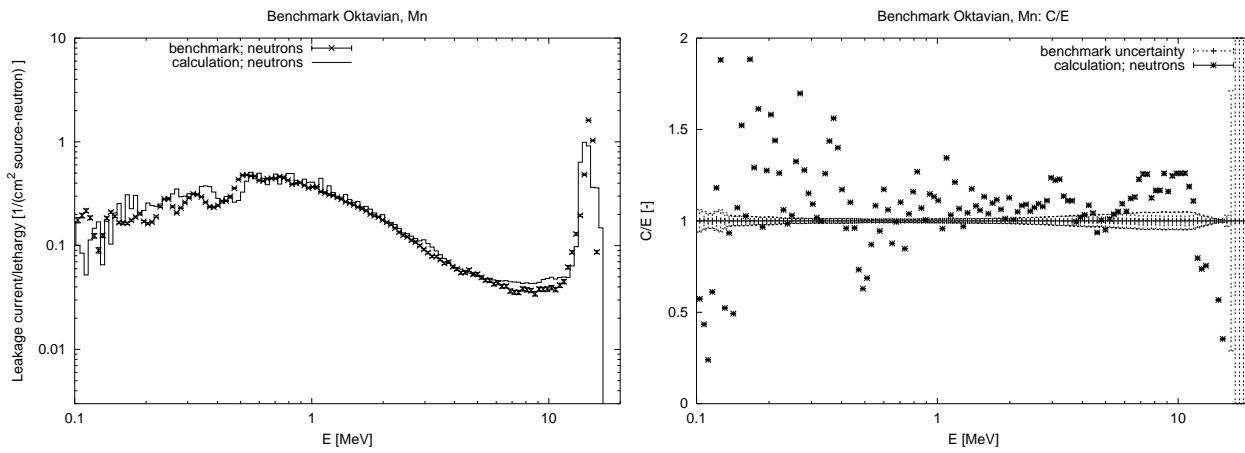


Figure 3.11 The result for the neutron leakage spectrum for the Oktavian Mn benchmark.

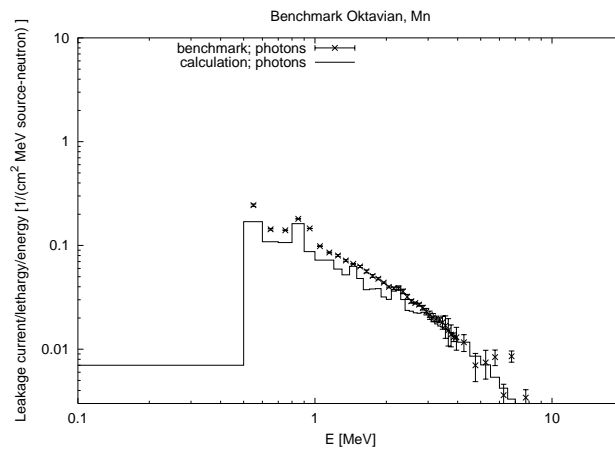


Figure 3.12 The result for the photon leakage spectrum for the Oktavian Mn benchmark.

	energy range		C/E
Mn	0.0–	0.1	0.38 ± 0.05
Mn	0.1–	1.0	1.05 ± 0.01
Mn	1.0–	5.0	1.09 ± 0.01
Mn	5.0–	10.0	1.12 ± 0.01
Mn	10.0–	20.0	1.00 ± 0.01

Table 3.6 C/E values for the neutron spectrum of the Oktavian Mn benchmark.

3.1.7 Oktavian, Mo

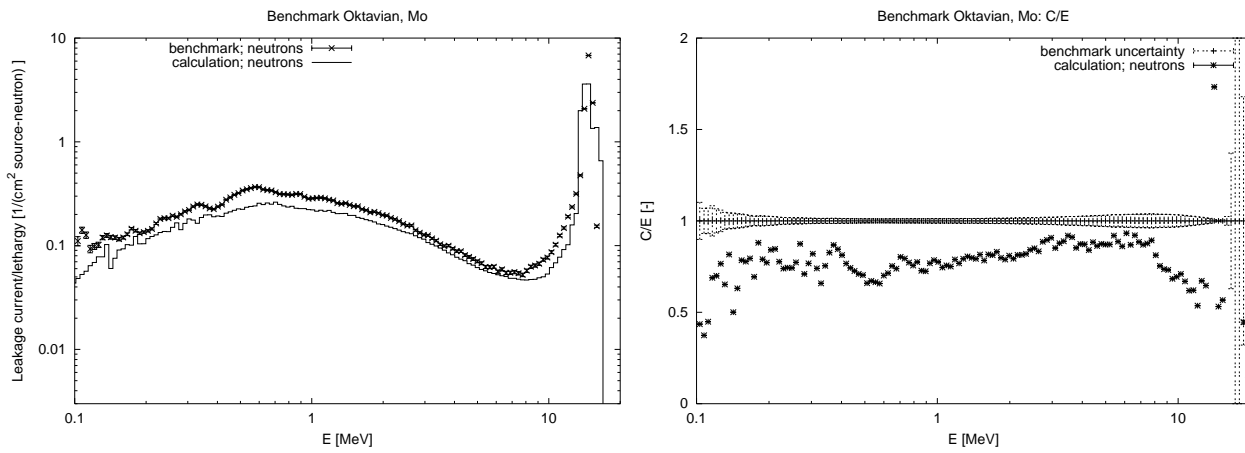


Figure 3.13 The result for the neutron leakage spectrum for the Oktavian Mo benchmark.

	energy range		C/E
Mo	0.0–	0.1	0.27 ± 0.19
Mo	0.1–	1.0	0.73 ± 0.01
Mo	1.0–	5.0	0.81 ± 0.01
Mo	5.0–	10.0	0.84 ± 0.01
Mo	10.0–	20.0	1.02 ± 0.01

Table 3.7 C/E values for the neutron spectrum of the Oktavian Mo benchmark.

3.1.8 Oktavian, Si

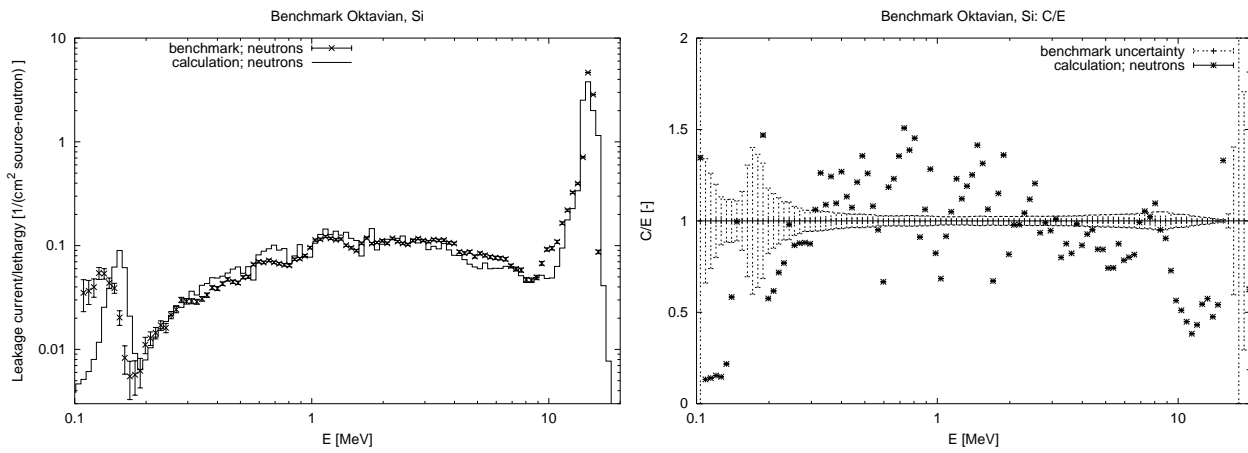


Figure 3.14 The result for the neutron leakage spectrum for the Oktavian Si benchmark.

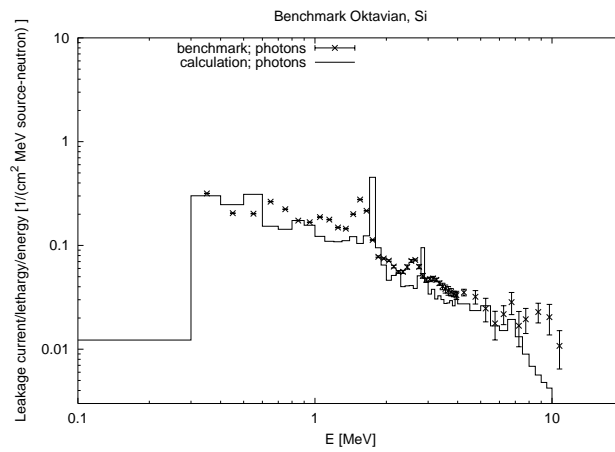


Figure 3.15 The result for the photon leakage spectrum for the Oktavian Si benchmark.

	energy range		C/E
Si	0.1–	1.0	1.09 ± 0.02
Si	1.0–	5.0	1.00 ± 0.01
Si	5.0–	10.0	0.85 ± 0.01
Si	10.0–	20.0	1.09 ± 0.01

Table 3.8 C/E values for the neutron spectrum of the Oktavian Si benchmark.

3.1.9 Oktavian, Ti

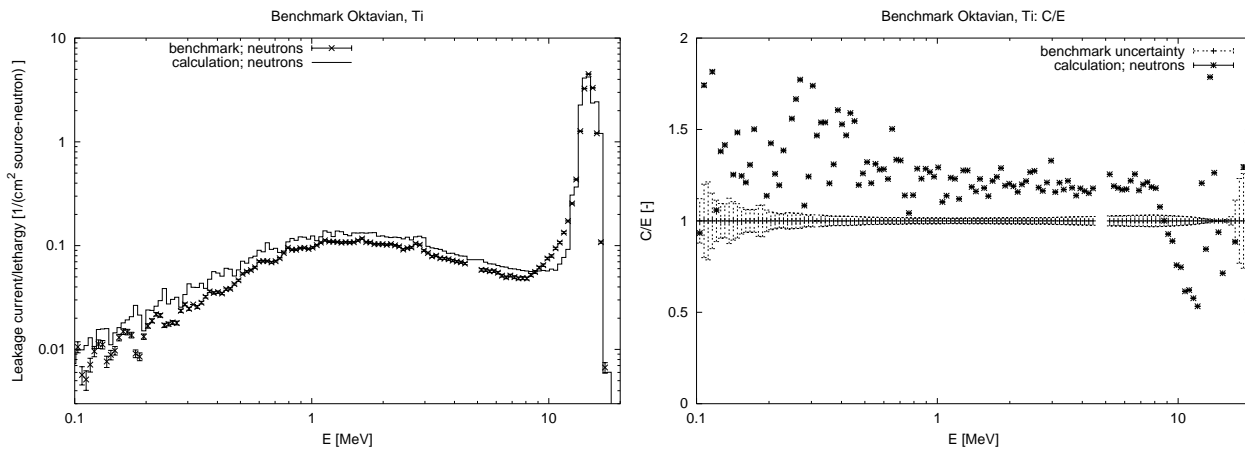


Figure 3.16 The result for the neutron leakage spectrum for the Oktavian Ti benchmark.

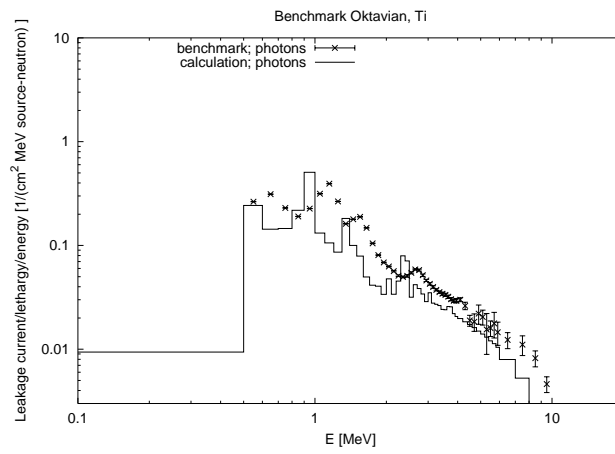


Figure 3.17 The result for the photon leakage spectrum for the Oktavian Ti benchmark.

	energy range		C/E
Ti	0.0–	0.1	1.17 ± 0.11
Ti	0.1–	1.0	1.33 ± 0.01
Ti	1.0–	5.0	1.20 ± 0.01
Ti	5.0–	10.0	1.14 ± 0.01
Ti	10.0–	20.0	1.18 ± 0.01

Table 3.9 C/E values for the neutron spectrum of the Oktavian Ti benchmark.

3.1.10 Oktavian, W

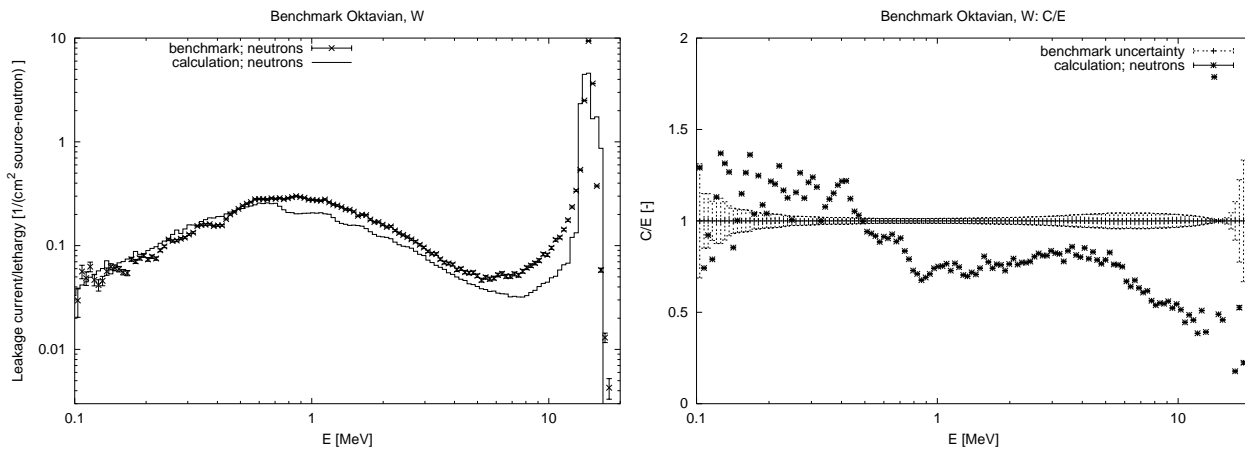


Figure 3.18 The result for the neutron leakage spectrum for the Oktavian W benchmark.

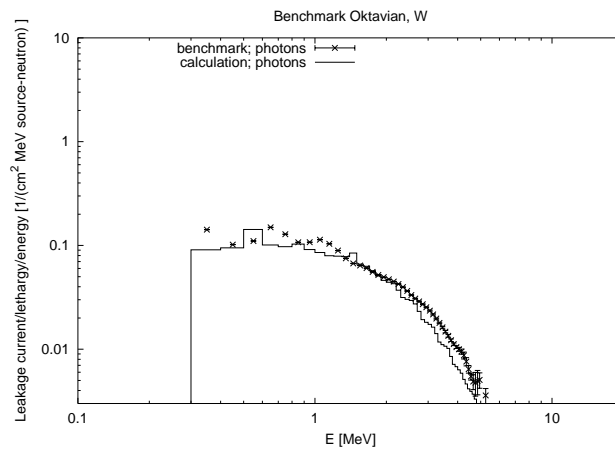


Figure 3.19 The result for the photon leakage spectrum for the Oktavian W benchmark.

	energy range		C/E
W	0.0–	0.1	0.30 ± 0.16
W	0.1–	1.0	0.97 ± 0.01
W	1.0–	5.0	0.76 ± 0.01
W	5.0–	10.0	0.64 ± 0.01
W	10.0–	20.0	0.91 ± 0.01

Table 3.10 C/E values for the neutron spectrum of the Oktavian W benchmark.

3.1.11 Oktavian, Zr

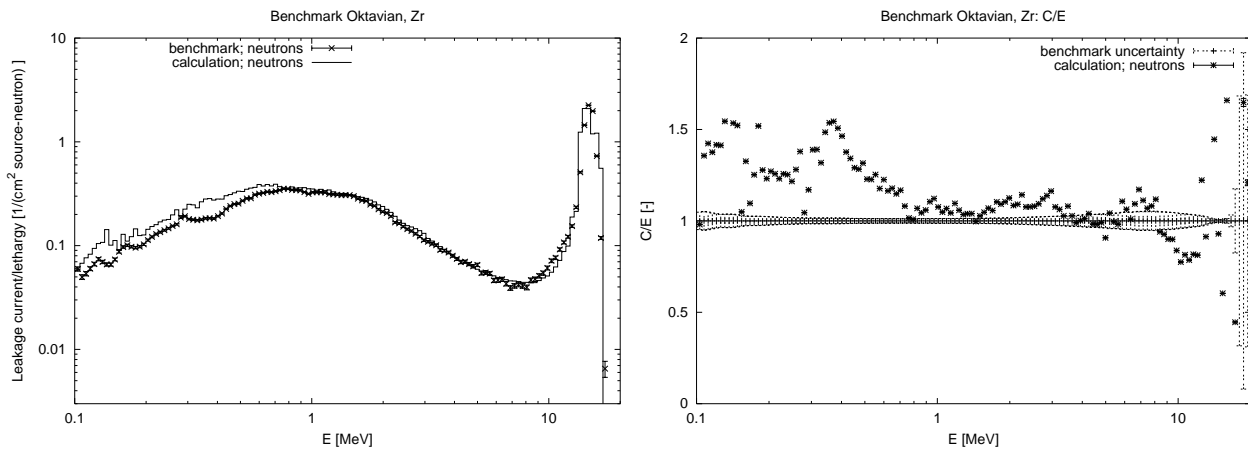


Figure 3.20 The result for the neutron leakage spectrum for the Oktavian Zr benchmark.

	energy range		C/E
Zr	0.0–	0.1	0.97 ± 0.04
Zr	0.1–	1.0	1.23 ± 0.01
Zr	1.0–	5.0	1.06 ± 0.01
Zr	5.0–	10.0	1.02 ± 0.01
Zr	10.0–	20.0	1.16 ± 0.01

Table 3.11 C/E values for the neutron spectrum of the Oktavian Zr benchmark.

3.2 FNS

3.2.1 Calculational methods

For each of the experiments mentioned in Section 2 the neutron source spectrum was taken from the underlying reference. Hence, in Oktavian and FNS analyses an isotropic neutron distribution was assumed. However, it is known that the neutron source has a peak energy of 14.8 MeV in the forward direction, and a peak at 13.3 MeV in the backward direction (see Ref. [9]).

The assumption of isotropy will slightly influence the calculated angular spectra for the FNS benchmarks. This influence is expected to be of the order of several percent only.

3.2.2 FNS, Be, 5 cm

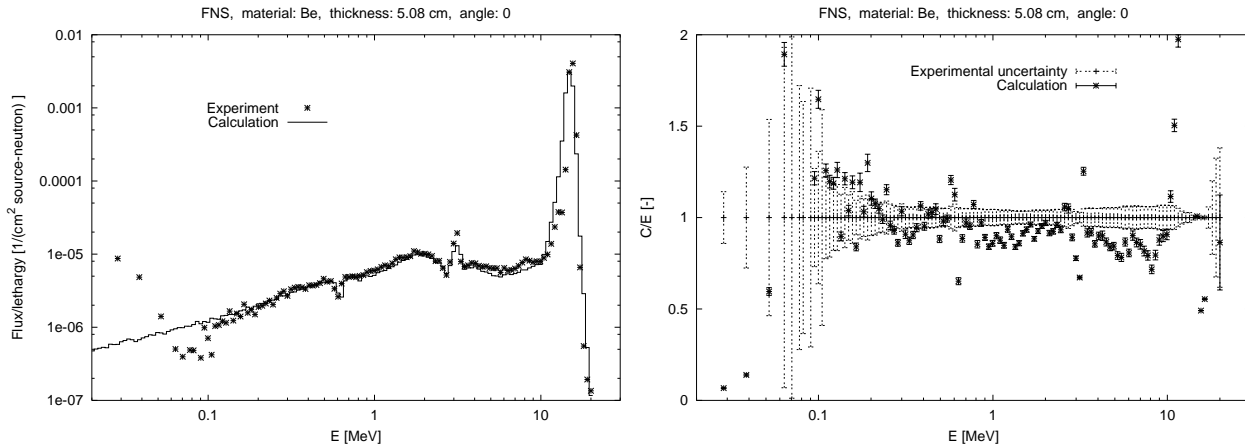


Figure 3.21 Neutron spectrum for the FNS, Be, d=5cm benchmark at 0° angle.

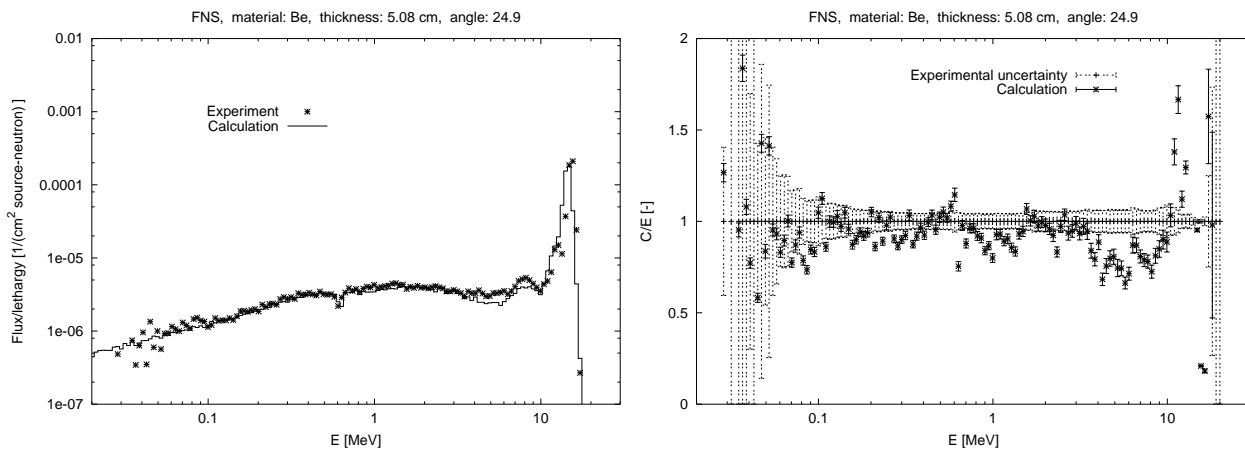


Figure 3.22 Neutron spectrum for the FNS, Be, d=5cm benchmark at 24.9° angle.

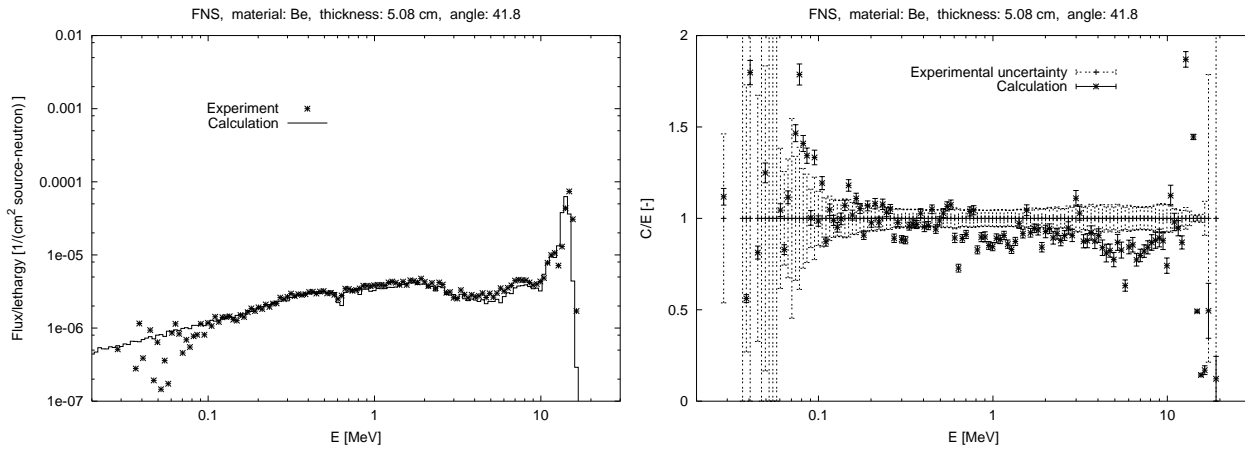


Figure 3.23 Neutron spectrum for the FNS, Be, d=5cm benchmark at 42.8° angle.

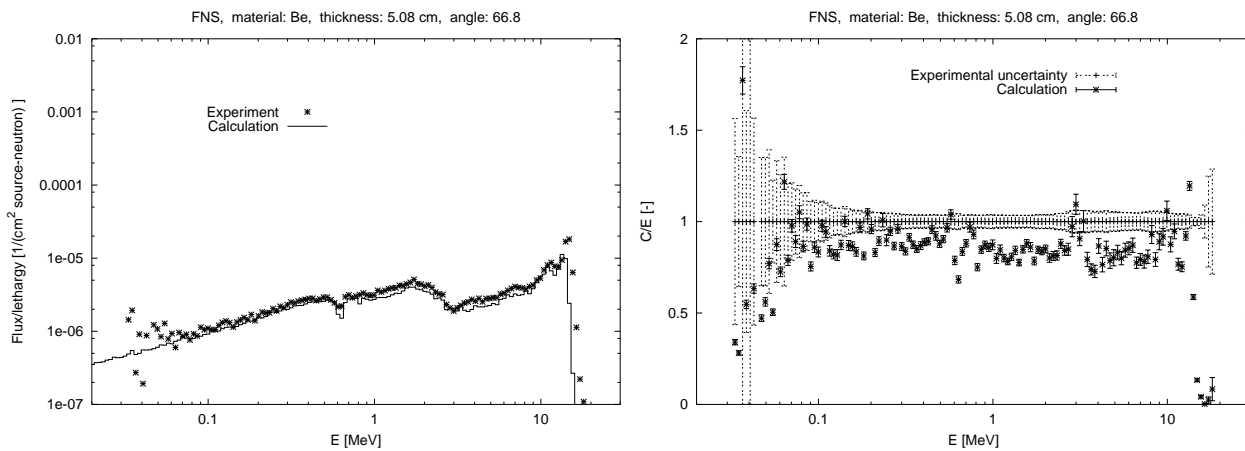


Figure 3.24 Neutron spectrum for the FNS, Be, d=5cm benchmark at 66.8° angle.

energy range	0°	12.2°	24.9°	42.8°	66.8°
0.1– 1.0	0.95 ± 0.01		0.93 ± 0.01	0.95 ± 0.01	0.87 ± 0.01
1.0– 5.0	0.90 ± 0.01		0.93 ± 0.01	0.91 ± 0.01	0.84 ± 0.01
5.0– 10.0	0.81 ± 0.01		0.78 ± 0.01	0.81 ± 0.01	0.80 ± 0.01
10.0– 20.0	0.96 ± 0.01		0.96 ± 0.01	0.94 ± 0.01	0.69 ± 0.01

Table 3.12 C/E values for the neutron spectrum of the FNS Be 5cm benchmark.

3.2.3 FNS, Be, 15 cm

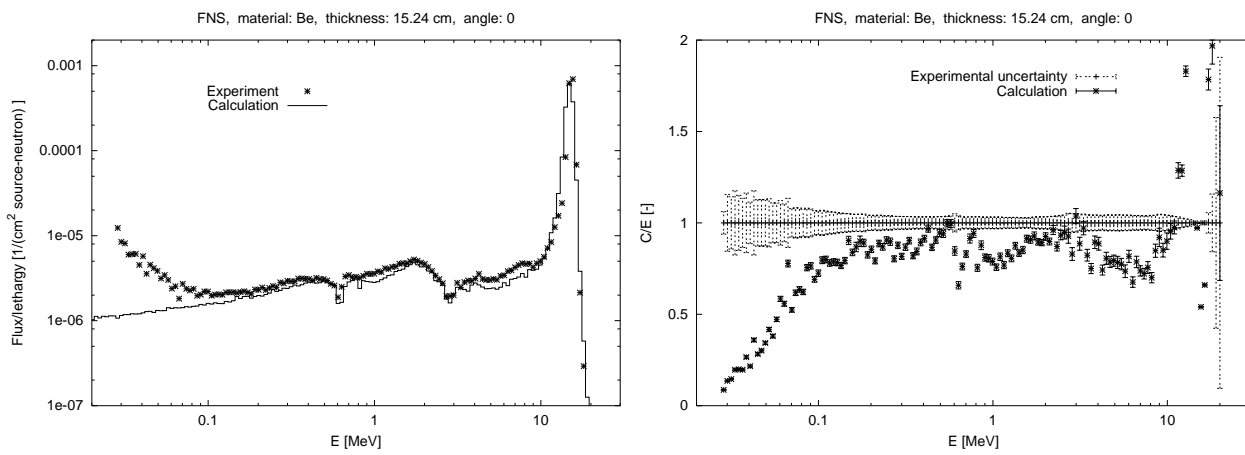


Figure 3.25 Neutron spectrum for the FNS, Be, d=15cm benchmark at 0° angle.

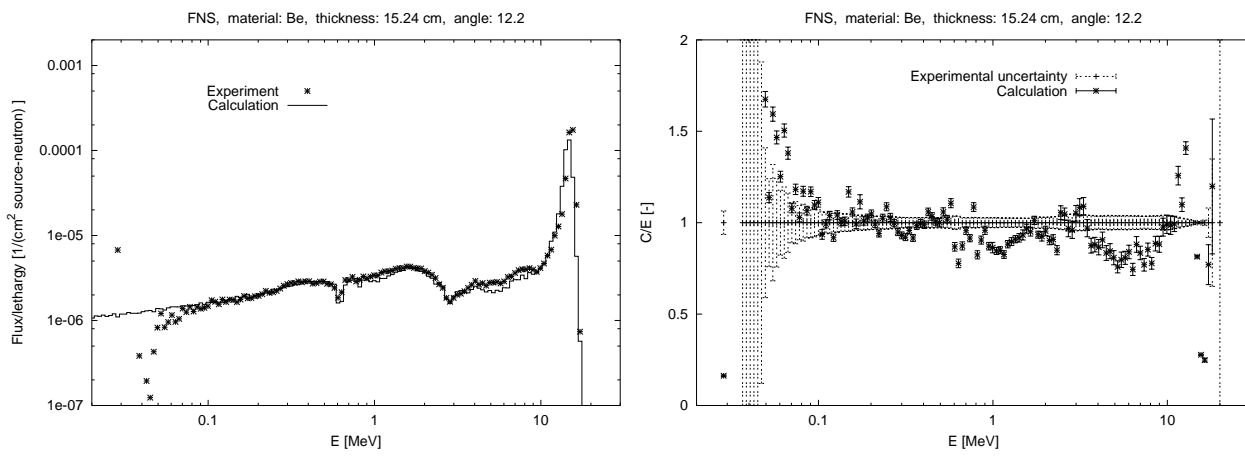


Figure 3.26 Neutron spectrum for the FNS, Be, d=15cm benchmark at 12.2° angle.

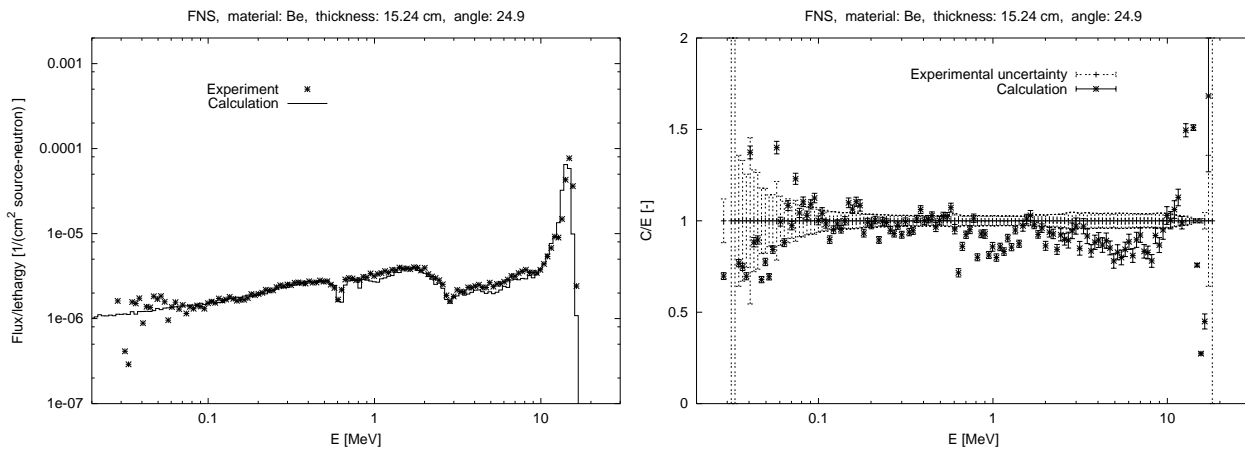


Figure 3.27 Neutron spectrum for the FNS, Be, d=15cm benchmark at 24.9° angle.

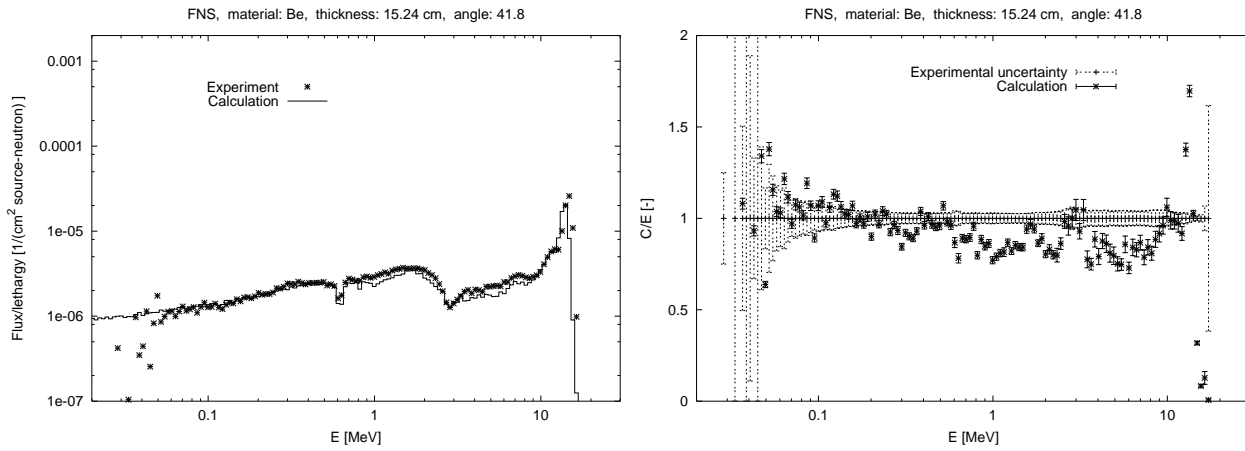


Figure 3.28 Neutron spectrum for the FNS, Be, d=15cm benchmark at 42.8° angle.

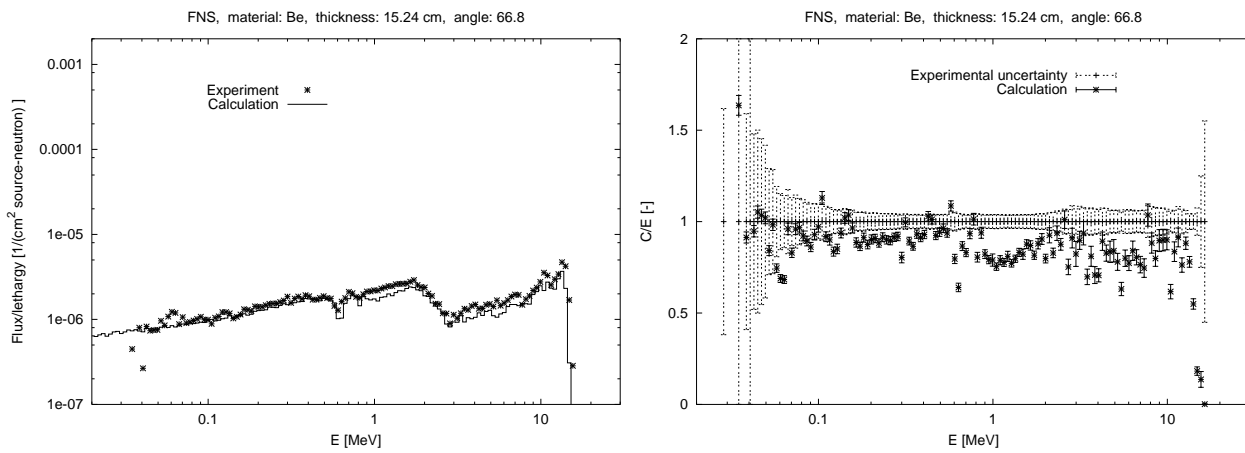


Figure 3.29 Neutron spectrum for the FNS, Be, d=15cm benchmark at 66.8° angle.

energy range	0°	12.2°	24.9°	42.8°	66.8°
0.1– 1.0	0.85 ± 0.01	0.97 ± 0.01	0.95 ± 0.01	0.94 ± 0.01	0.89 ± 0.01
1.0– 5.0	0.87 ± 0.01	0.93 ± 0.01	0.91 ± 0.01	0.87 ± 0.01	0.84 ± 0.01
5.0– 10.0	0.75 ± 0.01	0.81 ± 0.01	0.83 ± 0.01	0.81 ± 0.01	0.78 ± 0.02
10.0– 20.0	0.98 ± 0.01	0.81 ± 0.01	1.01 ± 0.01	0.83 ± 0.01	0.80 ± 0.02

Table 3.13 C/E values for the neutron spectrum of the FNS Be 15cm benchmark.

3.2.4 FNS, C, 5 cm

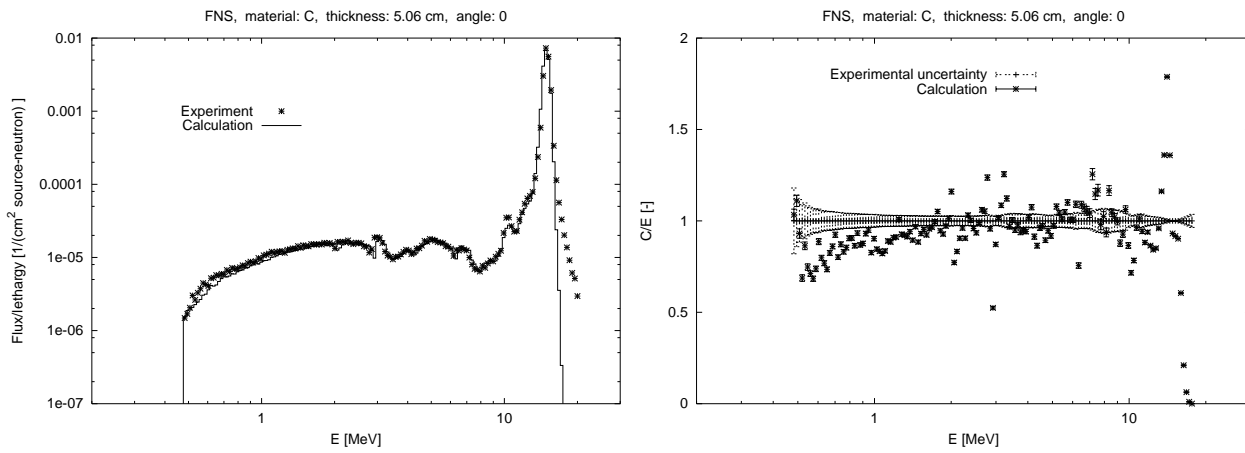


Figure 3.30 Neutron spectrum for the FNS, C, d=5cm benchmark at 0° angle.

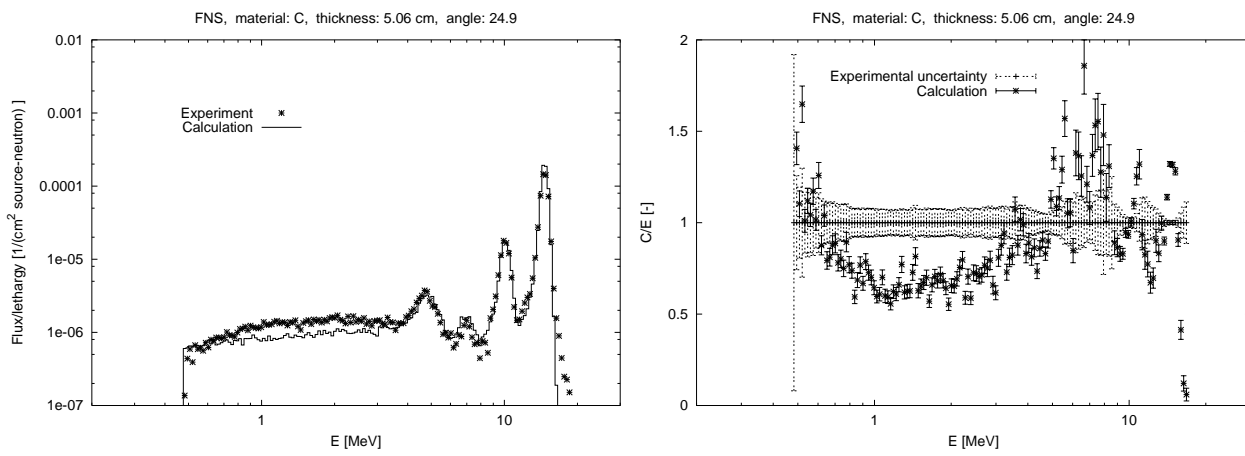


Figure 3.31 Neutron spectrum for the FNS, C, d=5cm benchmark at 24.9° angle.

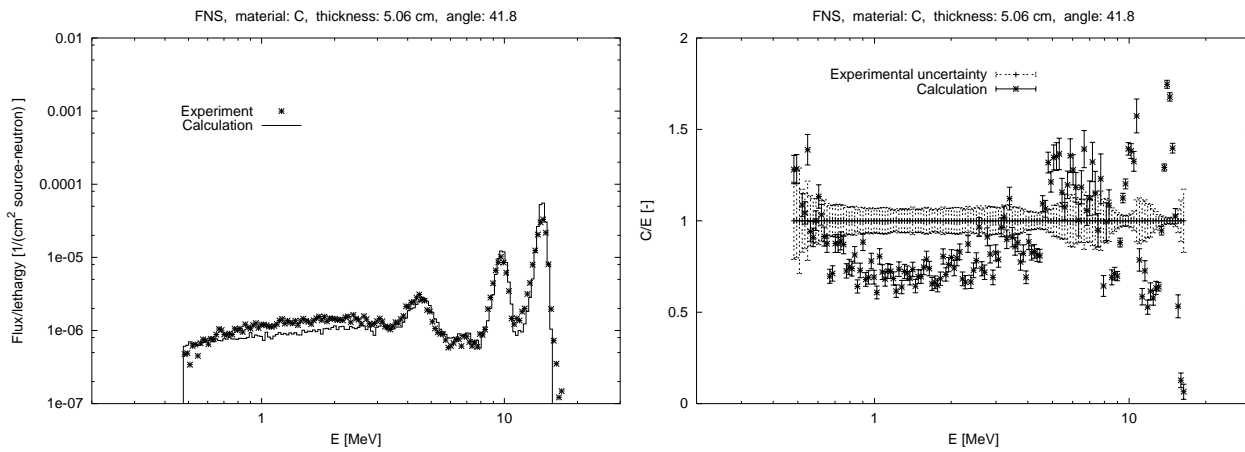


Figure 3.32 Neutron spectrum for the FNS, C, d=5cm benchmark at 42.8° angle.

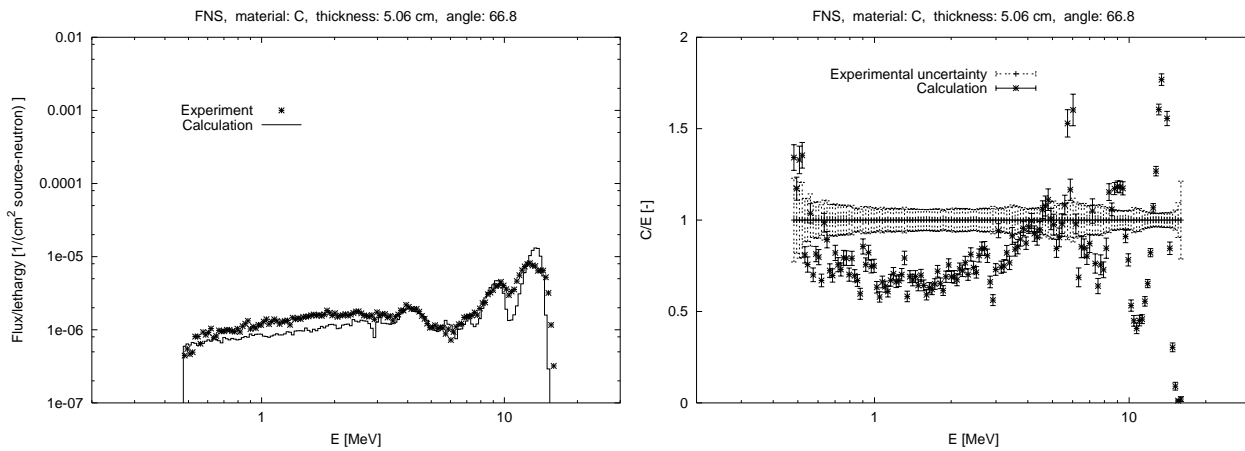


Figure 3.33 Neutron spectrum for the FNS, C, d=5cm benchmark at 66.8° angle.

energy range	0°	12.2°	24.9°	42.8°	66.8°
0.1– 1.0	0.81 ± 0.01		0.84 ± 0.01	0.83 ± 0.01	0.77 ± 0.01
1.0– 5.0	0.94 ± 0.01		0.73 ± 0.01	0.79 ± 0.01	0.76 ± 0.01
5.0– 10.0	1.01 ± 0.01		0.83 ± 0.01	0.93 ± 0.01	0.95 ± 0.01
10.0– 20.0	1.01 ± 0.01		1.23 ± 0.01	1.39 ± 0.01	1.01 ± 0.01

Table 3.14 C/E values for the neutron spectrum of the FNS C 5cm benchmark.

3.2.5 FNS, C, 20 cm

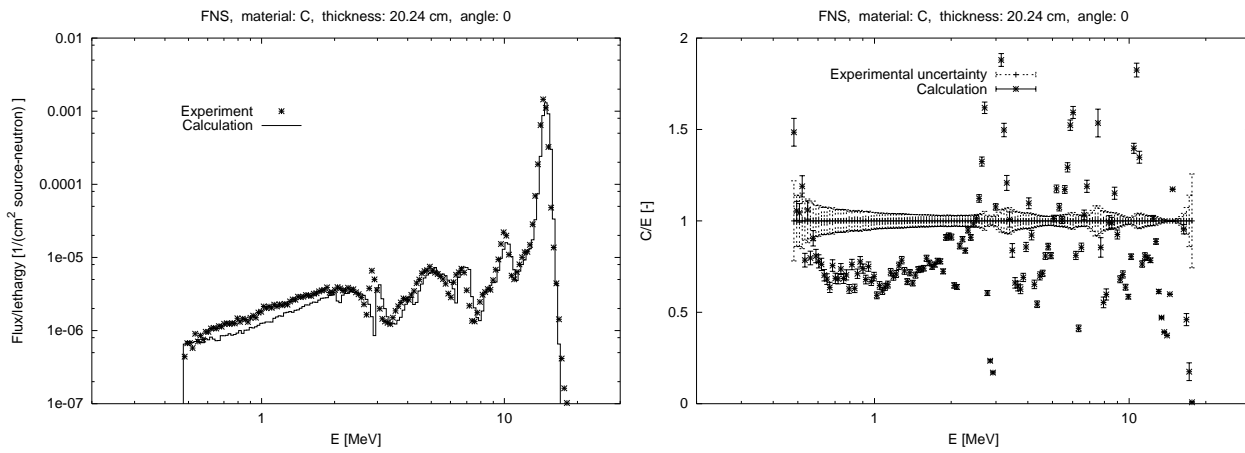


Figure 3.34 Neutron spectrum for the FNS, C, d=20cm benchmark at 0° angle.

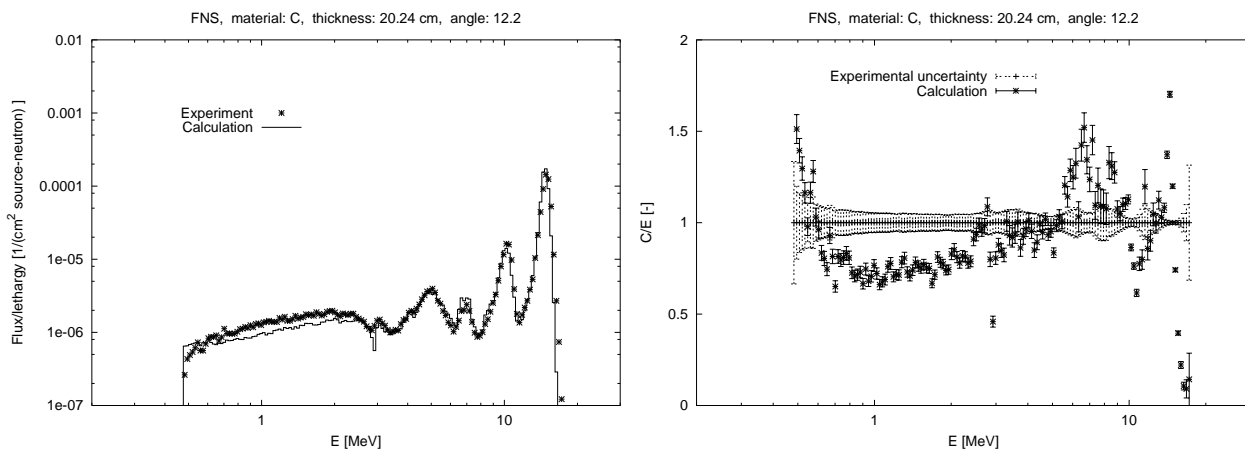


Figure 3.35 Neutron spectrum for the FNS, C, d=20cm benchmark at 12.2° angle.

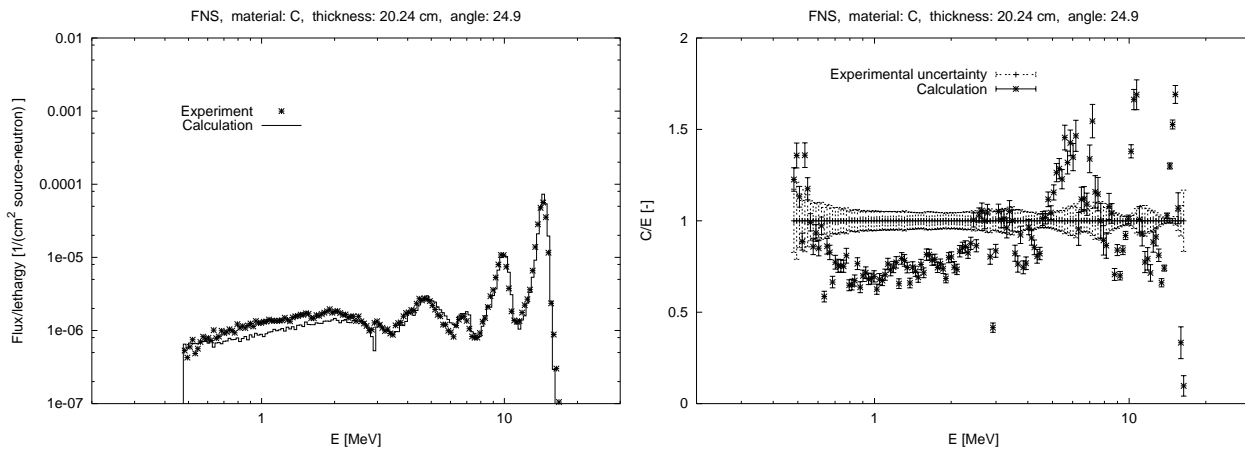


Figure 3.36 Neutron spectrum for the FNS, C, d=20cm benchmark at 24.9° angle.

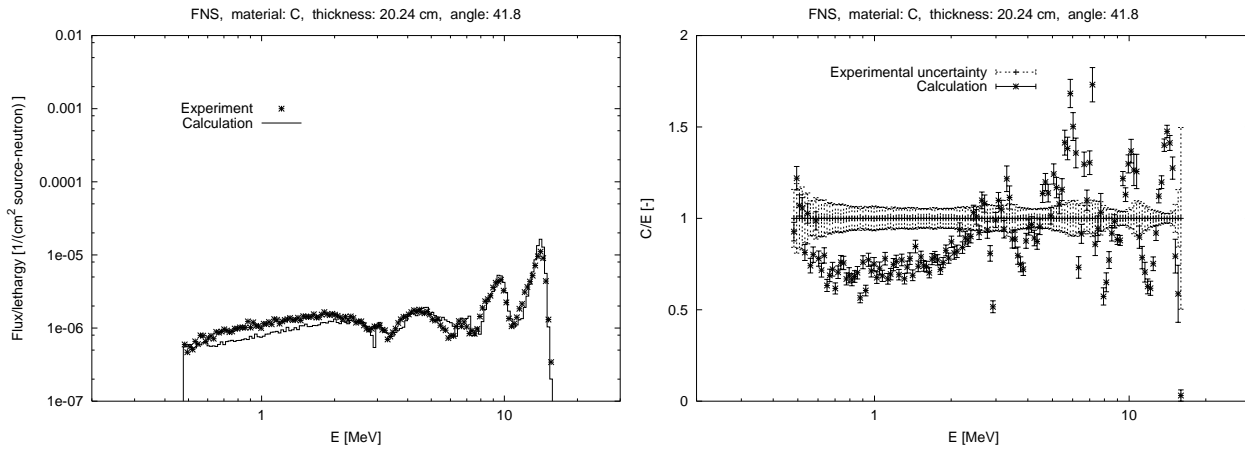


Figure 3.37 Neutron spectrum for the FNS, C, d=20cm benchmark at 42.8° angle.

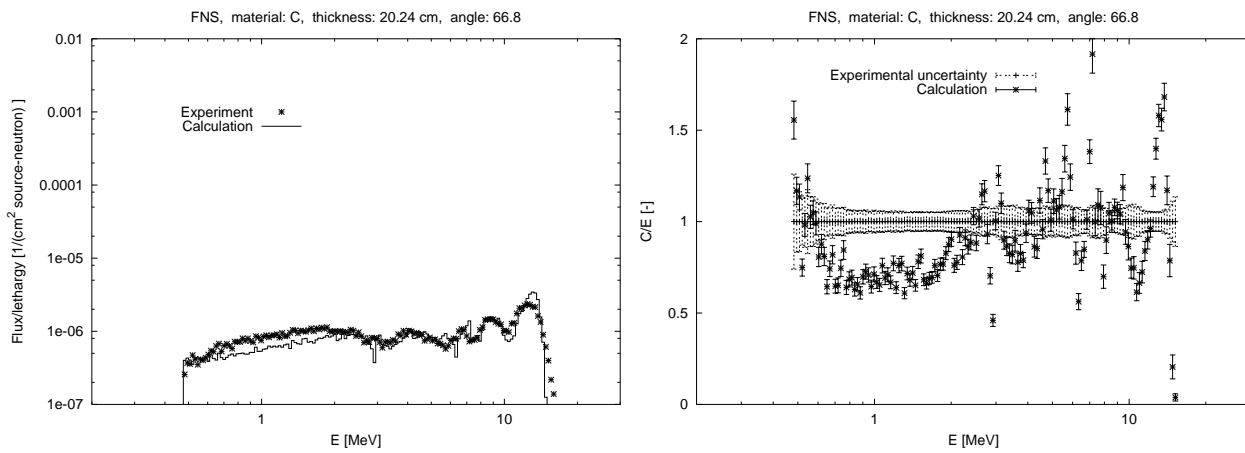


Figure 3.38 Neutron spectrum for the FNS, C, d=20cm benchmark at 66.8° angle.

energy range	0°	12.2°	24.9°	42.8°	66.8°
0.1– 1.0	0.72 ± 0.01	0.82 ± 0.01	0.76 ± 0.01	0.72 ± 0.01	0.75 ± 0.01
1.0– 5.0	0.77 ± 0.01	0.81 ± 0.01	0.81 ± 0.01	0.84 ± 0.01	0.83 ± 0.01
5.0– 10.0	0.90 ± 0.01	1.01 ± 0.01	0.89 ± 0.01	1.01 ± 0.01	1.04 ± 0.01
10.0– 20.0	0.98 ± 0.01	1.07 ± 0.01	1.20 ± 0.01	1.24 ± 0.01	1.07 ± 0.01

Table 3.15 C/E values for the neutron spectrum of the FNS C 20cm benchmark.

3.2.6 FNS, C, 40 cm

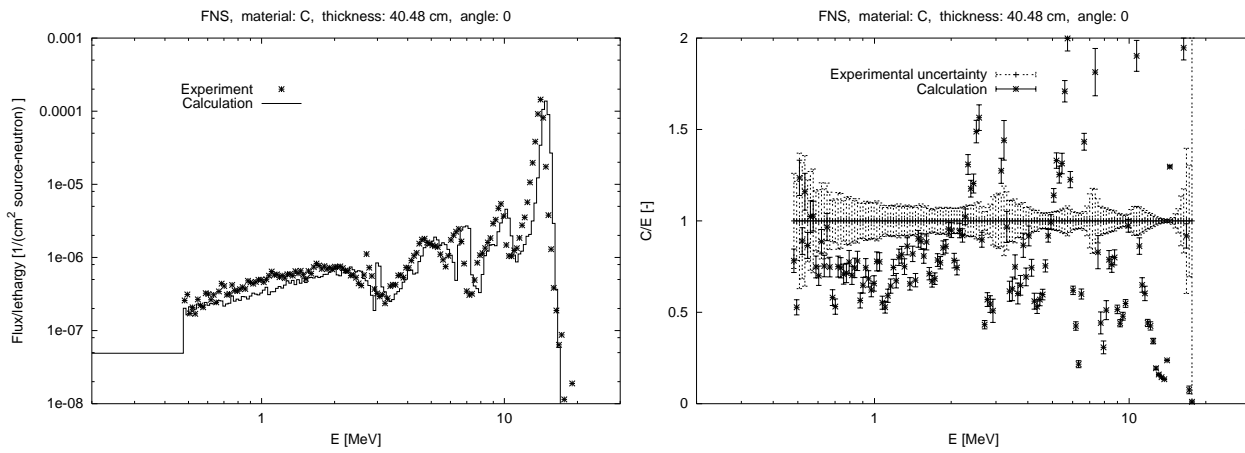


Figure 3.39 Neutron spectrum for the FNS, C, d=40cm benchmark at 0° angle.

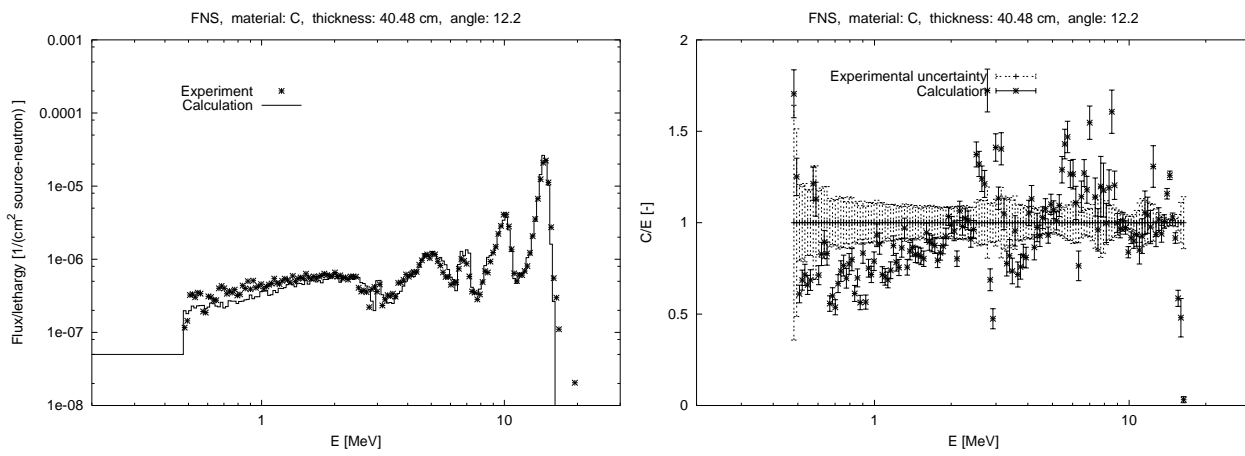


Figure 3.40 Neutron spectrum for the FNS, C, d=40cm benchmark at 12.2° angle.

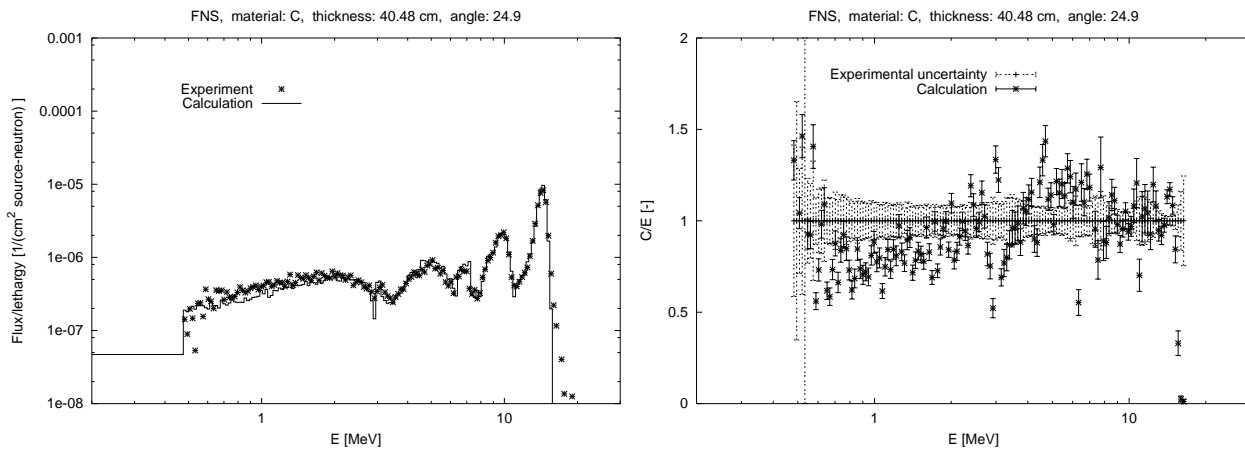


Figure 3.41 Neutron spectrum for the FNS, C, d=40cm benchmark at 24.9° angle.

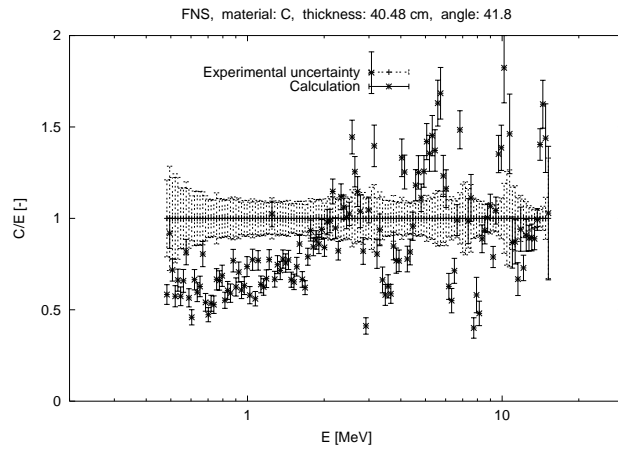
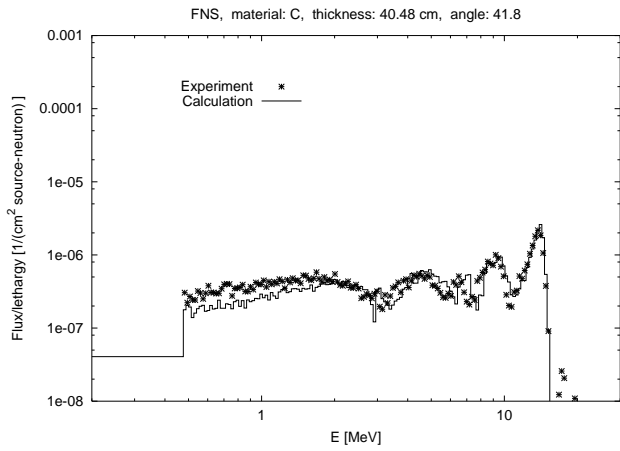


Figure 3.42 Neutron spectrum for the FNS, C, d=40cm benchmark at 42.8° angle.

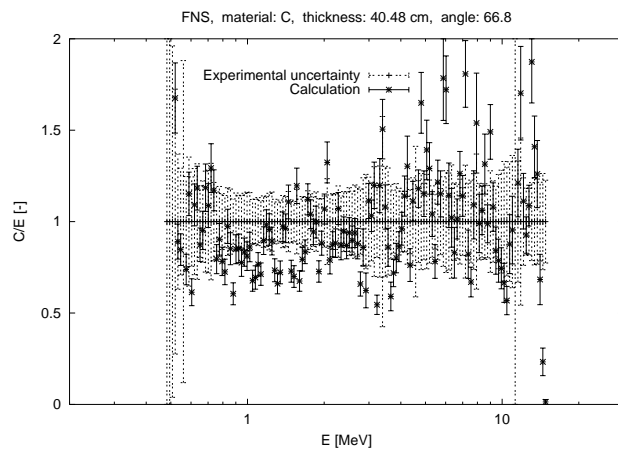
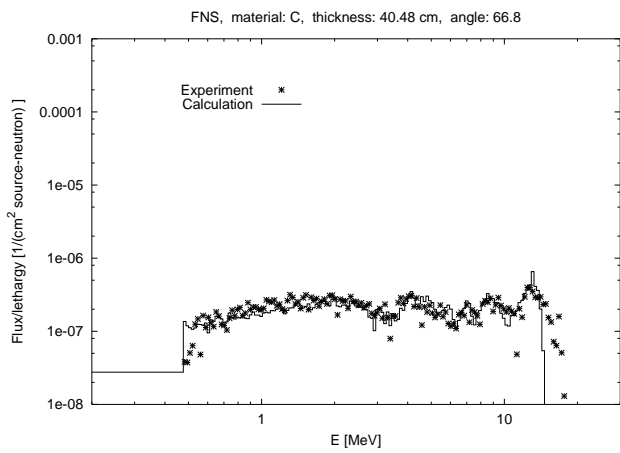


Figure 3.43 Neutron spectrum for the FNS, C, d=40cm benchmark at 66.8° angle.

energy range	0°	12.2°	24.9°	42.8°	66.8°
0.1– 1.0	0.71 ± 0.01	0.70 ± 0.01	0.80 ± 0.01	0.60 ± 0.02	0.94 ± 0.02
1.0– 5.0	0.78 ± 0.01	0.90 ± 0.01	0.91 ± 0.01	0.86 ± 0.01	0.91 ± 0.01
5.0– 10.0	0.85 ± 0.01	1.02 ± 0.01	1.01 ± 0.01	1.05 ± 0.02	1.12 ± 0.02
10.0– 20.0	1.03 ± 0.01	1.08 ± 0.01	1.09 ± 0.01	1.14 ± 0.02	0.94 ± 0.04

Table 3.16 C/E values for the neutron spectrum of the FNS C 40cm benchmark.

3.2.7 FNS, N, 20 cm

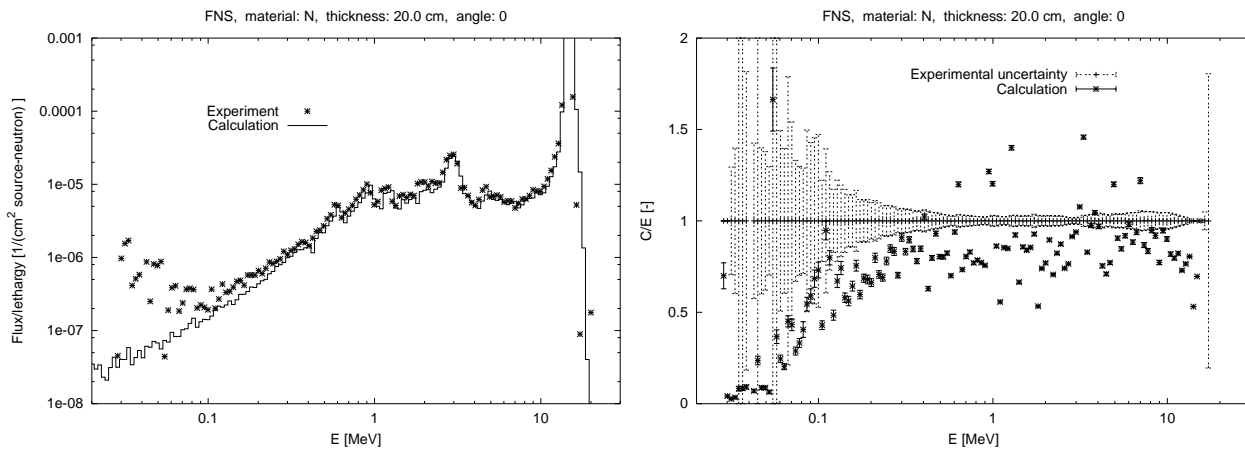


Figure 3.44 Neutron spectrum for the FNS, N, d=20cm benchmark at 0° angle.

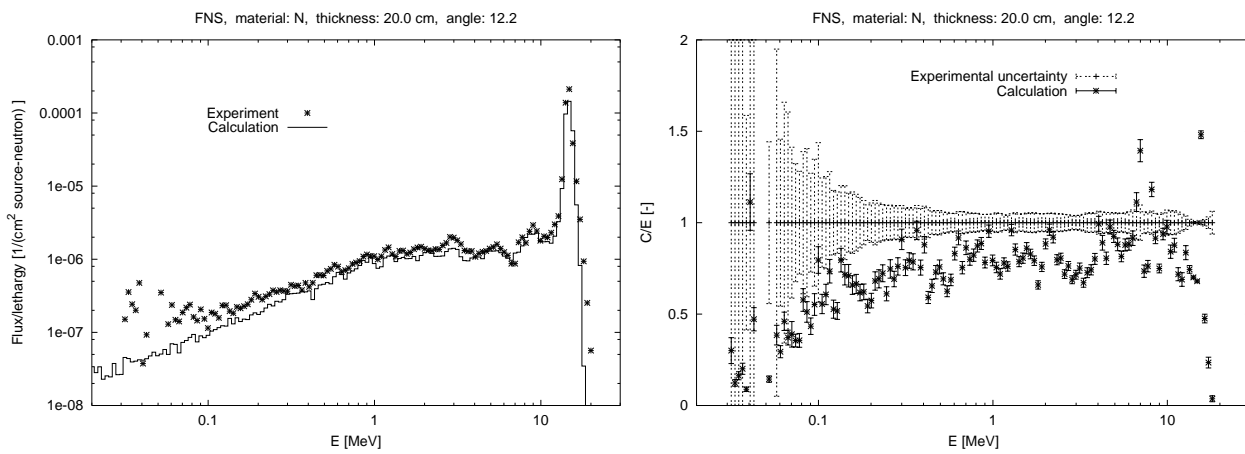


Figure 3.45 Neutron spectrum for the FNS, N, d=20cm benchmark at 12.2° angle.

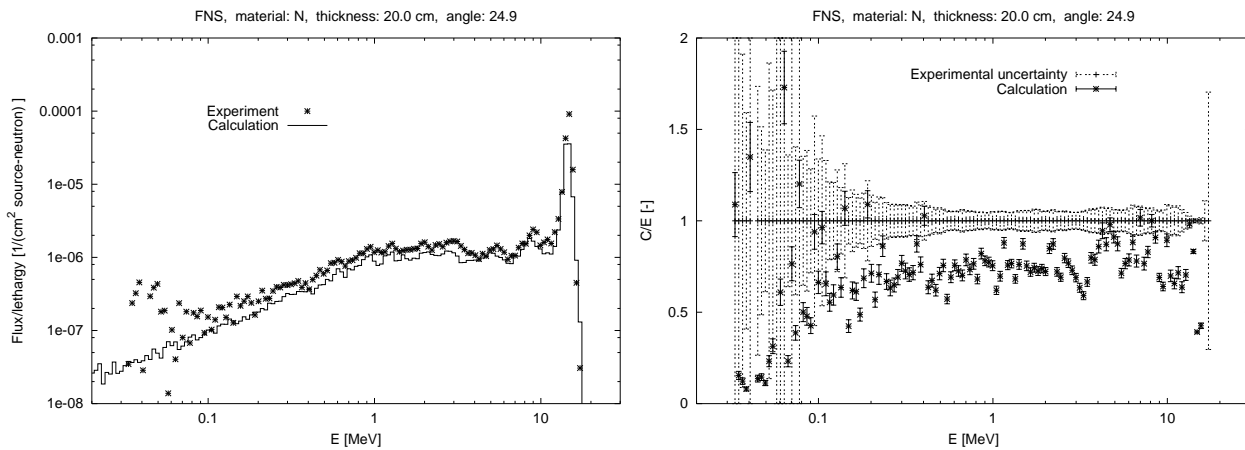


Figure 3.46 Neutron spectrum for the FNS, N, d=20cm benchmark at 24.9° angle.

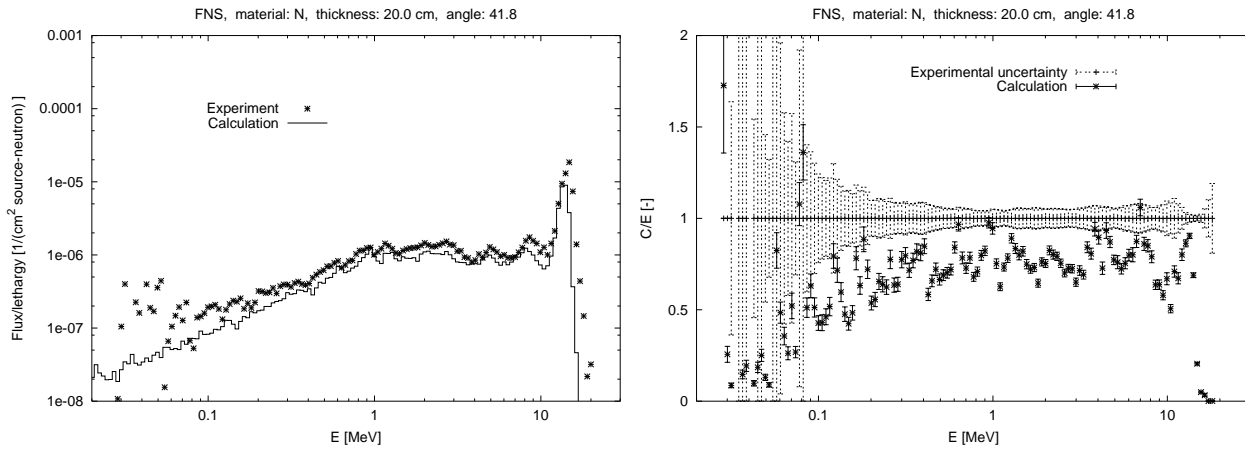


Figure 3.47 Neutron spectrum for the FNS, N, d=20cm benchmark at 42.8° angle.

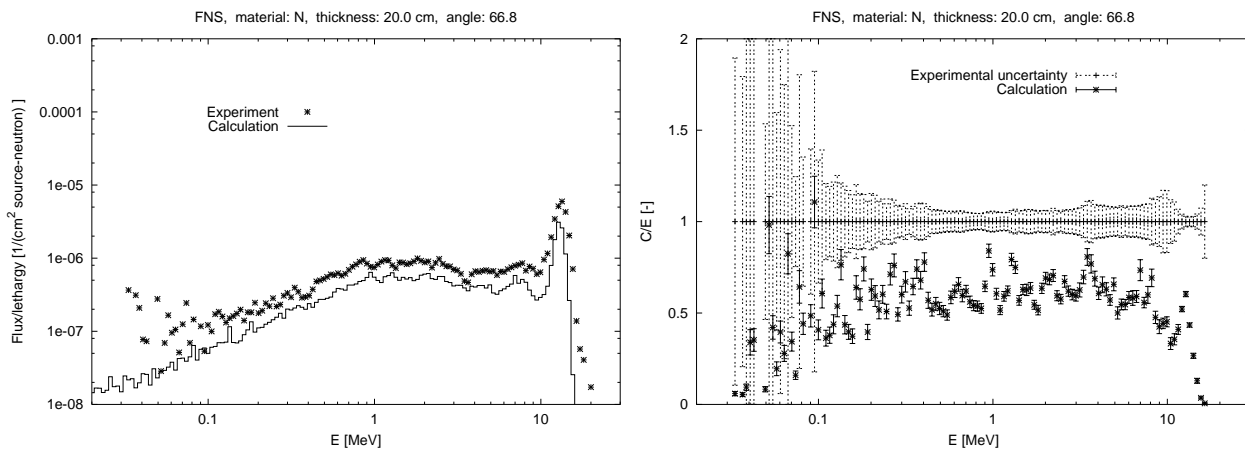


Figure 3.48 Neutron spectrum for the FNS, N, d=20cm benchmark at 66.8° angle.

energy range	0°	12.2°	24.9°	42.8°	66.8°
0.1– 1.0	0.80 ± 0.01	0.73 ± 0.01	0.69 ± 0.01	0.71 ± 0.01	0.56 ± 0.01
1.0– 5.0	0.86 ± 0.01	0.79 ± 0.01	0.75 ± 0.01	0.77 ± 0.01	0.64 ± 0.01
5.0– 10.0	0.92 ± 0.01	0.89 ± 0.01	0.80 ± 0.01	0.77 ± 0.01	0.57 ± 0.02
10.0– 20.0	0.85 ± 0.01	0.76 ± 0.01	0.57 ± 0.01	0.50 ± 0.01	0.41 ± 0.01

Table 3.17 C/E values for the neutron spectrum of the FNS N 20cm benchmark.

3.2.8 FNS, O, 20 cm

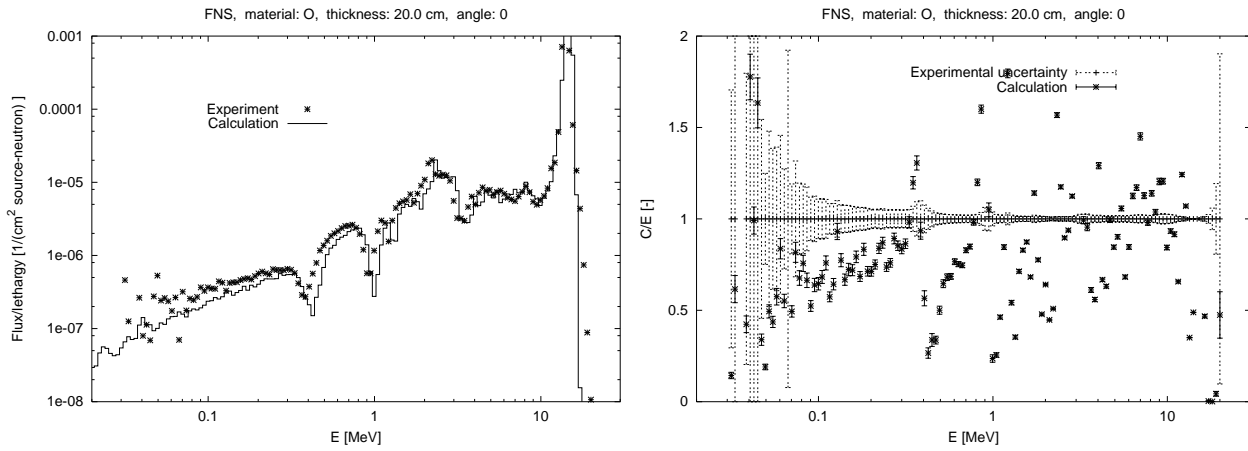


Figure 3.49 Neutron spectrum for the FNS, O, d=20cm benchmark at 0° angle.

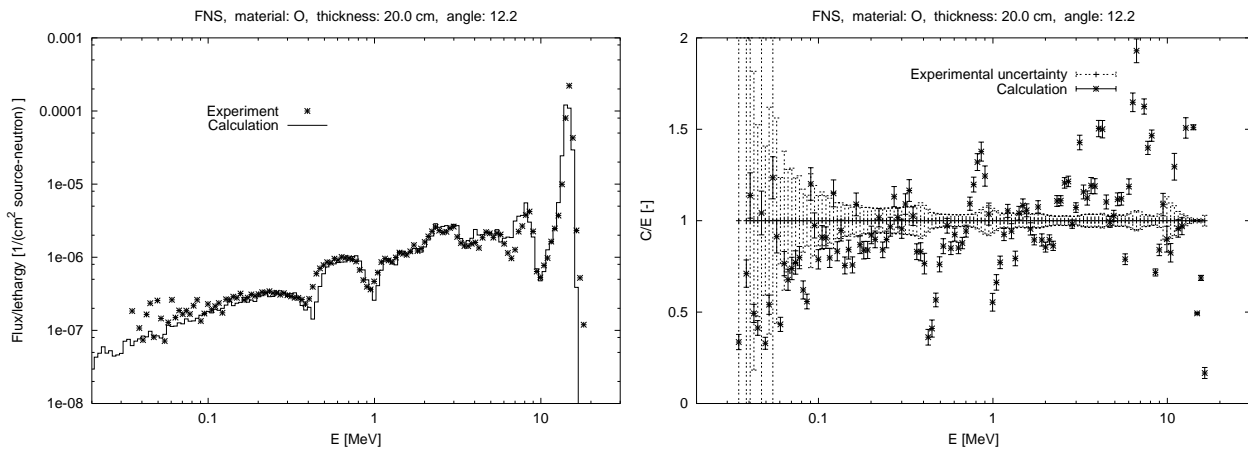


Figure 3.50 Neutron spectrum for the FNS, O, d=20cm benchmark at 12.2° angle.

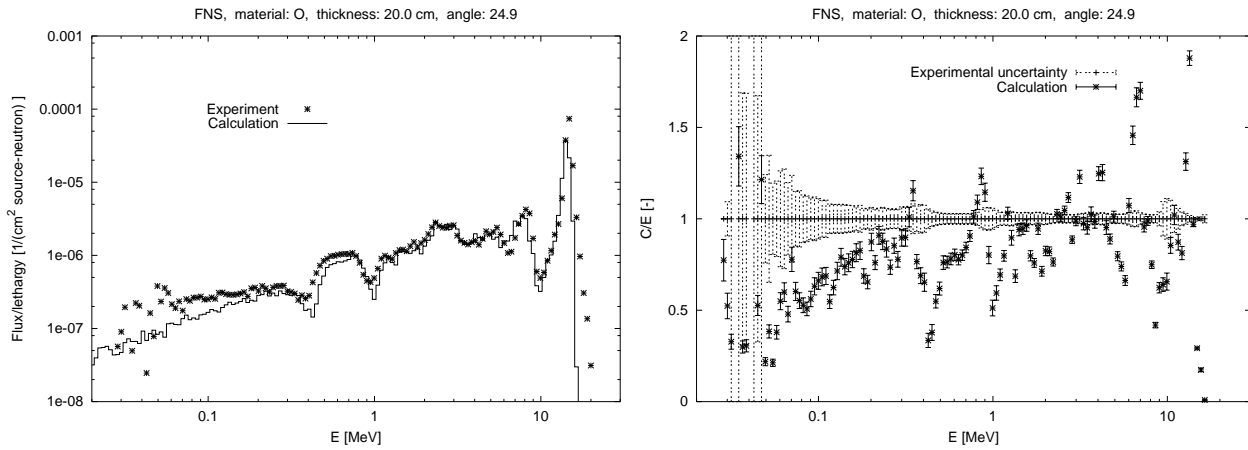


Figure 3.51 Neutron spectrum for the FNS, O, d=20cm benchmark at 24.9° angle.

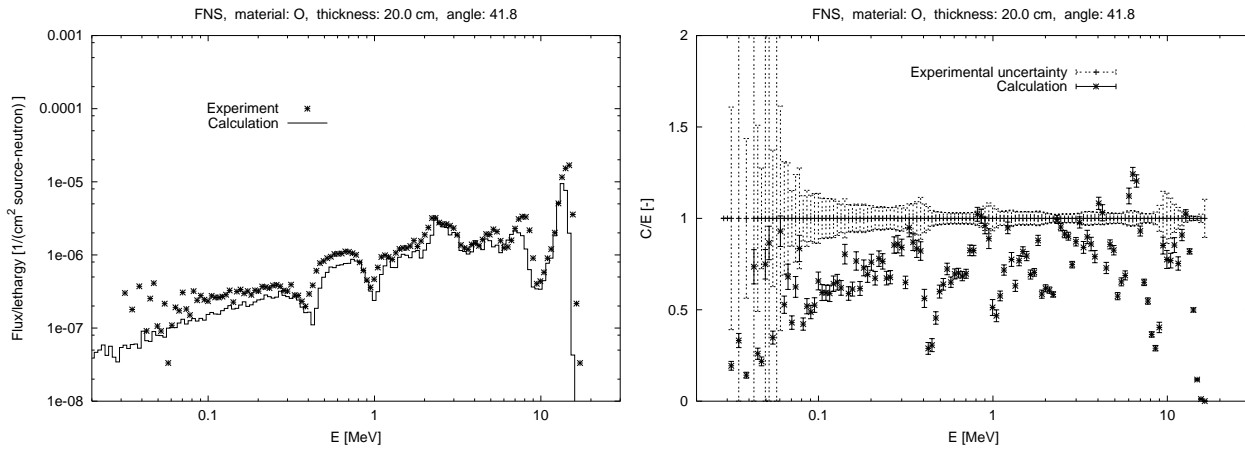


Figure 3.52 Neutron spectrum for the FNS, O, d=20cm benchmark at 42.8° angle.

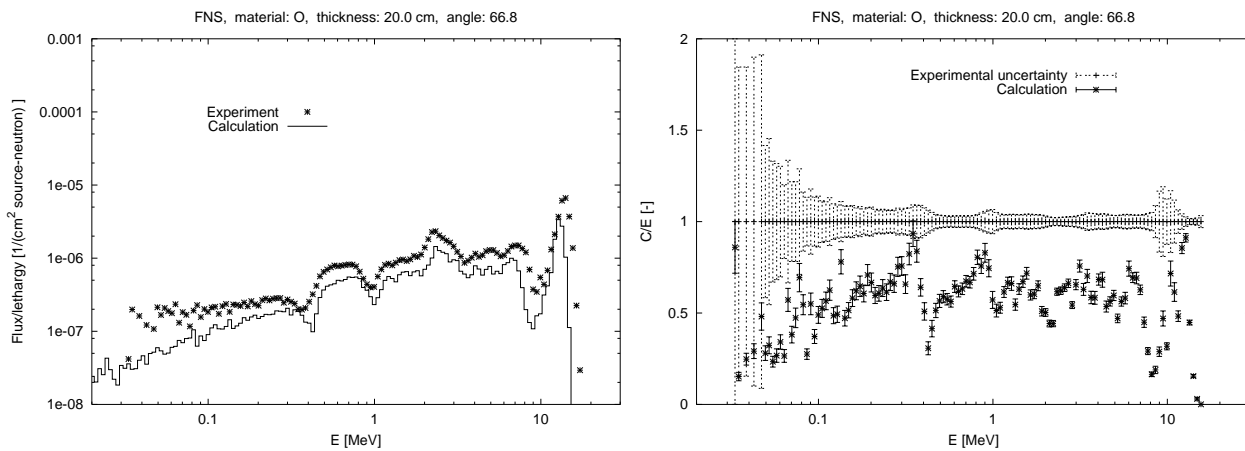


Figure 3.53 Neutron spectrum for the FNS, O, d=20cm benchmark at 66.8° angle.

energy range	0°	12.2°	24.9°	42.8°	66.8°
0.1– 1.0	0.80 ± 0.01	0.91 ± 0.01	0.79 ± 0.01	0.70 ± 0.01	0.63 ± 0.01
1.0– 5.0	0.84 ± 0.01	1.03 ± 0.01	0.92 ± 0.01	0.78 ± 0.01	0.58 ± 0.01
5.0– 10.0	1.06 ± 0.01	1.30 ± 0.01	0.93 ± 0.01	0.72 ± 0.01	0.54 ± 0.02
10.0– 20.0	0.89 ± 0.01	0.81 ± 0.01	0.55 ± 0.01	0.50 ± 0.01	0.40 ± 0.01

Table 3.18 C/E values for the neutron spectrum of the FNS O 20cm benchmark.

3.2.9 FNS, Fe, 5 cm

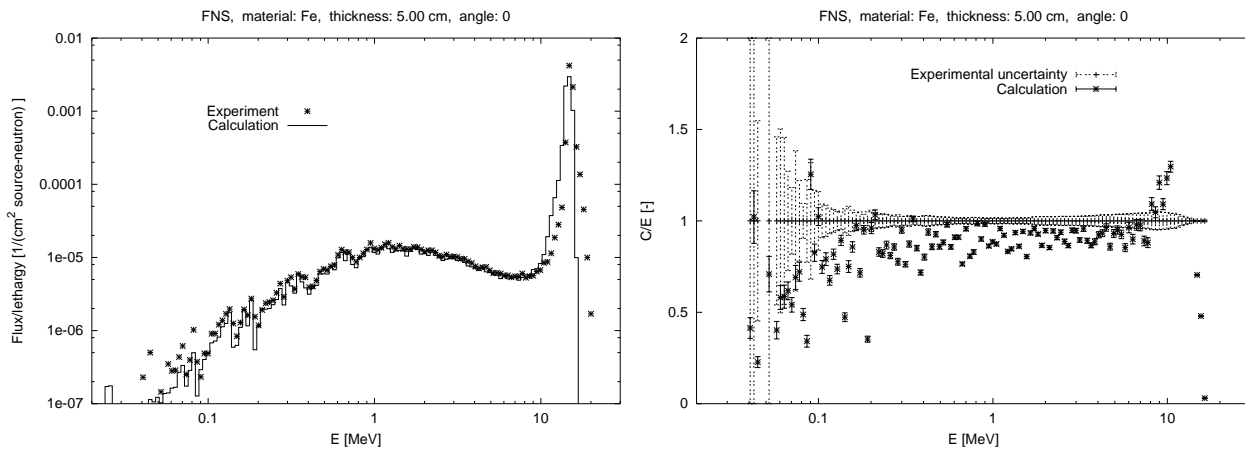


Figure 3.54 Neutron spectrum for the FNS, Fe, d=5cm benchmark at 0° angle.

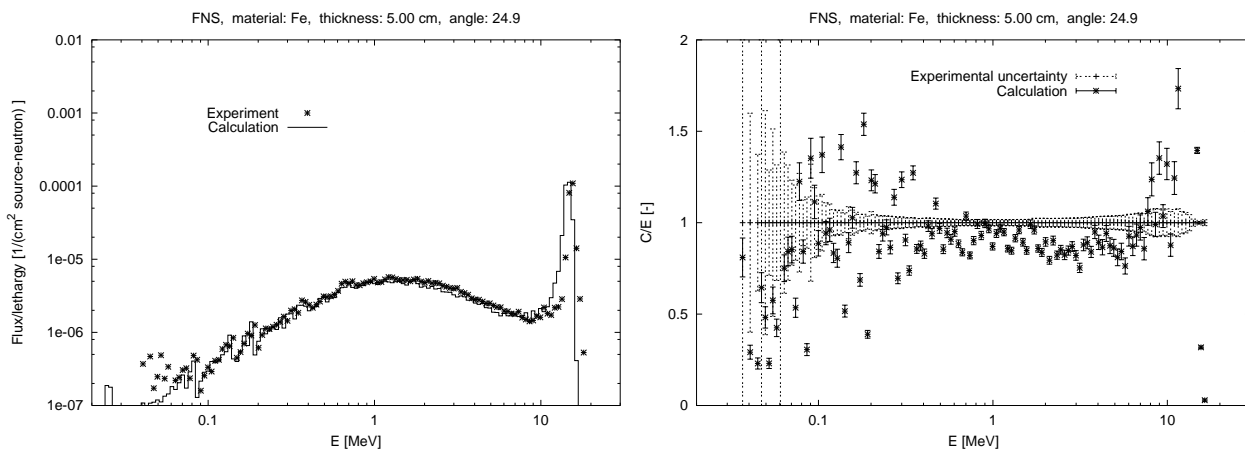


Figure 3.55 Neutron spectrum for the FNS, Fe, d=5cm benchmark at 24.9° angle.

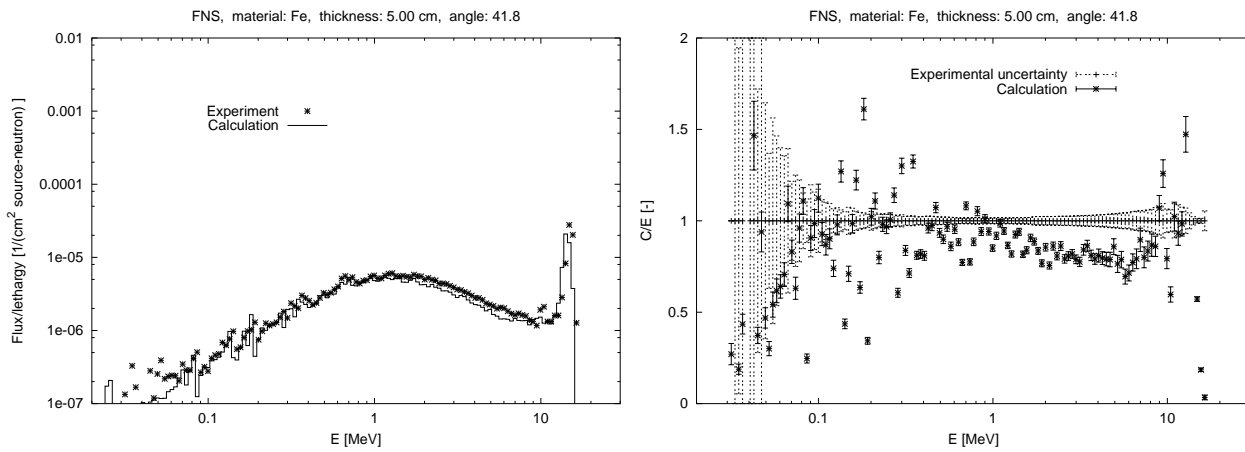


Figure 3.56 Neutron spectrum for the FNS, Fe, d=5cm benchmark at 42.8° angle.

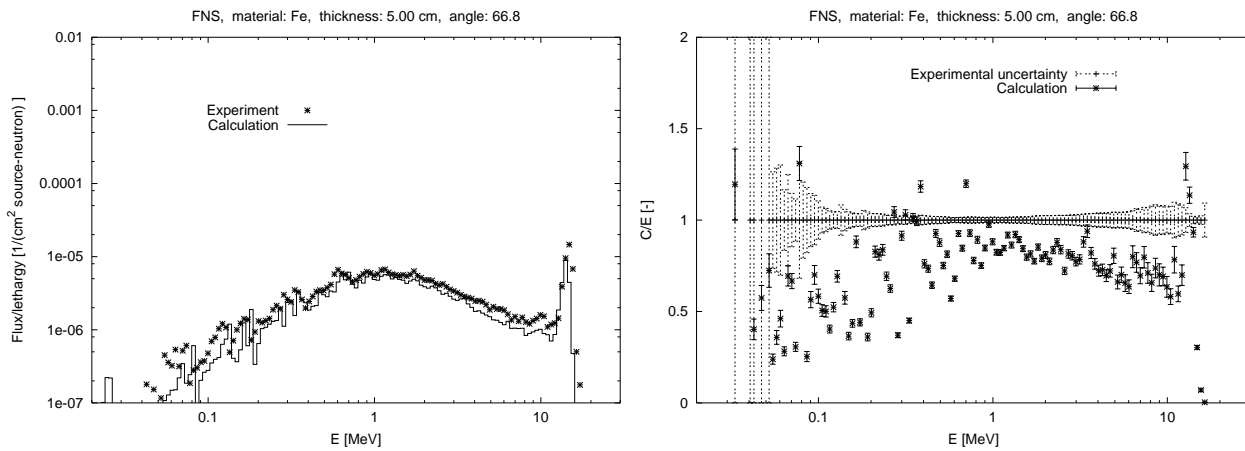


Figure 3.57 Neutron spectrum for the FNS, Fe, d=5cm benchmark at 66.8° angle.

energy range	0°	12.2°	24.9°	42.8°	66.8°
0.1– 1.0	0.83 ± 0.01		0.89 ± 0.01	0.88 ± 0.01	0.78 ± 0.01
1.0– 5.0	0.92 ± 0.01		0.90 ± 0.01	0.87 ± 0.01	0.85 ± 0.01
5.0– 10.0	0.98 ± 0.01		0.98 ± 0.02	0.85 ± 0.02	0.72 ± 0.02
10.0– 20.0	0.92 ± 0.01		1.27 ± 0.01	0.84 ± 0.01	0.58 ± 0.02

Table 3.19 C/E values for the neutron spectrum of the FNS Fe 5cm benchmark.

3.2.10 FNS, Fe, 20 cm

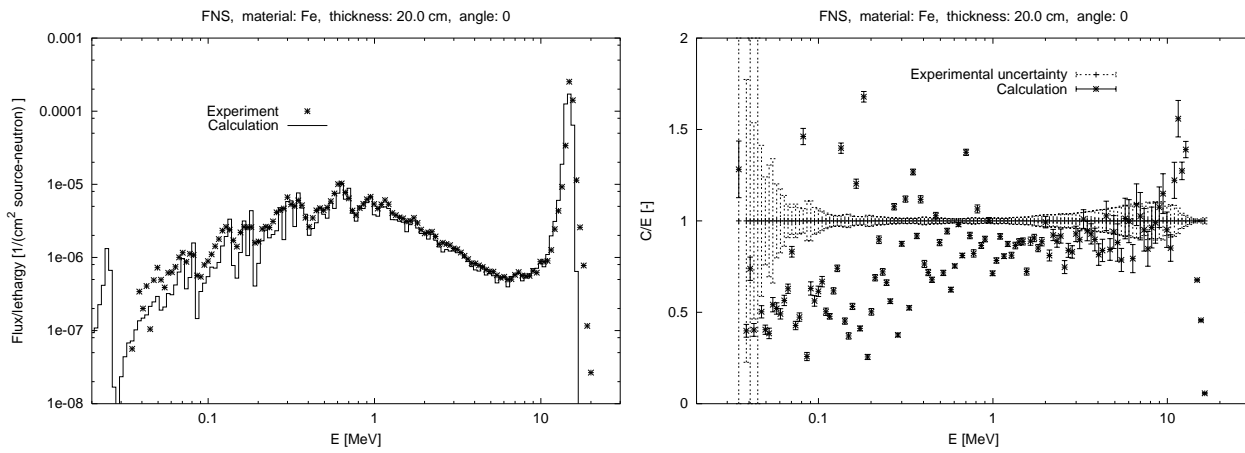


Figure 3.58 Neutron spectrum for the FNS, Fe, d=20cm benchmark at 0° angle.

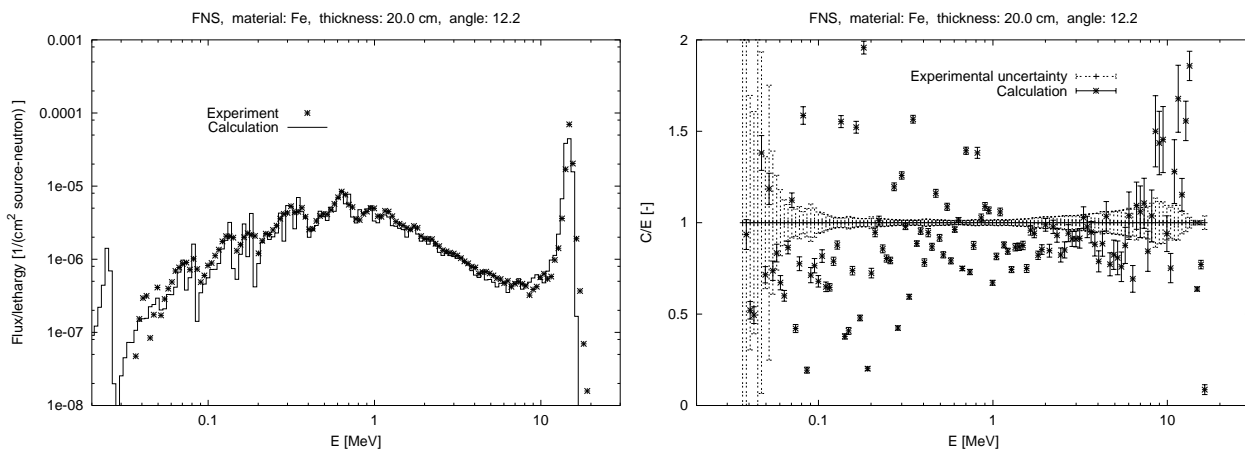


Figure 3.59 Neutron spectrum for the FNS, Fe, d=20cm benchmark at 12.2° angle.

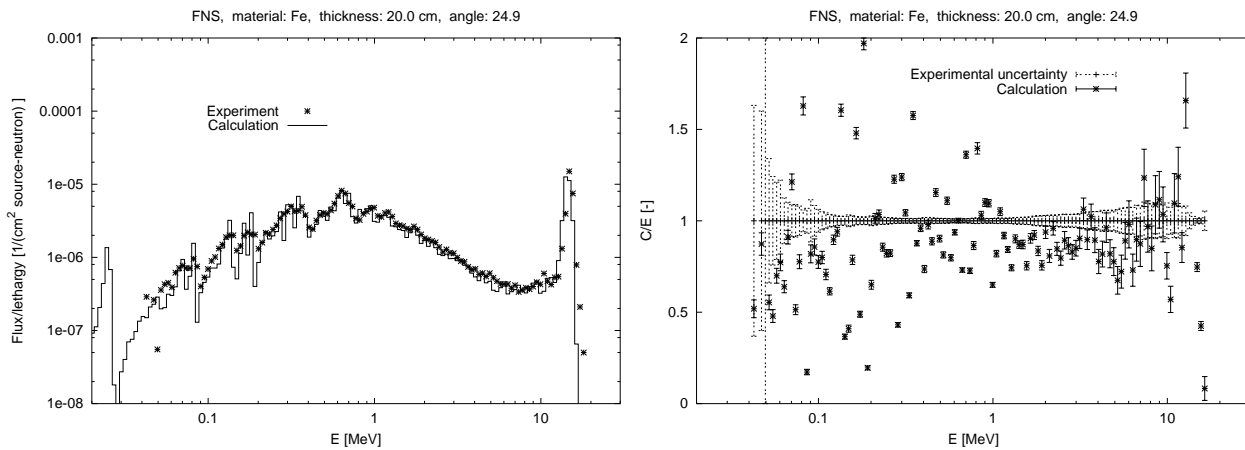


Figure 3.60 Neutron spectrum for the FNS, Fe, d=20cm benchmark at 24.9° angle.

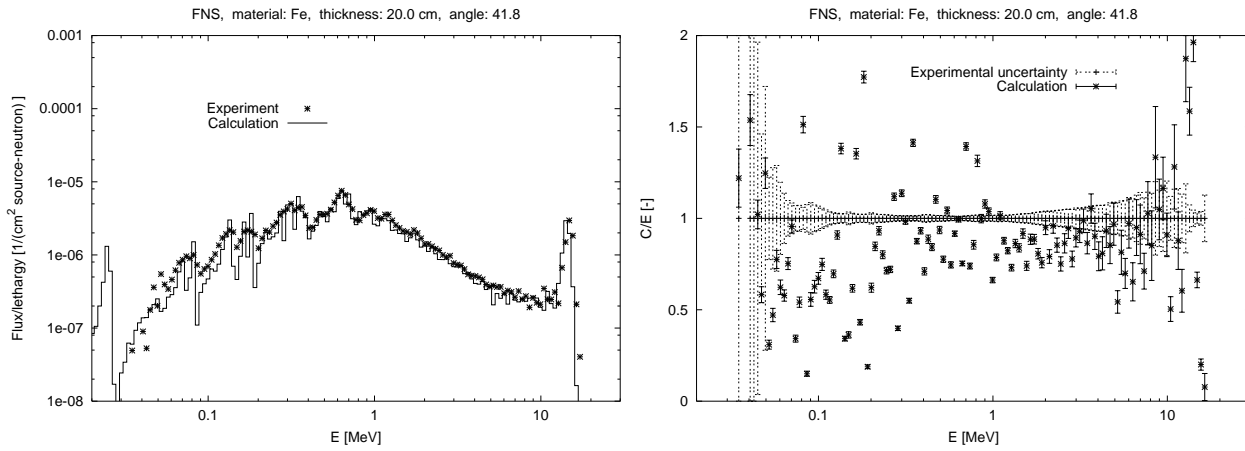


Figure 3.61 Neutron spectrum for the FNS, Fe, d=20cm benchmark at 42.8° angle.

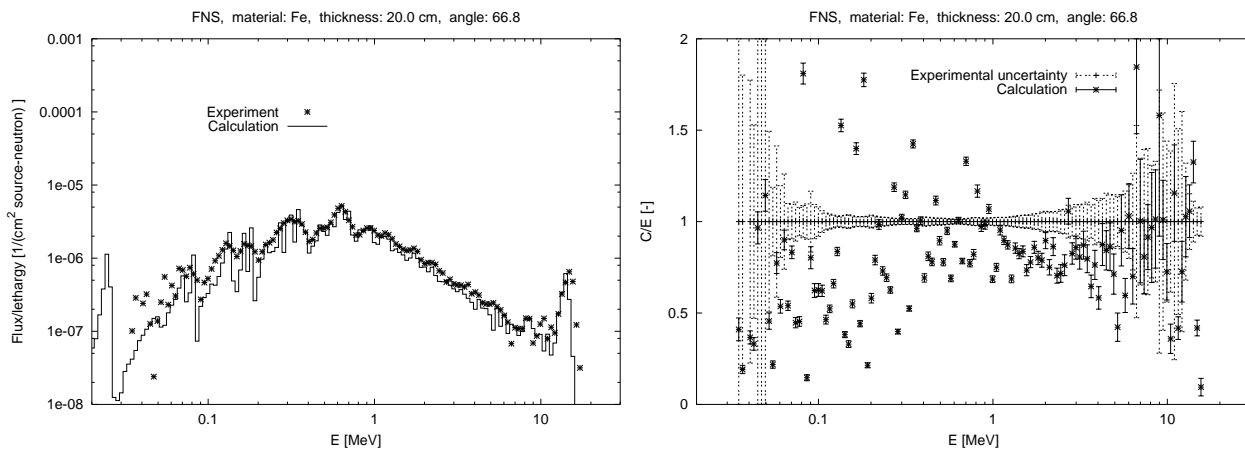


Figure 3.62 Neutron spectrum for the FNS, Fe, d=20cm benchmark at 66.8° angle.

energy range	0°	12.2°	24.9°	42.8°	66.8°
0.1– 1.0	0.84 ± 0.01	0.93 ± 0.01	0.93 ± 0.01	0.89 ± 0.01	0.87 ± 0.01
1.0– 5.0	0.91 ± 0.01	0.93 ± 0.01	0.91 ± 0.01	0.90 ± 0.01	0.86 ± 0.01
5.0– 10.0	0.94 ± 0.03	1.01 ± 0.03	0.93 ± 0.04	0.91 ± 0.04	0.92 ± 0.07
10.0– 20.0	0.85 ± 0.01	0.95 ± 0.01	1.06 ± 0.02	0.91 ± 0.03	0.67 ± 0.05

Table 3.20 C/E values for the neutron spectrum of the FNS Fe 20cm benchmark.

3.2.11 FNS, Fe, 40 cm

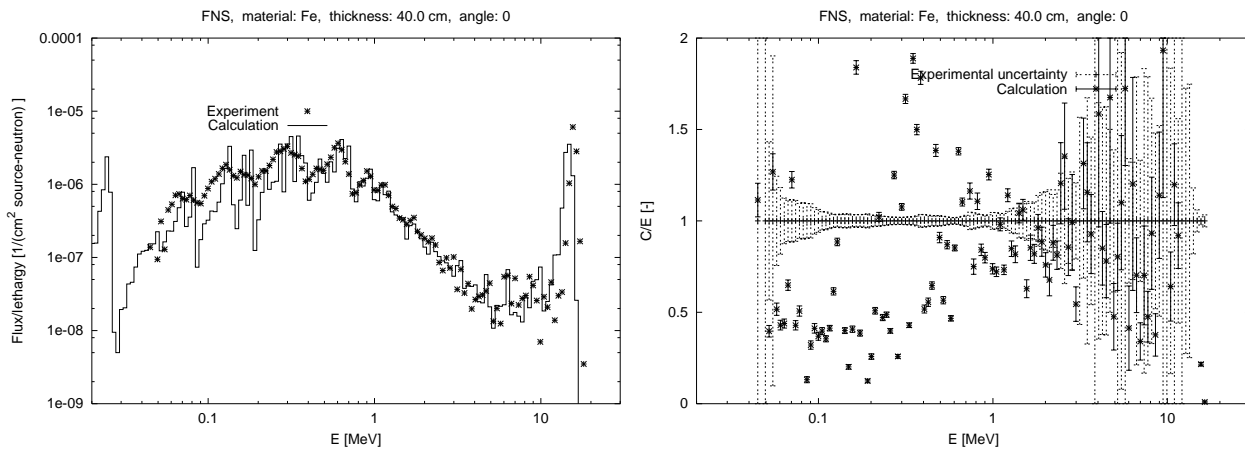


Figure 3.63 Neutron spectrum for the FNS, Fe, d=40cm benchmark at 0° angle.

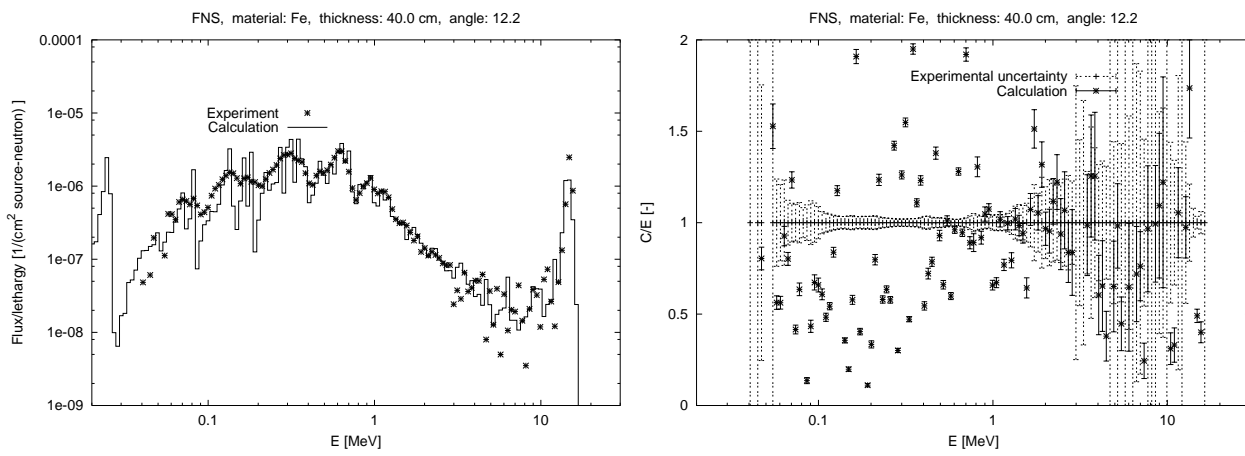


Figure 3.64 Neutron spectrum for the FNS, Fe, d=40cm benchmark at 12.2° angle.

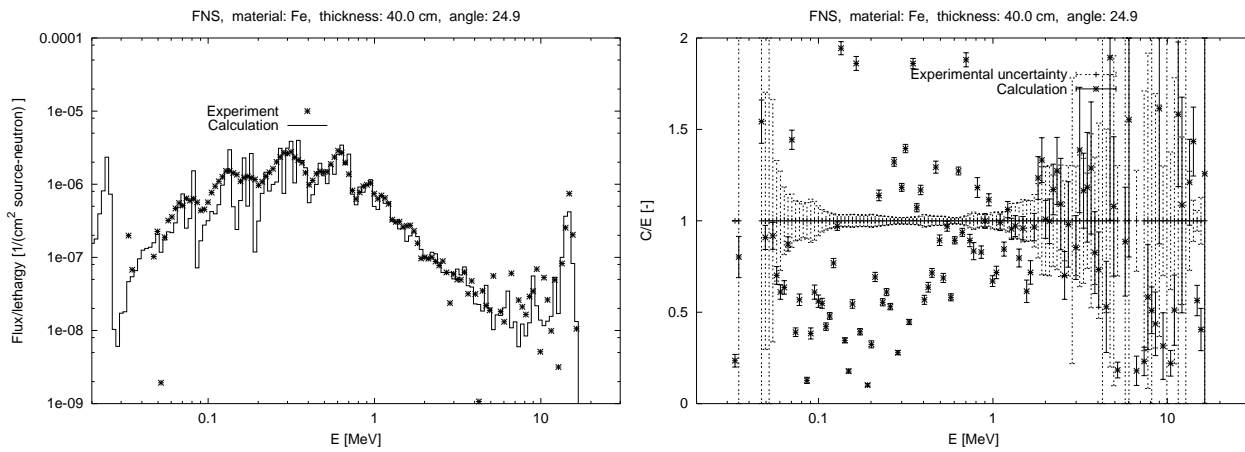


Figure 3.65 Neutron spectrum for the FNS, Fe, d=40cm benchmark at 24.9° angle.

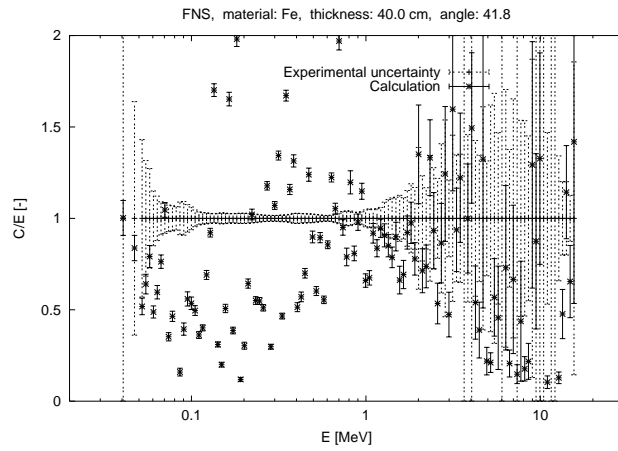
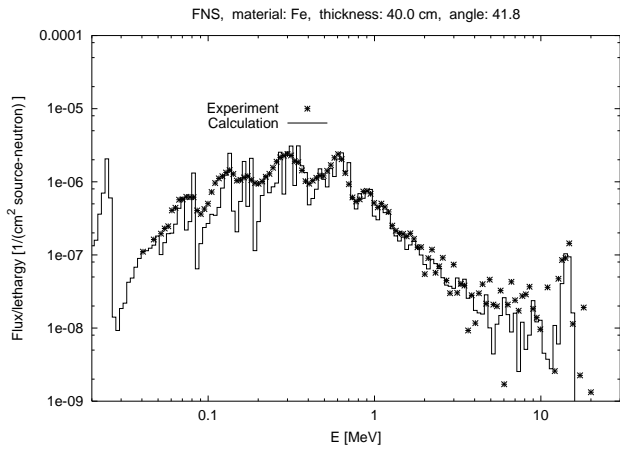


Figure 3.66 Neutron spectrum for the FNS, Fe, d=40cm benchmark at 42.8° angle.

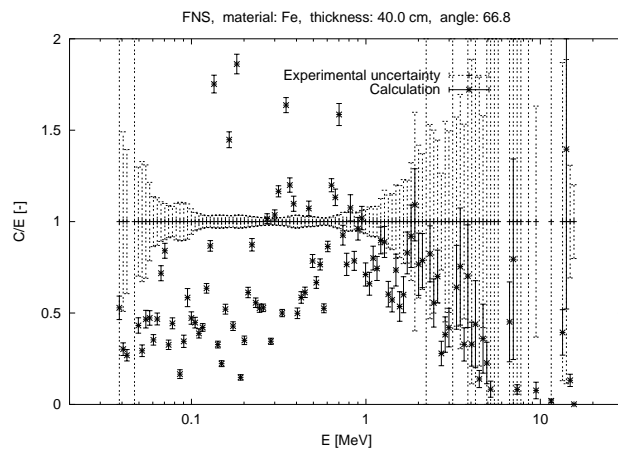
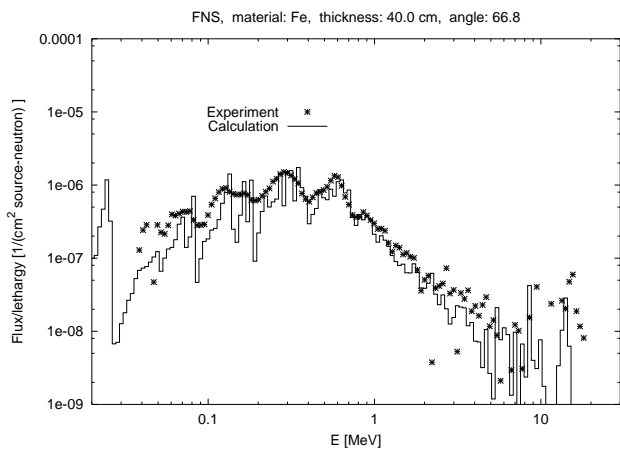


Figure 3.67 Neutron spectrum for the FNS, Fe, d=40cm benchmark at 66.8° angle.

energy range	0°	12.2°	24.9°	42.8°	66.8°
0.1– 1.0	0.91 ± 0.01	0.98 ± 0.01	0.92 ± 0.01	0.87 ± 0.01	0.81 ± 0.01
1.0– 5.0	0.97 ± 0.01	1.03 ± 0.01	1.02 ± 0.02	0.92 ± 0.02	0.80 ± 0.03
5.0– 10.0	0.85 ± 0.13	1.06 ± 0.13	0.91 ± 0.15	0.54 ± 0.16	
10.0– 20.0	0.81 ± 0.02	0.77 ± 0.05	0.79 ± 0.08	0.68 ± 0.14	0.33 ± 0.33

Table 3.21 C/E values for the neutron spectrum of the FNS Fe 40cm benchmark.

3.2.12 FNS, Fe, 60 cm

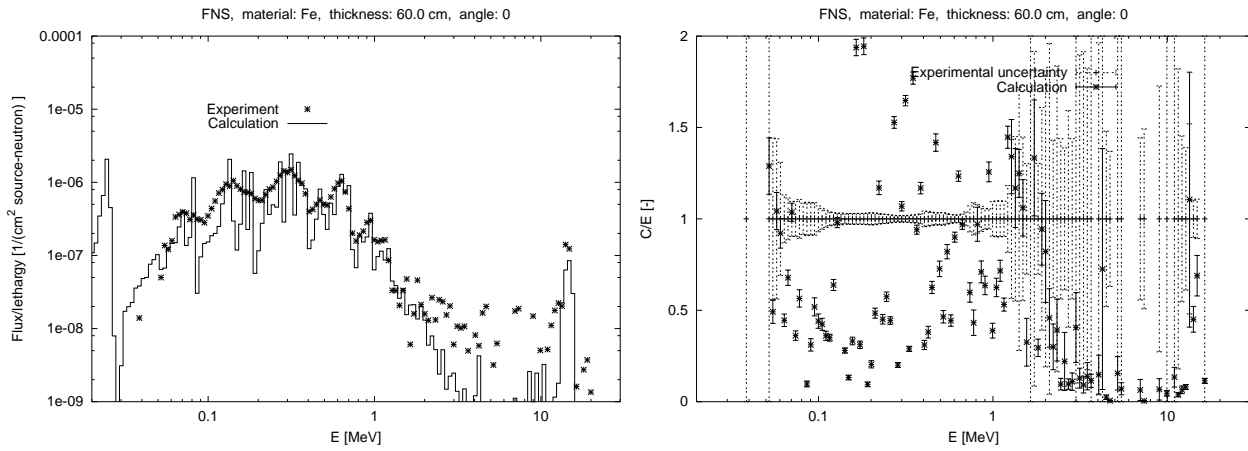


Figure 3.68 Neutron spectrum for the FNS, Fe, d=60cm benchmark at 0° angle.

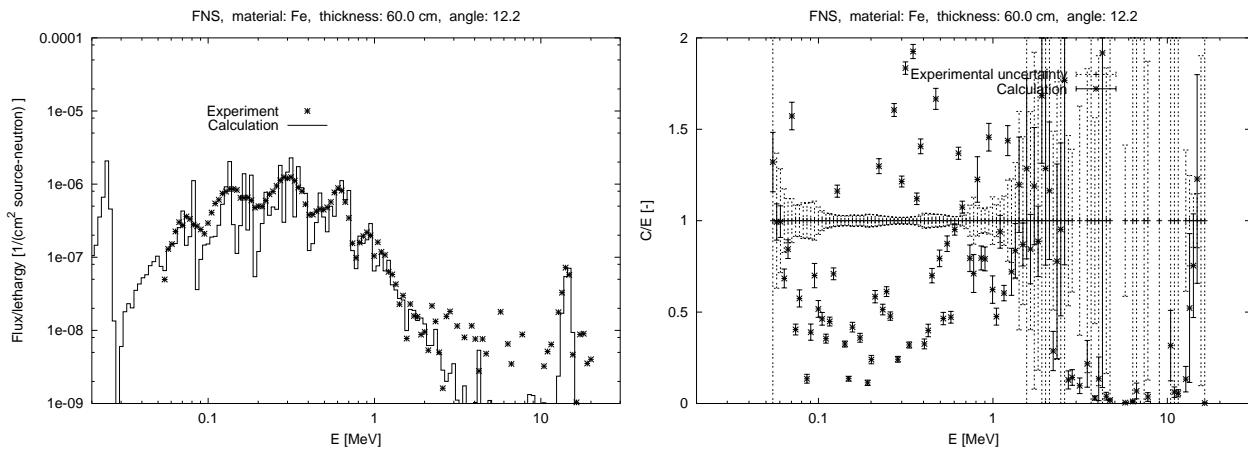


Figure 3.69 Neutron spectrum for the FNS, Fe, d=60cm benchmark at 12.2° angle.

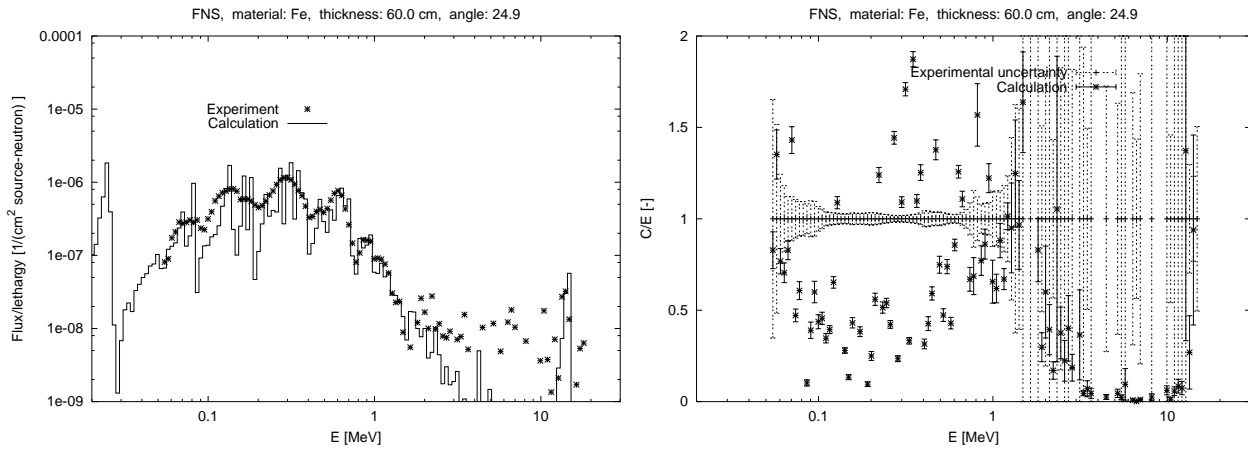


Figure 3.70 Neutron spectrum for the FNS, Fe, d=60cm benchmark at 24.9° angle.

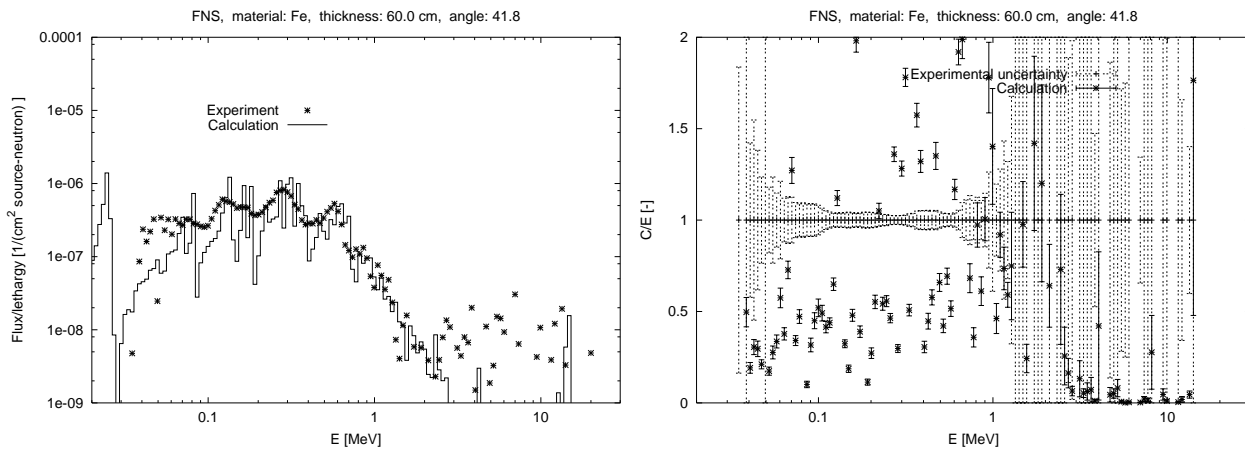


Figure 3.71 Neutron spectrum for the FNS, Fe, d=60cm benchmark at 42.8° angle.

energy range	0°	12.2°	24.9°	42.8°
0.1– 1.0	0.86 ± 0.01	0.95 ± 0.01	0.88 ± 0.01	0.91 ± 0.01
1.0– 5.0	0.73 ± 0.03	0.84 ± 0.04	0.98 ± 0.05	0.96 ± 0.07
5.0– 10.0	0.36 ± 0.31		0.11 ± 0.37	0.03 ± 0.22
10.0– 20.0	0.62 ± 0.11	0.73 ± 0.26	0.94 ± 0.44	3.50 ± 0.57

Table 3.22 C/E values for the neutron spectrum of the FNS Fe 60cm benchmark.

3.2.13 FNS, Pb, 5 cm

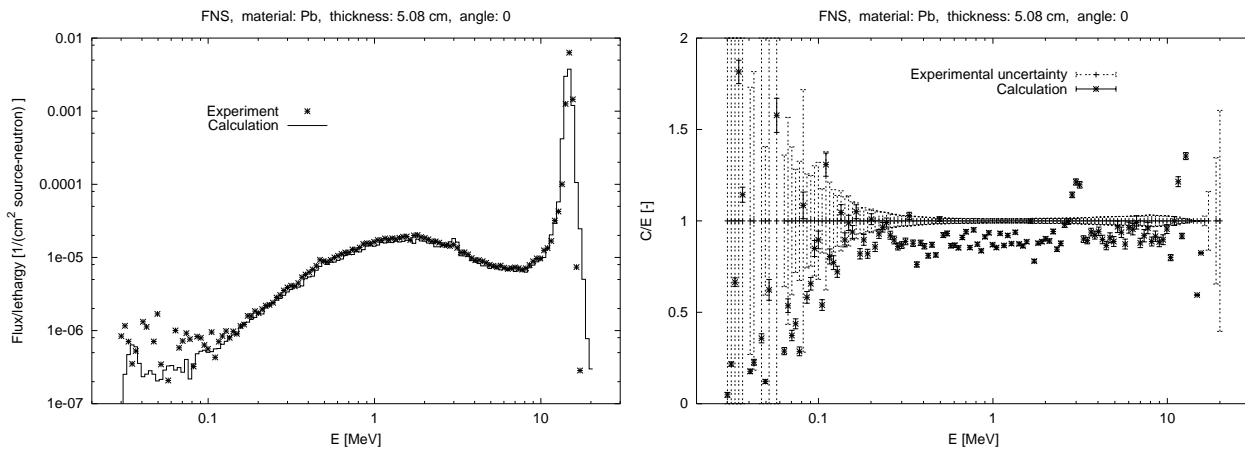


Figure 3.72 Neutron spectrum for the FNS, Pb, d=5cm benchmark at 0° angle.

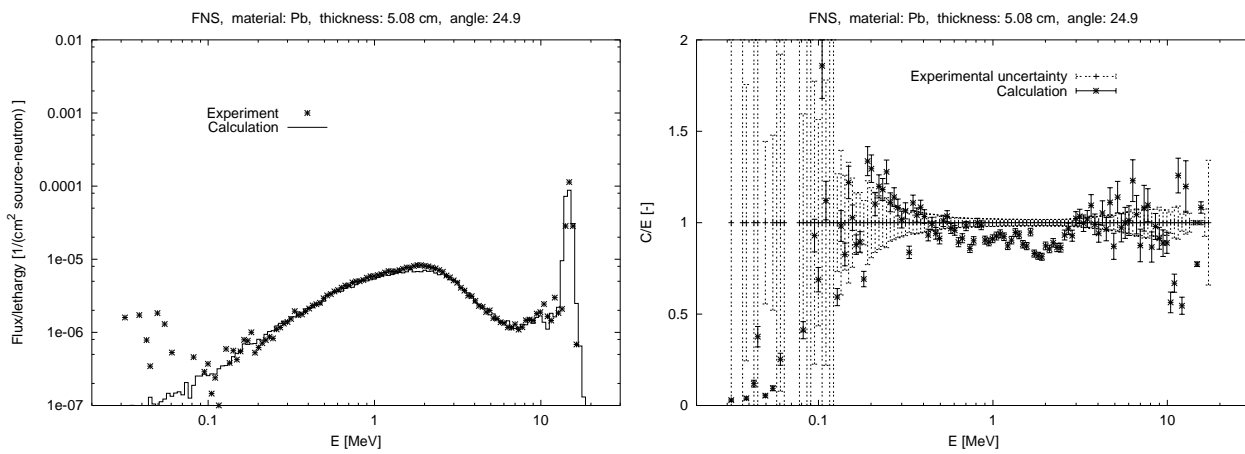


Figure 3.73 Neutron spectrum for the FNS, Pb, d=5cm benchmark at 24.9° angle.

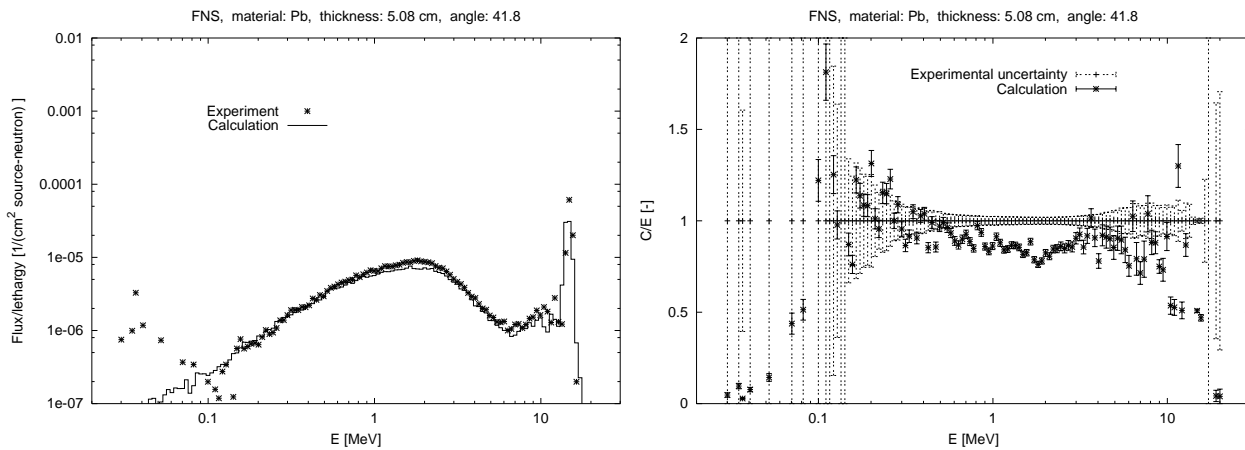


Figure 3.74 Neutron spectrum for the FNS, Pb, d=5cm benchmark at 42.8° angle.

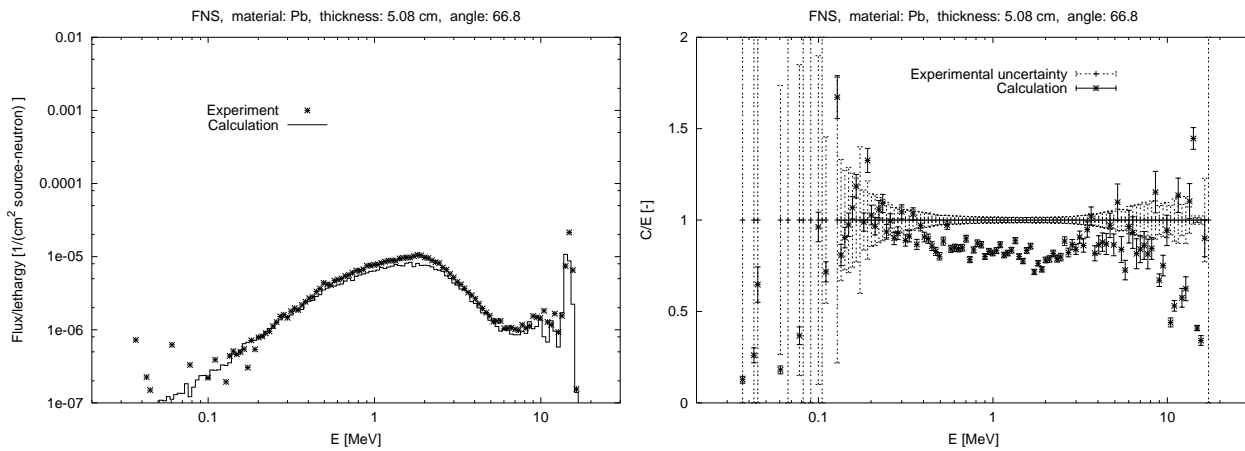


Figure 3.75 Neutron spectrum for the FNS, Pb, d=5cm benchmark at 66.8° angle.

energy range	0°	12.2°	24.9°	42.8°	66.8°
0.1– 1.0	0.84 ± 0.01		0.92 ± 0.01	0.89 ± 0.01	0.84 ± 0.01
1.0– 5.0	0.94 ± 0.01		0.93 ± 0.01	0.87 ± 0.01	0.84 ± 0.01
5.0– 10.0	0.91 ± 0.01		0.99 ± 0.02	0.84 ± 0.02	0.87 ± 0.02
10.0– 20.0	0.93 ± 0.01		1.16 ± 0.01	0.81 ± 0.01	0.67 ± 0.02

Table 3.23 C/E values for the neutron spectrum of the FNS Pb 5cm benchmark.

3.2.14 FNS, Pb, 20 cm

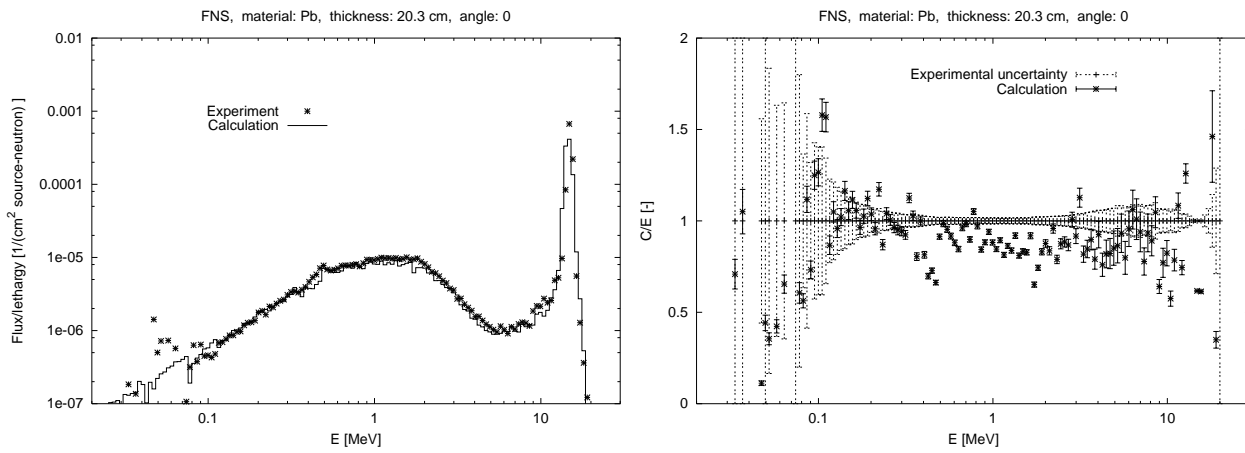


Figure 3.76 Neutron spectrum for the FNS, Pb, d=20cm benchmark at 0° angle.

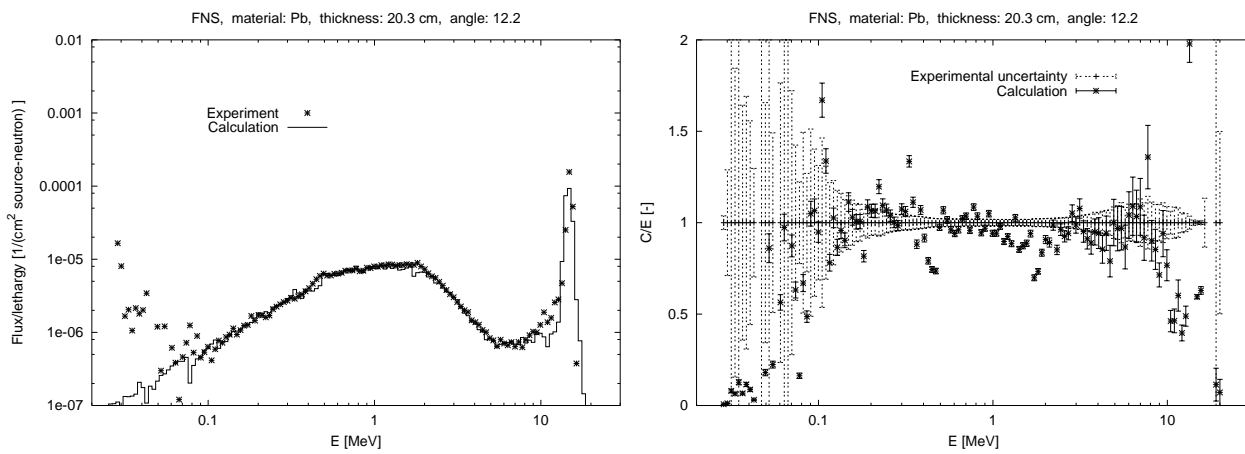


Figure 3.77 Neutron spectrum for the FNS, Pb, d=20cm benchmark at 12.2° angle.

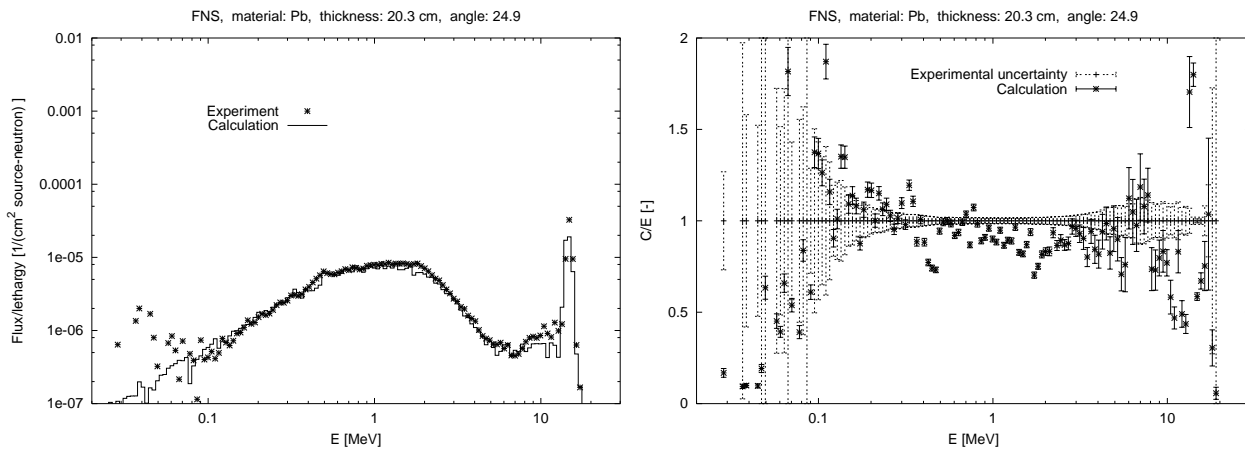


Figure 3.78 Neutron spectrum for the FNS, Pb, d=20cm benchmark at 24.9° angle.

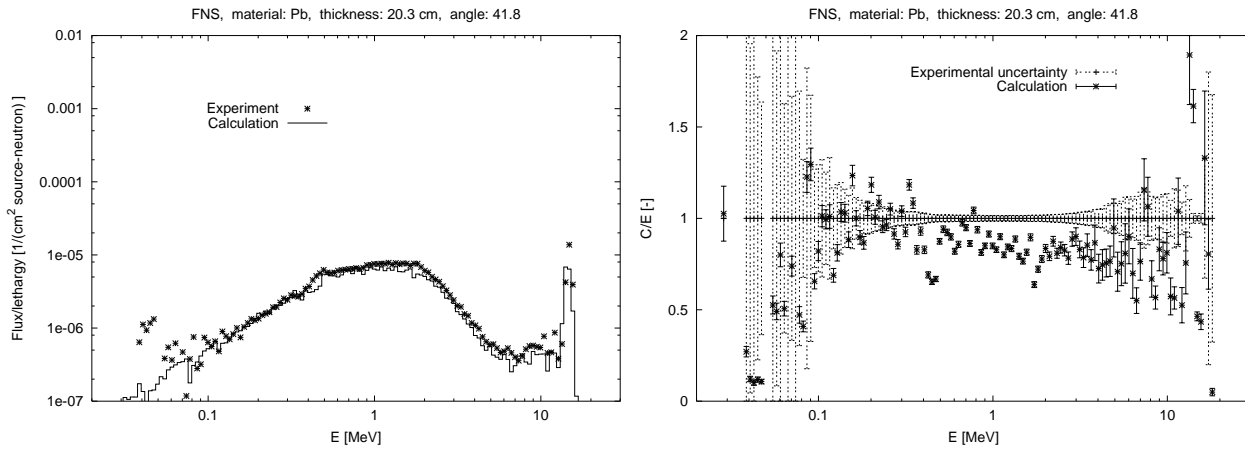


Figure 3.79 Neutron spectrum for the FNS, Pb, d=20cm benchmark at 42.8° angle.

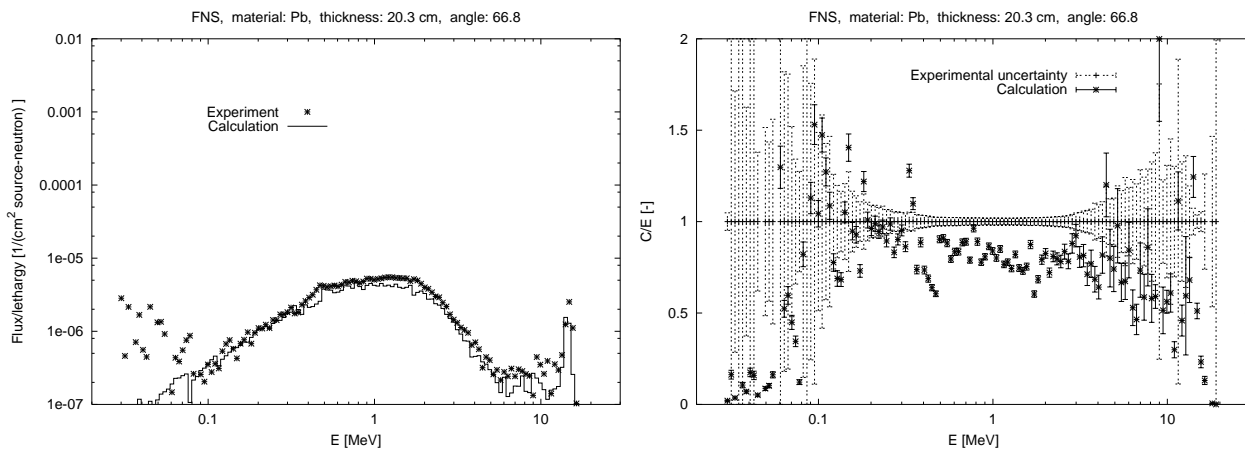


Figure 3.80 Neutron spectrum for the FNS, Pb, d=20cm benchmark at 66.8° angle.

energy range	0°	12.2°	24.9°	42.8°	66.8°
0.1– 1.0	0.88 ± 0.01	0.95 ± 0.01	0.93 ± 0.01	0.86 ± 0.01	0.82 ± 0.01
1.0– 5.0	0.89 ± 0.01	0.94 ± 0.01	0.91 ± 0.01	0.85 ± 0.01	0.82 ± 0.01
5.0– 10.0	0.82 ± 0.03	0.93 ± 0.03	0.89 ± 0.04	0.79 ± 0.04	0.72 ± 0.06
10.0– 20.0	0.95 ± 0.01	0.88 ± 0.01	0.83 ± 0.02	0.73 ± 0.03	0.63 ± 0.05

Table 3.24 C/E values for the neutron spectrum of the FNS Pb 20cm benchmark.

3.2.15 FNS, Pb, 40 cm

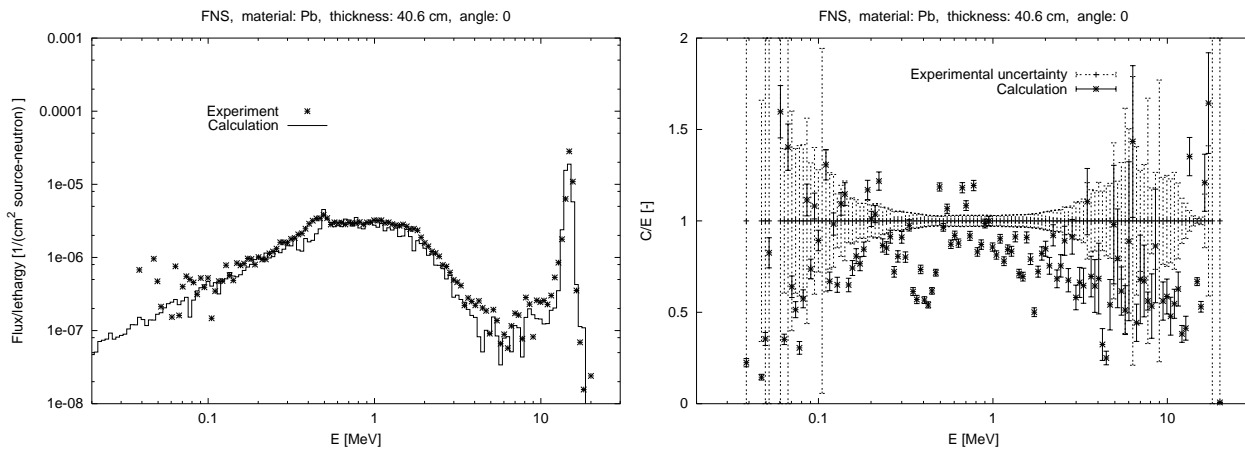


Figure 3.81 Neutron spectrum for the FNS, Pb, d=40cm benchmark at 0° angle.

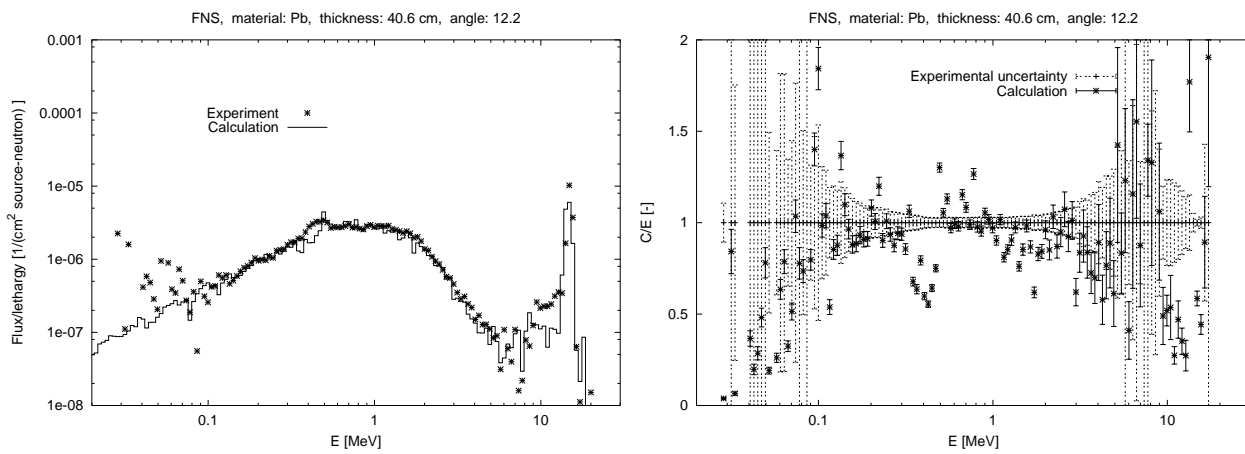


Figure 3.82 Neutron spectrum for the FNS, Pb, d=40cm benchmark at 12.2° angle.

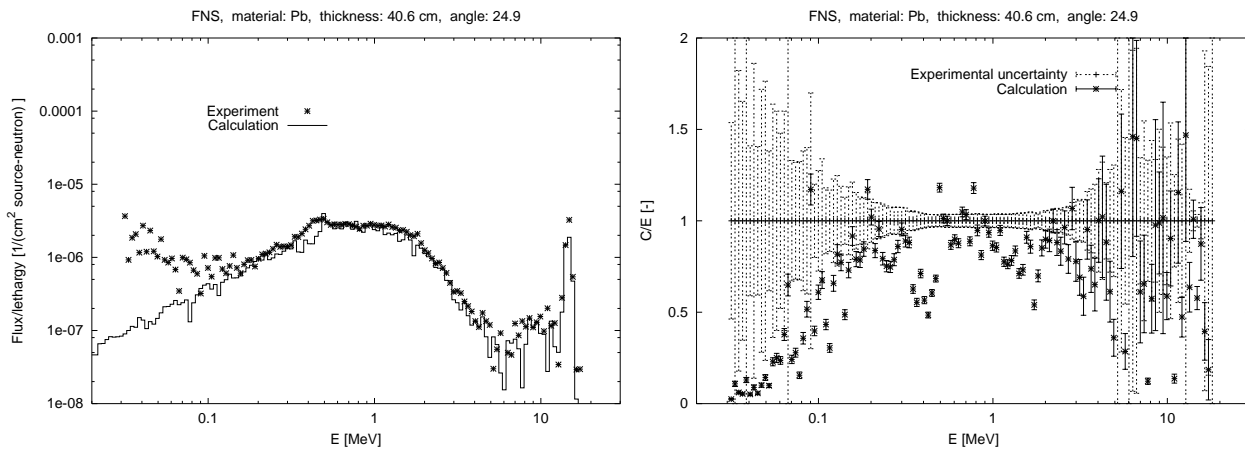


Figure 3.83 Neutron spectrum for the FNS, Pb, d=40cm benchmark at 24.9° angle.

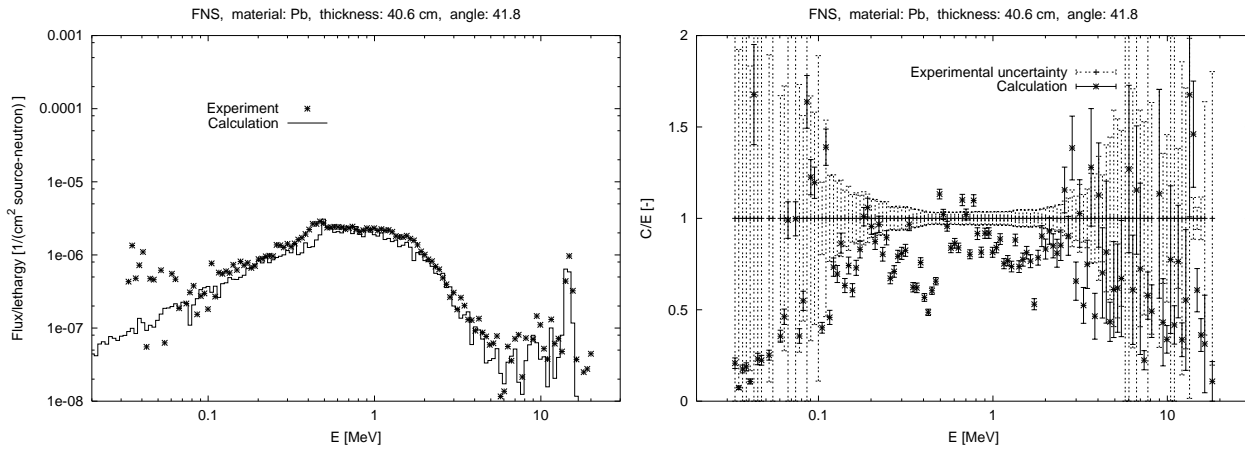


Figure 3.84 Neutron spectrum for the FNS, Pb, d=40cm benchmark at 42.8° angle.

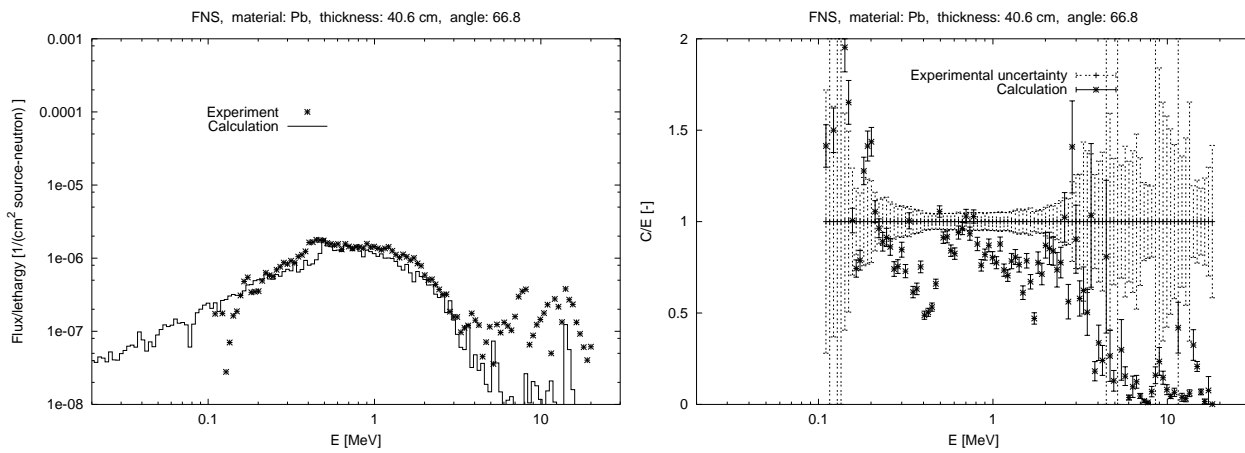


Figure 3.85 Neutron spectrum for the FNS, Pb, d=40cm benchmark at 66.8° angle.

energy range	0°	12.2°	24.9°	42.8°	66.8°
0.1– 1.0	0.86 ± 0.01	0.92 ± 0.01	0.82 ± 0.01	0.81 ± 0.01	0.85 ± 0.01
1.0– 5.0	0.84 ± 0.01	0.94 ± 0.01	0.87 ± 0.01	0.86 ± 0.01	0.80 ± 0.01
5.0– 10.0	0.69 ± 0.09	0.97 ± 0.11	0.76 ± 0.15	0.71 ± 0.14	0.12 ± 0.21
10.0– 20.0	0.89 ± 0.02	0.80 ± 0.04	0.73 ± 0.06	0.77 ± 0.11	0.12 ± 0.13

Table 3.25 C/E values for the neutron spectrum of the FNS Pb 40cm benchmark.

3.3 LLNL Pulsed Spheres

3.3.1 LLNL Pulsed Spheres, Concrete, 21 cm

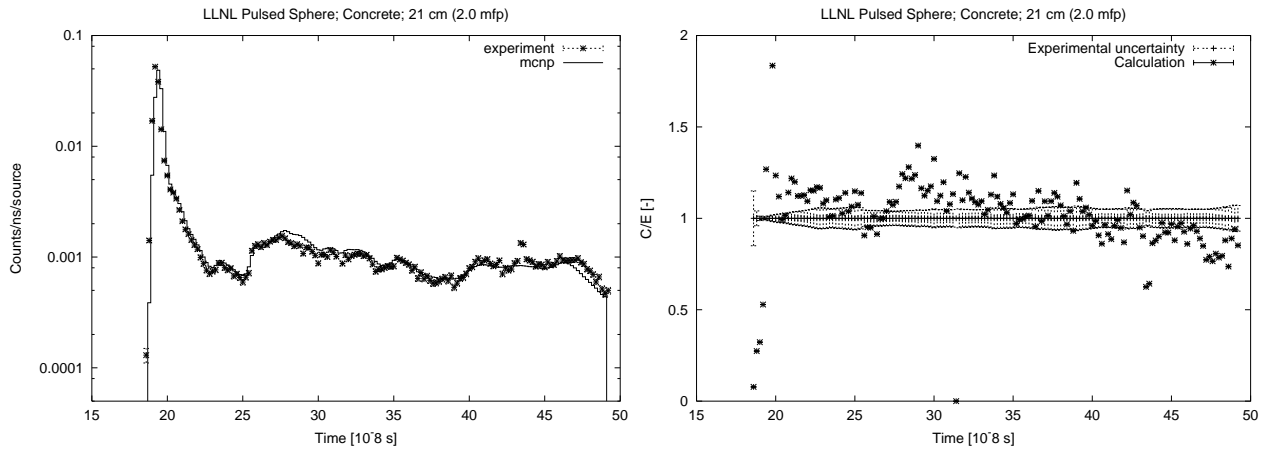


Figure 3.86 Neutron spectrum for the LLNL Pulsed Sphere, concrete, 21 cm (2.0 mfp) benchmark.

3.3.2 LLNL Pulsed Spheres, Concrete, 35.5 cm

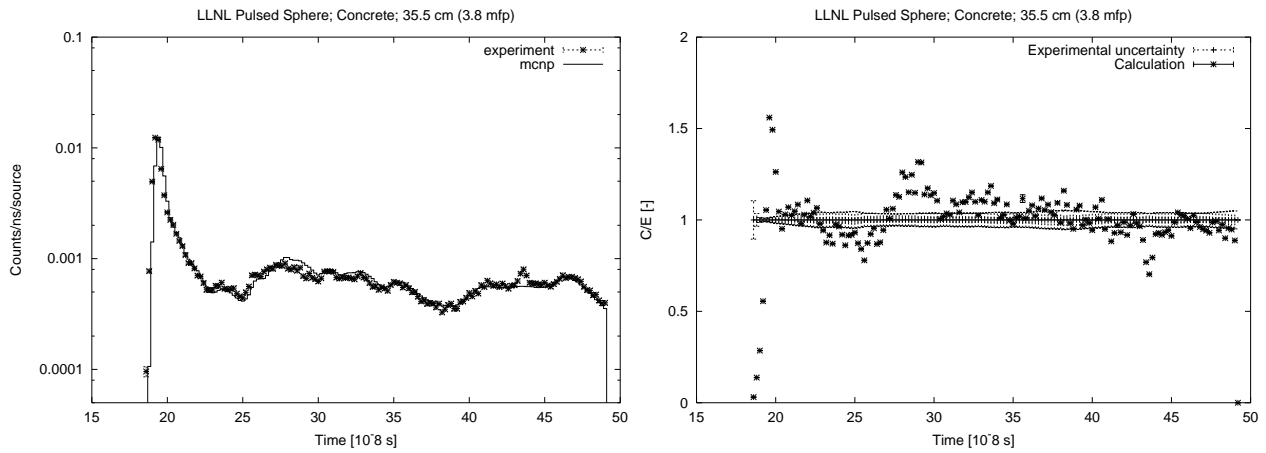


Figure 3.87 Neutron spectrum for the LLNL Pulsed Sphere, concrete, 35.5 cm (3.8 mfp) benchmark.

3.4 NIST Water Spheres

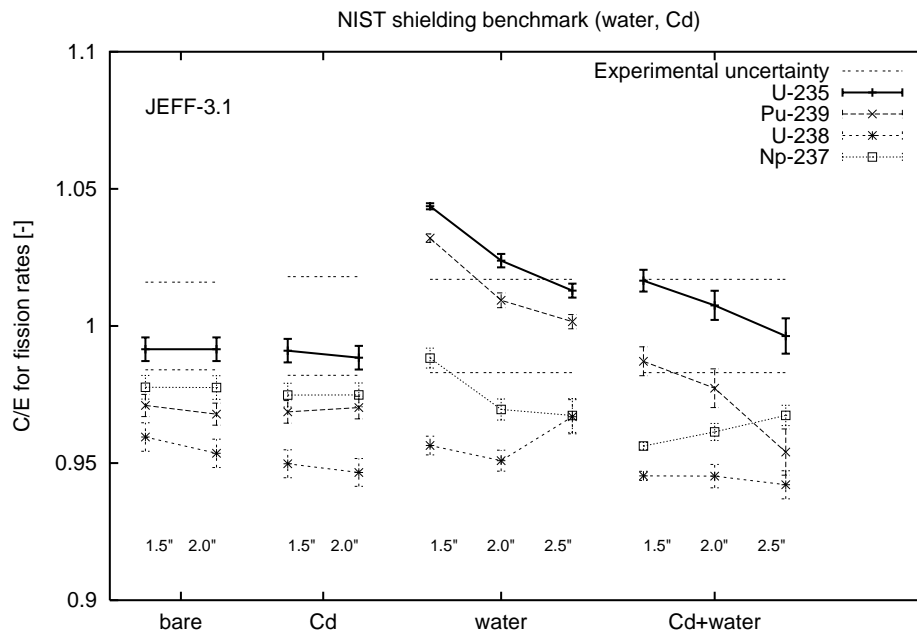


Figure 3.88 C/E values for the fission rate in fission foils in the NIST experiments.

material	radius	U-235	Pu-239	U-238	Np-237
bare	1.5"	0.992±0.004	0.971±0.004	0.960±0.005	0.978±0.004
bare	2.0"	0.992±0.004	0.968±0.004	0.954±0.005	0.978±0.004
Cd	1.5"	0.991±0.004	0.969±0.004	0.950±0.005	0.975±0.004
Cd	2.0"	0.988±0.004	0.970±0.004	0.947±0.005	0.975±0.004
H ₂ O	1.5"	1.044±0.001	1.032±0.002	0.956±0.003	0.988±0.004
H ₂ O	2.0"	1.023±0.003	1.009±0.003	0.951±0.004	0.970±0.004
H ₂ O	2.5"	1.013±0.003	1.002±0.003	0.967±0.006	0.967±0.006
Cd+H ₂ O	1.5"	1.017±0.004	0.987±0.005	0.945±0.002	0.956±0.001
Cd+H ₂ O	2.0"	1.008±0.005	0.977±0.007	0.945±0.004	0.961±0.003
Cd+H ₂ O	2.5"	0.996±0.006	0.954±0.008	0.942±0.005	0.967±0.004

Table 3.26 C/E values for the fission rates in the NIST benchmark.

4. Summary

The JEFF-3.1 general purpose library has been validated, using MCNP-4C3, with the shielding benchmarks Oktavian, FNS, LLNL Pulsed Spheres, and NIST Water spheres. The first three of these are 14 MeV experiments.

This exercise provides insight in the global quality of a data library and also in particular problems of nuclear data for certain elements. Comparison with other data libraries and detailed inspection of the data files could reveal the origin of observed discrepancies. However, this is outside the scope of the present study.

References

- [1] J.F. Briesmeister (Ed.), *MCNP - A General Monte Carlo N-Particle Transport Code, Version 4C*, Technical Report LA-13709-M, Los Alamos National Laboratory, USA (2000)
J.S. Hendricks, *MCNP4C3*, Report X-5:RN(U)-JSH-01-17, Los Alamos National Laboratory, USA (2001)
- [2] M.C. Duijvestijn, A. Hogenbirk, S.C. van der Marck, *ENDF/B-VI.8-PBMR - Contents of the ENDF/B-VI.8 based MCNP neutron transport cross section libraries for PBMR*, NRG Report 21526/05.64901/C FAI/MD/AK (2005)
- [3] www-nds.iaea.or.at/fendl2/validation/benchmarks/jaerim94014/oktavian/n-leak
- [4] C. Ichihara, I. Kimura, S.A. Hayashi, J. Yamamoto, and A. Takahashi, *Measurement of leakage neutron spectra from a spherical pile of zirconium irradiated with 14 MeV neutrons and validation of its nuclear data*, J. Nucl. Sci. Techn. **40** (2003) 417–422
- [5] www-nds.iaea.or.at/fendl2/validation/benchmarks/jaerim94014/fns-tof
- [6] Y. Oyama, S. Yamaguchi, and H. Maekawa *Measurements and analyses of angular neutron flux spectra on graphite and lithium-oxide slabs irradiated with 14.8 MeV neutrons*, J. Nucl. Sci. Techn. **25** (1988) 419–428
- [7] C. Wong, J.D. Anderson, P. Brown, L.F. Hansen, J.L. Kammerdiener, C. Logan, and B. Pohl, *Livermore Pulsed Sphere Program: Program Summary through July 1971*, UCRL-51144, Rev. 1 (1972)
- [8] J. D. Court, R.C. Brockhoff, and J.S. Hendricks *Lawrence Livermore Pulsed Sphere Benchmark Analysis of MCNP ENDF/B-VI*, LA-12885 (1994)
- [9] M.Z. Youssef, A. Kumar, M.A. Abdou, Ch. Konno, F. Maekawa, M. Wada, Y. Oyama, H. Maekawa, and Y. Ikeda, *Verification of ITER shielding capability and FENDL data benchmarking through analysis of bulk shielding experiment on large SS316/water assembly bombarded with 14 MeV neutrons*, Fusion Engineering and Design **42** (1998) 235–245
- [10] Sinbad data base, NEA (2004), http://www.nea.fr/html/science/shielding/sinbad/nist_h2o/nist-abs.htm

**Criticality safety benchmark
calculations with MCNP-4C3
using JEFF-3.1 nuclear data**

S.C. van der Marck

Petten, October 7, 2005

21616/05.69456/P FAI/SVDM/MB

author : S.C. van der Marck

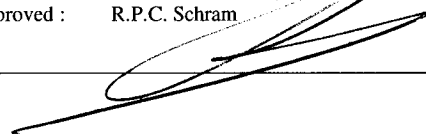


reviewed : A.J. Koning



54 page(s)

approved : R.P.C. Schram



© NRG 2005

Subject to agreement with the client, the information contained in this report may not be disclosed to any third party and NRG is not liable for any damage arising out of the use of such information.

Abstract

Criticality safety benchmark calculations were performed with MCNP-4C3 using the new JEFF-3.1 nuclear data library. The benchmarks used were almost all taken from the International Criticality Safety Benchmark Evaluation Project (ICSBEP). Additional benchmarks were a Proteus core, a Dimple core, two Kritz cores, and two TRX cores. The results of these calculations are reported in tabular and graphical form.

Keywords

MCNP-4C3

JEFF-3.1

nuclear data

criticality safety benchmarks

Contents

1	Introduction	5
2	Brief description of the criticality benchmarks	6
2.1	HEU benchmarks	6
2.1.1	Fast spectrum	6
2.1.2	Intermediate spectrum	8
2.1.3	Thermal spectrum	8
2.1.4	Mixed spectrum	12
2.2	IEU benchmarks	12
2.2.1	Fast spectrum	12
2.2.2	Intermediate spectrum	13
2.2.3	Thermal spectrum	14
2.3	LEU benchmarks	14
2.3.1	Fast spectrum	14
2.3.2	Intermediate spectrum	14
2.3.3	Thermal spectrum	14
2.4	PU benchmarks	20
2.4.1	Fast spectrum	20
2.4.2	Intermediate spectrum	20
2.4.3	Thermal spectrum	21
2.4.4	Mixed spectrum	22
2.5	MIX benchmarks	23
2.5.1	Fast spectrum	23
2.5.2	Intermediate spectrum	23
2.5.3	Thermal spectrum	23
2.6	U233 benchmarks	24
2.6.1	Fast spectrum	24
2.6.2	Intermediate spectrum	24
2.6.3	Thermal spectrum	24
2.7	Occurrence of elements	24
3	Results of validation calculations	26
3.1	HEU results	26
3.1.1	Fast spectrum	26
3.1.2	Intermediate spectrum	28
3.1.3	Thermal spectrum	28
3.1.4	Mixed spectrum	32
3.2	IEU results	32
3.2.1	Fast spectrum	32
3.2.2	Intermediate spectrum	33
3.2.3	Thermal spectrum	34
3.3	LEU results	34
3.3.1	Thermal spectrum	34

3.4	PU results	44
3.4.1	Fast spectrum	44
3.4.2	Intermediate spectrum	44
3.4.3	Thermal spectrum	45
3.4.4	Mixed spectrum	48
3.5	MIX results	48
3.5.1	Fast spectrum	48
3.5.2	Thermal spectrum	48
3.6	U233 results	50
3.6.1	Fast spectrum	50
3.6.2	Thermal spectrum	51
3.7	Summary	53
References		54

1. Introduction

In May 2005 a new version of the JEFF general purpose nuclear data library was released: JEFF-3.1. Over the last several years there has been a concerted effort by many people in several countries to bring the quality of this nuclear data library to a new, higher level. Especially the underprediction of k_{eff} for many criticality safety benchmark with a thermal spectrum has received much attention.

In this report, the results of many criticality safety benchmark runs are presented. The results show, among other things, that when using JEFF-3.1 nuclear data, the prediction of k_{eff} for the thermal spectrum benchmarks is much closer to the benchmark value.

All results reported in this report were obtained by use of the Monte Carlo neutronics code MCNP, version 4C3 [1].

2. Brief description of the criticality benchmarks

Almost all benchmarks were taken from the *International Handbook of Evaluated Criticality Safety Benchmark Experiments* from the OECD-NEA project ICSBEP [2]. In Ref. [2], these benchmarks are subdivided in main categories according to three criteria.

1. The main fissionable isotope. The systems containing uranium-235 are subdivided according to the enrichment in ^{235}U : there is low enriched uranium (LEU: wt% $^{235}\text{U} < 10$), intermediate enriched (IEU: $10 < \text{wt}\% ^{235}\text{U} < 60$) and high enriched (HEU: wt% $^{235}\text{U} > 60$). There are also plutonium systems (PU), mixed uranium/plutonium systems (MIX), and ^{233}U systems (U233).
2. The physical form of the fissile material: there are metal systems (MET), compound (COM), solution (SOL) and miscellaneous systems.
3. The neutron spectrum: if more than half of the fissions occurs for neutrons with energy below 0.625 eV the spectrum is thermal (THERM), if more than half occurs between 0.625 eV and 100 keV it is intermediate (INTER), and if more than half occurs over 100 keV it is fast (FAST). If none of these applies, the spectrum is classified as MIXED.

The benchmark series identifier consists of the three components mentioned above, plus an additional sequence number.

For each of the benchmark series for which calculations have been performed, a brief description is given below.

2.1 HEU benchmarks

2.1.1 Fast spectrum

heu-met-fast-001 (1 case, 'Godiva')

- A bare sphere of highly enriched uranium (LANL, 1950s).
- The uranium enrichment was 94% ^{235}U .
- The isotopes in this benchmark model are U-{234,235,238}.

heu-met-fast-005 (6 cases)

- Cores of uranium metal alloy and reflectors of molybdenum and beryllium (Obninsk, 1987). The amount of reflector material (Be-9) and the amount of molybdenum between fuel and reflector was varied.
- The uranium enrichment was 90% ^{235}U .
- The isotopes in these benchmark models are C-nat, Al-27, Si-{28–30}, Ti-{46–50}, Cr-{50,52–54}, Mn-55, Fe-{54,56–58}, Ni-{58,60–62,64}, Mo-{92,94–98,100}, and U-{234,235,236,238}.

In cases 2 – 6 Be-9 is also present.

heu-met-fast-007 (43 cases)

- Uranium metal slabs moderated with polyethylene, plexiglas and teflon (ORNL, 1960s). Some of the polyethylene moderated experiments also had a polyethylene reflector. The H/ ^{235}U ratio was varied between 0 and 5.
- The uranium enrichment was 93% ^{235}U .
- The isotopes in these benchmark models are H-1, C-nat, U-{234,235,236,238}. In cases 27–31 O-16 is also used, and in cases 32–34 F-19 is also used.

heu-met-fast-022 (1 case)

- A sphere of highly enriched uranium with C, Fe and W impurities, reflected by duraluminum (VNIIEF, Russia, 1962).
- The uranium enrichment was 90% ^{235}U .
- The isotopes in this benchmark model are C-nat, Al-27, Fe-{54,56–58}, Cu-{63,65}, W-{182–184,186}, U-{234,235,238}.

heu-met-fast-027 (1 case)

- A sphere of highly enriched uranium with C, Fe and W impurities, reflected by lead (VNIIEF, Russia, 1962).
- The uranium enrichment was 90% ^{235}U .
- The isotopes in this benchmark model are C-nat, Fe-{54,56–58}, W-{182–184,186}, Pb-{206–208}, U-{234,235,238}.

heu-met-fast-028 (1 case, 'Topsy', 'Flattop-25')

- A sphere of highly enriched uranium reflected by normal uranium (LANL, 1960s).
- The uranium enrichment was 93% ^{235}U .
- The isotopes in this benchmark model are U-{234,235,238}.

heu-met-fast-057 (6 cases)

- Uranium metal spheres and cylinders, reflected by lead (LLNL, 1950s).
- The uranium enrichment was 93% ^{235}U .
- The isotopes in these benchmark models are Be-9, Ca-{40,42–44,46,48}, Fe-{54,56–58}, Ni-{58,60–62,64}, Pb-{204,206–208}, U-{234,235,238}.

heu-met-fast-060 (1 case)

- A cylindrical assembly of uranium metal and tungsten, with aluminum reflectors (ZPR-9 assembly 4, ANL, 1960s).
- The uranium enrichment was 93% ^{235}U .
- The isotopes in this benchmark model are H-1, C-nat, F-19, Mg-{24–26}, Al-27, Si-{28–30}, Cl-{35,37}, Ti-{46–50}, Cr-{50,52–54}, Mn-55, Fe-{54,56–58}, Ni-{58,60–62,64}, Cu-{63,65}, Mo-{92,94–98,100}, W-{182–184,186}, U-{234,235,236,238}.

heu-met-fast-064 (3 cases)

- Three cylinders of lead reflected highly enriched uranium (VNIITF, Russia, 1991).
- The uranium enrichment was 96% ^{235}U .
- The isotopes in these benchmark models are C-nat, Si-{28–30}, Cr-{50,52–54}, Mn-55, Fe-{54,56–58}, W-{182–184,186}, Pb-{204,206–208}, U-{234,235,238}.

heu-met-fast-067 (2 cases)

- Cylindrical assemblies of uranium metal with tungsten, graphite (assembly 5) and aluminum assembly 6), reflected by dense aluminum. (ZPR-9 assemblies 5 and 6, ANL, 1960s).
- The uranium enrichment was 93% ^{235}U .
- The isotopes in these benchmark models are H-1, C-nat, F-19, Mg-{24–26}, Al-27, Si-{28–30}, Cl-{35,37}, Ti-{46–50}, Cr-{50,52–54}, Mn-55, Fe-{54,56–58}, Cu-{63,65}, Ni-{58,60–62,64}, Mo-{92,94–98,100}, W-{182–184,186}, U-{234,235,236,238}.

heu-met-fast-072 (1 case, 'Zeus')

- An iron/HEU core surrounded by a copper reflector in the Los Alamos Critical Experiment Facility (LANL, 2002). In this report only configuration 1 (out of two) was computed.

- The uranium enrichment was 93% ^{235}U .
- The isotopes in these benchmark models are B-{10,11}, C-nat, N-{14,15}, Mg-{24–26}, Al-27, Si-{28–30}, P-31, S-{32–34,36}, Ti-{46–50}, V-nat, Cr-{50,52–54}, Mn-55, Fe-{54,56–58}, Ni-{58,60–62,64}, Cu-{63,65}, Zn-nat, Ga-nat, Mo-{92,94–98,100}, Pb-{204,206–208}, U-{234,235,236,238}.

2.1.2 Intermediate spectrum

heu-comp-inter-004 (1 case)

- A k_{∞} experiment at the HECTOR reactor (Winfrith, UK, 1960s): a graphite moderated uranium oxide core. The benchmark model is an infinite medium with a material composition appropriate to the interpolated boron/ ^{235}U ratio.
- The uranium enrichment was 92% ^{235}U .
- The isotopes in these benchmark models are H-1, B-{10,11}, C-nat, O-16, Ca-{40,42–44,46,48}, U-{234,235,236,238}.

heu-comp-inter-005 (5 cases)

- Several k_{∞} experiments at the COBRA facility (Obninsk, Russia, 1980s, 1990s), containing uranium and nickel (KBR-7 assembly), stainless steel (KBR-9), stainless steel and molybdenum (KBR-10), chromium (KBR-15), and zirconium (KBR-16).
- The uranium enrichment was 90% ^{235}U .
- The isotopes in these benchmark models are C-nat, O-16, Si-{28–30}, Ti-{46–50}, Cr-{50,52–54}, Mn-55, Fe-{54,56–58}, Ni-{58,60–62,64}, U-{235,238}. Also used are Co-59 (case 1), Mo-{92,94–98,100} (case 3) and H-1, Zr-{90–92,94,96}, Hf-{174,176–180} (case 5).

heu-met-inter-001 (1 case)

- A cylindrical assembly of uranium and iron, reflected by stainless steel (ZPR-9 assembly 34, ANL, 1979).
- The uranium enrichment was 93% ^{235}U .
- The isotopes in this benchmark model are H-1, C-nat, F-19, Mg-{24–26}, Al-27, Si-{28–30}, Cl-{35,37}, Cr-{50,52–54}, Mn-55, Fe-{54,56–58}, Ni-{58,60–62,64}, Cu-{63,65}, Mo-{92,94–98,100}, U-{234,235,236,238}.

heu-met-inter-006 (4 cases, 'Zeus')

- The initial set of Zeus experiments at the Los Alamos Critical Experiments Facility (LANL, 1999–2001): uranium metal interspersed with graphite plates in a cylindrical stack, surrounded by copper reflector. The C/ ^{235}U ratio varied between 51.2 to 13.6.
- The uranium enrichment was 93% ^{235}U .
- The isotopes in these benchmark models are C-nat, Mg-{24–26}, Al-27, Si-{28–30}, Ti-{46–50}, Cr-{50,52–54}, Mn-55, Fe-{54,56–58}, Cu-{63,65}, U-{234,235,236,238}.

2.1.3 Thermal spectrum

heu-met-therm-001 (2 cases)

- A polyethylene moderated and reflected uranium system with silicon (LANL, 1999).
- The uranium enrichment was 93% ^{235}U .
- The isotopes in these benchmark models are H-1, C-nat, O-16, Si-{28–30}, U-{234,235,236,238}.

Thermal scattering data for H in CH₂ is used.

heu-met-therm-003 (7 cases)

- Lattices of oralloy cubes in water (LANL, 1955). The number of cubes and their spacing were varied.
 - The uranium enrichment was 94% ²³⁵U.
 - The isotopes in these benchmark models are H-1, C-nat, O-16, U-{234,235,238}.
- Thermal scattering data for H in H₂O is used.

heu-met-therm-006 (23 cases)

- Lattices of SPERT-D fuel elements, reported by ORNL, 1964-65. The fuel elements consisted of plates of a uranium-aluminium alloy. The experiments were water-moderated and water-reflected. In some of the cases uranyl nitrate solution (with and without boron) was substituted for the water. The lattice configuration was varied.
- The uranium enrichment was 93% ²³⁵U.
- The isotopes in these benchmark models are H-1, O-16, Mg-{24-26}, Al-27, Si-{28-30}, Ti-{46-50}, Cr-{50,52-54}, Mn-55, Fe-{54,56-58}, Cu-{63,65}, and U-{234,235,238}. Thermal scattering data for H in H₂O is used.

For cases 17 and 18 Cd-{106,108,110-114,116} is also present, while for cases 4 and 19-23 C-nat, N-14, P-31, S-{32-34,36}, and Ni-{58,60-62,64} are present too. Besides, cases 20-23 have B-{10,11}.

heu-met-therm-008 (2 cases)

- A polyethylene moderated and reflected uranium system with aluminium (LANL)
 - The uranium enrichment was 93% ²³⁵U.
 - The isotopes in these benchmark models are H-1, C-nat, Mg-{24-26}, Al-27, Si-{28-30}, Ti-{46-50}, Cr-{50,52-54}, Mn-55, Fe-{54,56-58}, Cu-{63,65}, U-{234,235,236,238}.
- Thermal scattering data for H in CH₂ is used.

heu-met-therm-009 (1 case)

- A polyethylene moderated and reflected uranium system with magnesium oxide (LANL, 2001)
 - The uranium enrichment was 93% ²³⁵U.
 - The isotopes in these benchmark models are H-1, Li-{6}, B-10, C-nat, O-16, Mg-{24-26}, Al-27, K-{39,40,41}, Ca-{40,42-44,46,48}, Mn-55, Fe-{54,56-58}, Cd-{106,108,110-114,116}, U-{234,235,236,238}.
- Thermal scattering data for H in CH₂ is used.

heu-met-therm-010 (2 cases)

- A polyethylene moderated and reflected uranium system with gadolinium (LANL, 2001). Two thicknesses of Gd foil were used.
 - The uranium enrichment was 93% ²³⁵U.
 - The isotopes in these benchmark models are H-1, C-nat, Gd-{152,154-158,160}, U-{234,235,236,238}.
- Thermal scattering data for H in CH₂ is used.

heu-met-therm-013 (2 cases)

- A polyethylene moderated and reflected uranium system with iron (LANL, ~2002). Two thicknesses of iron plates were used.

- The uranium enrichment was 93% ²³⁵U.
- The isotopes in these benchmark models are H-1, C-nat, Fe-{54,56–58}, U-{234,235,236,238}.

Thermal scattering data for H in CH₂ is used.

heu-met-therm-014 (1 case)

- 2 × 2 × 23 array of uranium with silicon oxide, moderated and reflected by polyethylene (LANL, ~2002)
- The uranium enrichment was 93% ²³⁵U.
- The isotopes in these benchmark models are H-1, C-nat, O-16, Si-{28–30}, U-{234,235,236,238}.

Thermal scattering data for H in CH₂ is used.

heu-met-therm-016 (2 cases)

- 2 × 2 × 23 array of uranium with Ni-Cr-Mo-Gd alloy, moderated and reflected by polyethylene (LANL)
- The uranium enrichment was 93% ²³⁵U.
- The isotopes in these benchmark models are H-1, B-{10,11}, C-nat, O-16, Mg-{24–26}, Al-27, Si-{28–30}, P-31, Ca-{40,42–44,46,48}, Ti-{46–50}, V-nat, Cr-{50,52–54}, Mn-55, Fe-{54,56–58}, Co-59, Ni-{58,60–62,64}, Cu-{63,65}, Br-79, Zr-{90–92,94,96}, Nb-93, Mo-{92,94–98,100}, Ag-{107,109}, Cd-{106,108,110–114,116}, Gd-{152,154–158,160}, Hf-{174,176,177,178,179,180}, Ta-181, W-{182–184,186}, Pb-{204,206–208}, U-{234,235,236,238}.

Thermal scattering data for H in CH₂ is used.

heu-met-therm-018 (2 cases)

- A polyethylene moderated and reflected uranium system with concrete (LANL, 2003).
- The uranium enrichment was 93% ²³⁵U.
- The isotopes in these benchmark models are H-1, Li-{6,7}, B-{10,11}, C-nat, O-16, Na-23, Mg-{24–26}, Al-27, Si-{28–30}, P-31, S-32, K-{39,40,41}, Ca-{40,42–44,46,48}, Sc-45, Ti-{46–50}, Fe-{54,56–58}, Rh-103, Cd-{106,108,110–114,116}, In-{113,115}, Eu-{151,153}, Gd-{152,154–158,160}, U-{234,235,236,238}.

Thermal scattering data for H in CH₂ is used.

heu-sol-therm-001 (10 cases)

- Cylindrical reflected tank with uranyl nitrate, minimally reflected. The uranium concentration was varied and the critical height was determined.
- The uranium enrichment was 93% ²³⁵U.
- The isotopes in these benchmark models are H-1, C-nat, N-14, O-16, Al-27, Si-{28–30}, P-31, S-{32–34,36}, Cr-{50,52–54}, Mn-55, Fe-{54,56–58}, Ni-{58,60–62,64}, Mo-{92,94–98,100}, U-{234,235,236,238}. Thermal scattering data for H in H₂O is used.

heu-sol-therm-002 (14 cases)

- Cylindrical reflected tank with uranyl nitrate, with a concrete reflector. The uranium concentration was varied and the critical height was determined.
- The uranium enrichment was 93% ²³⁵U.
- The isotopes in these benchmark models are H-1, C-nat, N-14, O-16, Na-23, Mg-{24–26}, Al-27, Si-{28–30}, S-{32–34,36}, K-{39–41}, Ca-{40,42–44,46,48}, Ti-{46–50}, Cr-

{50,52–54}, Mn-55, Fe-{54,56–58}, and U-{234,235,236,238}. Thermal scattering data for H in H₂O is used.

In cases 5 – 14 there is also Cu-{63,65}, in cases 1 – 4 P-31, Ni-{58,60–62,64}, and Mo-{92,94–98,100}.

heu-sol-therm-004 (6 cases)

- Reflected uranyl-fluoride solutions in heavy water (LANL, 1950s). The D/²³⁵U ratio varied from 34 to 431.
- The uranium enrichment was 94% ²³⁵U.
- The isotopes in these benchmark models are H-{1,2}, O-16, F-19, Si-{28–30}, Cr-{50,52–54}, Mn-55, Fe-{54,56–58}, Ni-{58,60–62,64}, U-{234,235,238}. Thermal scattering data for D in D₂O is used.

heu-sol-therm-009 (4 cases)

- Water reflected 6.4-liter spheres of highly enriched uranium oxyfluoride (UO₂F₂) solutions (ORNL, 1950s). The fuel concentration was varied.
- The uranium enrichment was 93% ²³⁵U.
- The isotopes in these benchmark models are H-1, O-16, F-19, Al-27, Si-{28–30}, Mn-55, Cu-{63,65}, U-{234,235,236,238}. Thermal scattering data for H in H₂O is used.

heu-sol-therm-010 (4 cases)

- Water reflected 9.7-liter spheres of highly enriched uranium oxyfluoride (UO₂F₂) solutions (ORNL, 1950s). The fuel concentration and the temperature were varied.
- The uranium enrichment was 93% ²³⁵U.
- The isotopes in these benchmark models are H-1, O-16, F-19, Al-27, Si-{28–30}, Mn-55, Cu-{63,65}, U-{234,235,236,238}. Thermal scattering data for H in H₂O is used.

heu-sol-therm-013 (4 cases, 'ORNL-1', . . . , 'ORNL-4')

- Uranyl nitrate solutions poisoned with boric acid in an unreflected sphere (at ORNL, 1950s).
- The uranium enrichment was 93% ²³⁵U.
- The isotopes in these benchmark models are H-1, N-14, O-16, Al-27, Si-{28–30}, Mn-55, Cu-{63,65}, U-{234,235,236,238}. Thermal scattering data for H in H₂O is used. For cases 1 – 3 B-{10,11} are also present.

heu-sol-therm-032 (1 case)

- Unreflected 48-inch sphere of highly enriched uranyl nitrate solution (ORNL, 1950s).
- The uranium enrichment was 93% ²³⁵U.
- The isotopes in this benchmark model are H-1, N-14, O-16, Al-27, Si-{28–30}, Mn-55, Fe-{54,56–58}, Cu-{63,65}, U-{233,234,235,236,238}. Thermal scattering data for H in H₂O is used.

heu-sol-therm-038 (30 cases)

- Two interacting slab tanks with highly enriched uranyl nitrate solution with various absorber-reflector plates (LANL, 1988). The absorber-reflector plates were made of poly-ethylene, borated poly-ethylene, boraflex, pyrex, stainless steel, hot rolled steel, lead, beryllium, depleted uranium, or cadmium.
- The uranium enrichment was 93% ²³⁵U.
- The isotopes in these benchmark models are H-1, Be-9, B-{10,11}, C-nat, N-14, O-16, Na-23, Mg-{24–26}, Al-27, Si-{28–30}, P-31, S-{32–34,36}, Ti-{46–50}, Cr-

{50,52–54}, Mn-55, Fe-{54,56–58}, Ni-{58,60–62,64}, Cu-{63,65}, Mo-{92,94–98,100}, Cd-{106,108,110–114,116}, Pb-{206–208}, U-{234,235,236,238}. Thermal scattering data for H in H₂O and for H in CH₂ is used.

heu-sol-therm-039 (6 cases)

- Mixture of highly enriched uranium hexafluoride (UF₆) and hydrofluoric acid (HF), low H/U ratio, in a hot-water reflected tank (Valduc, 1960s). The uranium concentration was varied.
- The uranium enrichment was 93% ²³⁵U.
- The isotopes in these benchmark models are H-1, C-nat, O-16, F-19, Si-{28–30}, Mn-55, Fe-{54,56–58}, Ni-{58,60–62,64}, Cu-{63,65}, U-{234,235,236,238}. Thermal scattering data for H in H₂O is used.

heu-sol-therm-042 (8 cases)

- Unreflected cylinders (5 ft and 9 ft diameter) of highly enriched uranyl nitrate solution. The uranium concentration was varied.
- The uranium enrichment was 93% ²³⁵U.
- The isotopes in these benchmark models are H-1, C-nat, N-14, O-16, Cr-{50,52–54}, Fe-{54,56–58}, Ni-{58,60–62,64}, Mo-{92,94–98,100}, U-{234,235,236,238}. Thermal scattering data for H in H₂O is used.

2.1.4 Mixed spectrum

heu-comp-mixed-003 (1 case)

- Heterogeneous assemblies of uranium dioxide fuel elements in a zirconium hydride moderator block, with beryllium reflector (RCC Kurchatov, 1992–1993).
- The uranium enrichment was 96% ²³⁵U.
- The isotopes in these benchmark models are H-1, Be-9, B-{10,11}, C-nat, O-16, Al-27, Si-{28–30}, Ti-{46–50}, Cr-{50,52–54}, Mn-55, Fe-{54,56–58}, Ni-{58,60–62,64}, Zr-{90–92,94,96}, Nb-93, Mo-{92,94–98,100}, Hf-{174,176,177,178,179,180}, W-{182–184,186}, U-{234,235,236,238}. Thermal scattering data for H in ZrH is used.

heu-met-mixed-005 (5 cases)

- Critical experiments with heterogeneous compositions of highly enriched uranium, silicon dioxide and polyethylene (Obninsk, 1999).
- The uranium enrichment was 90% ²³⁵U.
- The isotopes in these benchmark models are H-1, Li-{6,7}, B-{10,11}, C-nat, N-14, O-16, Na-23, Mg-{24–26}, Al-27, Si-{28–30}, S-32, K-{39,40,41}, Ca-{40,42–44,46,48}, Ti-{46–50}, V-nat, Cr-{50,52–54}, Mn-55, Fe-{54,56–58}, Ni-{58,60–62,64}, Cu-{63,65}, Mo-{92,94–98,100}, Cd-{106,108,110–114,116}, Pb-{206–208}, U-{234,235,236,238}. Thermal scattering data for H in H₂O is used.

2.2 IEU benchmarks

2.2.1 Fast spectrum

ieu-met-fast-001 (4 cases, 'Jemima')

- Bare cylindrical configurations of enriched and natural uranium (LANL, 1952–1954).
- The core average uranium enrichment was 36–55% ²³⁵U.

- The isotopes in these benchmark models are Mg-{24–26}, Al-27, Cr-{50,52–54}, Mn-55, Fe-{54,56–58}, Ni-{58,60–62,64}, Cu-{63,65}, U-{234,235,238}.

ieu-met-fast-002 (1 case)

- Cylindrical assembly with a core of alternating plates of enriched and natural uranium surrounded by a natural uranium reflector (LANL, 1956).
- The core average uranium enrichment was 16% ²³⁵U.
- The isotopes in this benchmark model are U-{234,235,238}.

ieu-met-fast-007 (3 cases, 'Big Ten')

- Three models of a large mixed-uranium-metal cylindrical core with 10% average uranium enrichment, surrounded by a thick depleted uranium reflector (LANL, 1971). The total uranium mass was ten metric tons. This core is modeled in three different benchmark models: detailed, simple and two-zone.
- The core average uranium enrichment was 10% ²³⁵U.
- The isotopes in these benchmark models are Si-{28–30}, Cr-{50,52–54}, Mn-55, Fe-{54,56–58}, Ni-{58,60–62,64}, Nb-93, U-{234,235,236,238}.

ieu-met-fast-010 (1 case)

- A cylindrical assembly of uranium metal, 9% average enrichment, with a thick depleted uranium reflector (ANL, ZPR-9, U9 benchmark assembly, 1980).
- The core average uranium enrichment was 9% ²³⁵U.
- The isotopes in these benchmark models are H-1, C-nat, F-19, Al-27, Si-{28–30}, Cl-{35,37}, Cr-{50,52–54}, Mn-55, Fe-{54,56–58}, Ni-{58,60–62,64}, Cu-{63,65}, Mo-{92,94–98,100}, U-{234,235,236,238}.

ieu-met-fast-012 (1 case)

- A critical assembly of uranium metal, aluminium and steel, reflected by depleted uranium (ZPR-3 assembly 41, 1962).
- The core average uranium enrichment was 16% ²³⁵U.
- The isotopes in this benchmark model are C-nat, Al-27, Si-{28–30}, Cr-{50,52–54}, Mn-55, Fe-{54,56–58}, Ni-{58,60–62,64}, and U-{234,235,236,238}.

ieu-met-fast-014 (2 cases)

- Cylindrical assemblies of uranium metal and tungsten with aluminum reflectors (ANL, ZPR-9 assemblies 2 and 3, 1964). Case 2 (assembly 3) had more tungsten than case 1 (assembly 1).
- The core average uranium enrichment was 16% ²³⁵U (case 1) and 21% ²³⁵U (case 2).
- The isotopes in these benchmark models are H-1, C-nat, F-19, Mg-{24–26}, Al-27, Si-{28–30}, Cl-{35,37}, Ti-{46–50}, Cr-{50,52–54}, Mn-55, Fe-{54,56–58}, Ni-{58,60–62,64}, Cu-{63,65}, Mo-{92,94–98,100}, W-{182–184,186}, U-{234,235,236,238}.

2.2.2 Intermediate spectrum

ieu-comp-inter-001 (4 cases)

- For k_{∞} experiments for combinations of uranium, thorium metal and varying amounts of polyethylene (IPPE, Obninsk, 1990–1994). The H/²³⁵U ratio varied from 0 to 70.
- Various combinations of 36% ²³⁵U and 90% ²³⁵U were used.
- The isotopes in these benchmark models are H-1, C-nat, O-16, Al-27, Si-{28–30}, Ti-{46–50}, Cr-{50,52–54}, Mn-55, Fe-{54,56–58}, Ni-{58,60–62,64}, Th-232, U-{235,238}

2.2.3 Thermal spectrum

ieu-comp-therm-002 (3 cases)

- Stainless steel clad UO₂ fuel rods in a water filled tank (MATR, Russia, 1970-1973). The fuel rods were arranged in a hexagonal lattice, with gadolinium absorber, cadmium absorber or no absorber. Cases 1, 3 and 5 were at room temperature, case 2 was at T=218.4°C, and cases 4 and 6 were at T=150.8°C.
- The uranium enrichment was 17% ²³⁵U.
- The isotopes in these benchmark models are H-1, C-nat, O-16, Si-{28–30}, Ti-{46–50}, Cr-{50,52–54}, Mn-55, Fe-{54,56–58}, Ni-{58,60–62,64}, and U-{234,235,238}. Thermal scattering data for H in H₂O is used.
For case 3 Al-27 and Gd-{152,154–158,160} are also present, for case 5 Al-27 and Cd-{106,108,110–114,116}.

ieu-comp-therm-003 (2 cases)

- Zirconium hydride fuel rods in water, with a graphite reflector (Triga Mark II reactor, Ljubljana, 1991). The two cases differ only in the position of the 7 outermost fuel elements.
- The uranium enrichment was 20% ²³⁵U.
- The isotopes in these benchmark models are H-1, B-{10,11}, C-nat, N-14, O-16, Al-27, Si-{28–30}, P-31, S-{32–34,36}, Cr-{50,52–54}, Mn-55, Fe-{54,56–58}, Ni-{58,60–62,64}, Zr-{90–92,94,96}, Mo-{92,94–98,100}, U-{235,238}. Thermal scattering data for graphite, for H in ZrH and for H in H₂O is used.

Proteus (1 case)

- Core 5 of Proteus, a graphite reflected pebble bed reactor, containing uranium-carbon fuel pebbles and graphite moderator pebbles (PSI, 1995–1996) [3].
- The uranium enrichment was 16.7% ²³⁵U.
- The isotopes in these benchmark models are H-1, Li-{6,7}, B-{10,11}, C-nat, N-14, O-16, Mg-{24–26}, Al-27, Si-{28–30}, S-{32–34,36}, Cl-{35,37}, Ca-{40,42–44,46,48}, Mn-55, Fe-{54,56–58}, Cu-{63,65}, Ga-nat, Cd-{106,108,110–114,116}, Gd-{154–158,160}, Sm-{144,147–150,152,154}, U-{234,235,236,238}. Thermal scattering data for graphite and for H in H₂O is used.

2.3 LEU benchmarks

2.3.1 Fast spectrum

No benchmark models in this category are available from the ICSBEP handbook.

2.3.2 Intermediate spectrum

No benchmark models in this category are available from the ICSBEP handbook.

2.3.3 Thermal spectrum

leu-comp-therm-001 (8 cases)

- Clusters of aluminium clad UO₂ fuel rods in a water filled tank. The clusters were square, with no absorber plates, reflecting walls, dissolved poison or gadolinium impurities. The number of clusters and the separation between them was varied.

- The uranium enrichment was 2.4% ^{235}U .
- The isotopes in these benchmark models are H-1, C-nat, O-16, Mg-{24–26}, Al-27, Si-{28–30}, Ti-{46–50}, Cr-{50,52–54}, Mn-55, Fe-{54,56–58}, Cu-{63,65}, and U-{234,235,236,238}. Thermal scattering data for H in H_2O and for H in CH_2 is used.

leu-comp-therm-002 (5 cases)

- Water moderated UO_2 fuel rods, aluminium clad, in square arrays (pitch 2.54 cm, Pacific Northwest Laboratories). The shape of the rod cluster was varied, as well as the distance between clusters (for cases 4 and 5).
- The uranium enrichment was 4.31% ^{235}U .
- The isotopes in these benchmark models are H-1, C-nat, O-16, Mg-{24–26}, Al-27, Si-{28–30}, S-{32–34,36}, Ca-{40,42–44,46,48}, Ti-{46–50}, Cr-{50,52–54}, Mn-55, Fe-{54,56–58}, Cu-{63,65}, U-{234,235,236,238}. Thermal scattering data for H in H_2O and for H in CH_2 is used.

leu-comp-therm-003 (22 cases)

- Water moderated UO_2 fuel rods, aluminium clad, in square arrays (pitch 1.684 cm), with gadolinium impurity in water (Pacific Northwest Laboratories). The shape of the rod clusters was varied, as well as the distance between clusters.
- The uranium enrichment was 2.35% ^{235}U .
- The isotopes in these benchmark models are H-1, C-nat, O-16, Mg-{24–26}, Al-27, Si-{28–30}, Ti-{46–50}, Cr-{50,52–54}, Mn-55, Fe-{54,56–58}, Cu-{63,65}, Gd-{152,154–158,160}, U-{234,235,236,238}. Thermal scattering data for H in H_2O and for H in CH_2 is used.

leu-comp-therm-005 (16 cases)

- UO_2 fuel rods, aluminium clad, in water containing dissolved gadolinium (Pacific Northwest Laboratories, early 1980s). The lattice pitch and the gadolinium concentration were varied.
- The uranium enrichment was 2.35% ^{235}U (cases 1–13) and 4.31% ^{235}U (cases 14–16).
- The isotopes in these benchmark models are H-1, C-nat, N-14, O-16, Mg-{24–26}, Al-27, Si-{28–30}, S-{32–34,36}, Ca-{40,42–44,46,48}, Ti-{46–50}, Cr-{50,52–54}, Mn-55, Fe-{54,56–58}, Cu-{63,65}, Gd-{152,154–158,160}, U-{234,235,236,238}. Thermal scattering data for H in H_2O and for H in CH_2 is used.

leu-comp-therm-006 (18 cases)

- Arrays of UO_2 fuel rods with water-to-fuel ratios from 1.5 to 3.0 in a Tank-type Critical Assembly (TCA, Japan, 1963–1975). The lattice pitch and the number of fuel rods were varied.
- The uranium enrichment was 2.6% ^{235}U .
- The isotopes in these benchmark models are H-1, O-16, Al-27, U-{234,235,238}. Thermal scattering data for H in H_2O is used.

leu-comp-therm-007 (10 cases)

- Water moderated UO_2 fuel rod arrays (Valduc, 1978). In four cases the arrays were square, with varying pitch. In the other cases the arrays had a triangular pitch, with either hexagonal or pseudo-cylindrical section, and with varying pitch.
- The uranium enrichment was 4.738% ^{235}U .
- The isotopes in these benchmark models are H-1, B-{10,11}, C-nat, N-14, O-16, Mg-

{24–26}, Al-27, Si-{28–30}, P-31, S-{32–34,36}, Cr-{50,52–54}, Mn-55, Fe-{54,56–58}, Ni-{58,60–62,64}, Zn-nat, U-{234,235,236,238}.

Thermal scattering data for H in H₂O is used.

leu-comp-therm-009 (27 cases)

- Clusters of aluminium-clad UO₂ fuel rods in a large water-filled tank (Pacific Northwest Laboratories, 1977). There were three square-pitched clusters with two absorber plates in between. These plates were stainless steel, borated stainless steel, boral, copper, copper with 1% cadmium, cadmium, aluminium or zircaloy-4.
- The uranium enrichment was 4.3% ²³⁵U.
- The isotopes in these benchmark models are H-1, C-nat, O-16, Na-23, Mg-{24–26}, Al-27, Si-{28–30}, S-{32–34,36}, Ca-{40,42–44,46,48}, Ti-{46–50}, Cr-{50,52–54}, Mn-55, Fe-{54,56–58}, Cu-{63,65}, and U-{234,235,236,238}. Thermal scattering data for H in H₂O and for H in CH₂ is used.

In some cases Na-23 (case 9 – 13) is present, in others B-{10,11} (case 5 – 9, 14, 15), Cd-{106,108,110–114,116} (case 14 – 23), Ni-{58,60–62,64} (cases 1 – 9, 14, 15), Mo-{92,94–98,100} (cases 1 – 8), Sn-{112,114–120,122,124} (cases 14, 15, 26, 27), and Zr-{90–92,94,96} (cases 26, 27).

leu-comp-therm-010 (30 cases)

- Rectangular clusters of water moderated UO₂ fuel rods, reflected by two lead, uranium or steel walls. Also the pitch and the number of fuel rods were varied.
- The uranium enrichment was 4.31% ²³⁵U.
- The isotopes in these benchmark models are H-1, C-nat, O-16, Mg-{24–26}, Al-27, Si-{28–30}, P-31, S-{32–34,36}, Ca-{40,42–44,46,48}, Ti-{46–50}, Cr-{50,52–54}, Mn-55, Fe-{54,56–58}, Ni-{58,60–62,64}, Cu-{63,65}, Mo-{92,94–98,100}, Pb-{206–208}, U-{234,235,236,238}. Thermal scattering data for H in H₂O and for H in CH₂ is used.

leu-comp-therm-016 (32 cases)

- Low enriched uranium pin assemblies placed in water and separated by absorber plates. The absorber material was steel, borated steel, boral, copper, copper with cadmium, cadmium, aluminium or zircaloy-4.
 - The uranium enrichment was 93% ²³⁵U.
 - The isotopes in these benchmark models are H-1, C-nat, O-16, Mg-{24–26}, Al-27, Si-{28–30}, Ti-{46–50}, Cr-{50,52–54}, Mn-55, Fe-{54,56–58}, Cu-{63,65}, and U-{234,235,236,238}. Thermal scattering data for H in H₂O and for H in CH₂ is used.
- In some cases B-{10,11} is also present (cases 8 – 14, 20), in others Na-23 (cases 12 – 19), S-{32–34,36} (cases 12 – 19, 28 – 30), Ni-{58,60–62,64} (cases 1 – 14, 20), Zr-{90–92,94,96} (cases 31, 32), Mo-{92,94–98,100} (cases 1 – 11), Cd-{106,108,110–114,116} (cases 20 – 27), and Sn-{112,114–120,122,124} (cases 20, 31, 32).

leu-comp-therm-017 (19 cases)

- Low enriched uranium pin assemblies placed in water and reflected by steel or lead reflector plates. The separation between the clusters and the distance between the fuel and the reflector were varied.
- The uranium enrichment was 2.35% ²³⁵U.
- The isotopes in these benchmark models are H-1, C-nat, O-16, Mg-{24–26}, Al-27, Si-{28–30}, Ti-{46–50}, Cr-{50,52–54}, Mn-55, Fe-{54,56–58}, Cu-{63,65} and U-

{234,235,236,238}. Thermal scattering data for H in H₂O and for H in CH₂ is used.
In cases 1–3, 23–25 there is also Pb-{206–208}, in the other cases there P-31, S-{32–34,36}, Ni-{58,60–62,64}, and Mo-{92,94–98,100}.

leu-comp-therm-019 (3 cases)

- Water-moderated hexagonally pitched lattices with low enriched cylindrical fuel rods with stainless steel cladding (RRC Kurchatov Institute, 1961). The pitch of the lattice was varied.
- The uranium enrichment was 5% ²³⁵U.
- The isotopes in these benchmark models are H-1, C-nat, O-16, Mg-{24–26}, Al-27, Si-{28–30}, Ti-{46–50}, Cr-{50,52–54}, Mn-55, Fe-{54,56–58}, Ni-{58,60–62,64}, Cu-{63,65}, and U-{234,235,236,238}. Thermal scattering data for H in H₂O is used.

leu-comp-therm-039 (17 cases)

- Incomplete arrays of water moderated and reflected UO₂ fuel rods (Valduc, 1978). All arrays were square, with a varying number of positions not filled.
- The uranium enrichment was 4.738% ²³⁵U.
- The isotopes in these benchmark models are H-1, B-{10,11}, C-nat, N-14, O-16, Mg-{24–26}, Al-27, Si-{28–30}, P-31, S-{32–34,36}, Cr-{50,52–54}, Mn-55, Fe-{54,56–58}, Ni-{58,60–62,64}, Zn-nat, U-{234,235,236,238}.
Thermal scattering data for H in H₂O is used.

leu-comp-therm-051 (19 cases)

- Aluminium-clad uranium oxide in 9 assemblies of 14×14 fuel rods. (Babcock-Wilcox Lynchberg Research Center, 1978-79). The moderator and reflector was borated water, and the absorbers were stainless steel and boron. The loading pattern, water height and boron concentration were varied.
- The uranium enrichment was 2.5% ²³⁵U.
- The isotopes in these benchmark models are H-1, B-10, B-11, O-16, Mg-{24–26}, Al-27, Si-{28–30}, Ti-{46–50}, Cr-{50,52–54}, Mn-55, Fe-{54,56–58}, Cu-{63,65}, and U-{234,235,236,238}. Thermal scattering data for H in H₂O is used.
For cases 2 – 9 there are also: C-nat, P-31, S-{32–34,36}, Co-59, Ni-{58,60–62,64}, and Mo-{92,94–98,100}.

leu-comp-therm-060 (28 cases)

- Configurations of UO₂ fuel assemblies in an RBMK-type graphite moderated reactor. Some configurations had empty channels, some had water in the fuel channels, and some had boron or thorium absorber rods. Also the enrichment was varied.
- The uranium enrichment was 1.8% ²³⁵U (cases 1 and 2), 2.4% ²³⁵U (cases 5 and 6) or 2.0% ²³⁵U (all other cases).
- The isotopes in these benchmark models are H-1, B-{10,11}, C-nat, N-14, O-16, F-19, Mg-{24–26}, Al-27, Si-{28–30}, P-31, S-{32–34,36}, Ca-{40,42–44,46,48}, Ti-{46–50}, V-nat, Cr-{50,52–54}, Mn-55, Fe-{54,56–58}, Ni-{58,60–62,64}, Cu-{63,65}, As-75, Zr-{90–92,94,96}, Nb-93, Mo-{92,94–98,100}, Ag-{107,109}, Cd-{106,108,110–114,116}, Sn-{112,114–120,122,124}, Hf-{174,176–180}, W-{182–184,186}, Au-197, Pb-{206–208}, Bi-209, Th-{230,232}, U-{234,235,236,238}. Thermal scattering data for graphite and for H in H₂O is used.

Dimple (1 case)

- Assembly S01A, a cylindrical arrangement of uranium dioxide fuel pins on a square pitch of 1.32 cm, water moderated and reflected (Winfrith, UK) [4].
- The uranium enrichment was 3% ^{235}U .
- The isotopes in these benchmark models are H-{1,2}, C-nat, N-14 O-16 Mg-{24–26}, Al-27, Si-{28–30}, P-31 S-{32–34,36}, Cl-{35,37}, Ti-{46–50}, V-nat, Cr-{50,52–54}, Mn-55 Fe-{54,56–58}, Co-nat, Ni-{58,60–62,64}, Cu-{63,65}, Sr-{84,86–88}, Nb-93 Mo-{92,94–98,100}, Sn-{112,114–120,122,124}, U-{234,235,236,238}. Thermal scattering data for graphite and for H in H_2O and for H in CH_2 is used.

TRX (2 cases)

- Light-water moderated UO_2 pins with aluminium cladding in a hexagonal lattice [5]. The pitch was 1.806 cm (case 1) or 2.174 cm (case 2).
- The uranium enrichment was 1.3% ^{235}U .
- The isotopes in these benchmark models are H-1, O-16, Al-27, Fe-{54,56–58}, U-{235,238}. Thermal scattering data for graphite and for H in H_2O is used.

leu-met-therm-001 (1 case)

- A natural uranium, heavy water moderated critical assembly (Yugoslavia, 1958).
- The uranium enrichment was 0.72% ^{235}U .
- The isotopes in this benchmark model are H-{1,2}, B-{10,11}, C-nat, N-14, O-16, Mg-{24–26}, Al-27, Si-{28–30}, Ti-{46–50}, Cr-{50,52–54}, Mn-55, Fe-{54,56–58}, Ni-{58,60–62,64}, Cu-{63,65}, Cd-{106,108,110–114,116}, U-{234,235,238}. Thermal scattering data for D in D_2O and for H in H_2O is used.

leu-sol-therm-001 (1 case, 'Sheba-II')

- An unreflected $\text{UO}_2\text{F}_2+\text{H}_2\text{O}$ cylindrical assembly (LANL).
- The uranium enrichment was 5% ^{235}U .
- The isotopes in this benchmark model are H-1, N-14, O-16, F-19, Cr-{50,52–54}, Mn-55, Fe-{54,56–58}, Ni-{58,60–62,64}, U-{234,235,236,238}. Thermal scattering data for H in H_2O is used.

leu-sol-therm-003 (9 cases)

- Full and truncated bare spheres of 10% enriched uranyl nitrate water solutions (Obninsk, 1965). The uranium concentration and the sphere diameters were varied.
- The uranium enrichment was 10% ^{235}U .
- The isotopes in these benchmark models are H-1, N-14, O-16, Si-{28–30}, Ti-{46–50}, Cr-{50,52–54}, Mn-55, Fe-{54,56–58}, Ni-{58,60–62,64}, U-{234,235,238}. Thermal scattering data for H in H_2O is used.

leu-sol-therm-004 (7 cases)

- Water reflected uranyl nitrate solution in a 60 cm cylindrical water tank (STACY, Japan, 1995). The uranium concentration was varied.
- The uranium enrichment was 10% ^{235}U .
- The isotopes in these benchmark models are H-1, C-nat, N-14, O-16, Si-{28–30}, P-31, S-{32–34,36}, Cr-{50,52–54}, Mn-55, Fe-{54,56–58}, Ni-{58,60–62,64}, U-{234,235,236,238}. Thermal scattering data for H in H_2O is used.

leu-sol-therm-007 (5 cases)

- Unreflected uranyl nitrate solution in a 60 cm cylindrical water tank (STACY, Japan, 1995).

The uranium concentration was varied.

- The uranium enrichment was 10% ^{235}U .
- The isotopes in these benchmark models are H-1, C-nat, N-14, O-16, Si-{28–30}, P-31, S-{32–34,36}, Cr-{50,52–54}, Mn-55, Fe-{54,56–58}, Ni-{58,60–62,64}, U-{234,235,236,238}. Thermal scattering data for H in H_2O is used.

leu-sol-therm-016 (7 cases)

- Water reflected slabs (28 cm) of uranyl nitrate solutions (STACY, Japan, 1997). The uranium concentration was varied.
- The uranium enrichment was 10% ^{235}U .
- The isotopes in these benchmark models are H-1, C-nat, N-14, O-16, Si-{28–30}, P-31, S-{32–34,36}, Cr-{50,52–54}, Mn-55, Fe-{54,56–58}, Ni-{58,60–62,64}, U-{234,235,236,238}. Thermal scattering data for H in H_2O is used.

leu-sol-therm-017 (6 cases)

- Unreflected slabs (28 cm) of uranyl nitrate solutions (STACY, Japan, 1997). The uranium concentration was varied.
- The uranium enrichment was 10% ^{235}U .
- The isotopes in these benchmark models are H-1, C-nat, N-14, O-16, Si-{28–30}, P-31, S-{32–34,36}, Cr-{50,52–54}, Mn-55, Fe-{54,56–58}, Ni-{58,60–62,64}, U-{234,235,236,238}. Thermal scattering data for H in H_2O is used.

leu-sol-therm-018 (6 cases)

- Concrete reflected slabs (28 cm) of uranyl nitrate solutions (STACY, Japan, 1997). The thickness of the reflector was varied.
- The uranium enrichment was 10% ^{235}U .
- The isotopes in these benchmark models are H-1, C-nat, N-14, O-16, Na-23, Mg-{24–26}, Al-27, Si-{28–30}, P-31, S-{32–34,36}, Cl-{35,37}, K-{39–41}, Ca-{40,42–44,46,48}, Cr-{50,52–54}, Mn-55, Fe-{54,56–58}, Ni-{58,60–62,64}, Cu-{63,65}, and U-{234,235,236,238}. Thermal scattering data for H in H_2O is used.

leu-sol-therm-020 (4 cases)

- Water reflected uranyl nitrate solution in a 80 cm cylindrical water tank (STACY, Japan, 1998–1999). The uranium concentration was varied.
- The uranium enrichment was 10% ^{235}U .
- The isotopes in these benchmark models are H-1, C-nat, N-14, O-16, Si-{28–30}, P-31, S-{32–34,36}, Cr-{50,52–54}, Mn-55, Fe-{54,56–58}, Ni-{58,60–62,64}, U-{234,235,236,238}. Thermal scattering data for H in H_2O is used.

leu-sol-therm-021 (4 cases)

- Unreflected uranyl nitrate solution in a 80 cm cylindrical water tank (STACY, Japan, 1998–1999). The uranium concentration was varied.
- The uranium enrichment was 10% ^{235}U .
- The isotopes in these benchmark models are H-1, C-nat, N-14, O-16, Si-{28–30}, P-31, S-{32–34,36}, Cr-{50,52–54}, Mn-55, Fe-{54,56–58}, Ni-{58,60–62,64}, U-{234,235,236,238}. Thermal scattering data for H in H_2O is used.

2.4 PU benchmarks

2.4.1 Fast spectrum

pu-met-fast-001 (1 case, 'Jezebel')

- A bare sphere of plutonium (LANL, 1950s).
- The plutonium-239 enrichment was 95.2% ²³⁹Pu.
- The isotopes in this benchmark model are Ga-nat, Pu-{239,240,241}.

pu-met-fast-002 (1 case, 'Jezebel-240')

- A bare sphere of plutonium (LANL, 1964).
- The plutonium enrichment was 76.4% ²³⁹Pu and 20.1% ²⁴⁰Pu.
- The isotopes in this benchmark model are Ga-nat, Pu-{239,240,241,242}.

pu-met-fast-005 (1 case)

- A critical experiment of a plutonium sphere reflected by tungsten (LANL, 1958).
- The isotopes in these benchmark models are Ni-{58,60–62,64}, Cu-{63,65}, Ga-nat, Zr-{90–92,94,96}, W-{182–184,186}, U-{235,238}, Pu-{239,240,241}.

pu-met-fast-006 (1 case, 'Popsy', 'Flattop-Pu')

- A sphere of plutonium reflected by normal uranium (LANL, 1960s).
- The plutonium enrichment was 94.9% ²³⁹Pu.
- The isotopes in this benchmark model are Ga-nat, U-{234,235,238}, Pu-{239,240,241}.

pu-met-fast-008 (1 case, 'Thor')

- A sphere of plutonium reflected by thorium (LANL, 1961).
- The plutonium enrichment was 94.9% ²³⁹Pu.
- The isotopes in this benchmark model are Ga-nat, Th-232, Pu-{239,240,241}.

pu-met-fast-012 (1 case)

- A cylindrical arrangement of short, close-packed stainless steel clad rods of plutonium metal (97.6 at.% ²³⁹Pu), reflected on all sides by thick depleted uranium (IPPE, Obninsk, 1956).
- The isotopes in these benchmark models are C-nat, Si-{28–30}, Ti-{46–50}, Cr-{50,52–54}, Mn-55, Fe-{54,56–58}, Ni-{58,60–62,64}, Cu-{63,65}, Ga-nat, U-{235,238}, Pu-{238,239,240,241}.

pu-met-fast-013 (1 case)

-
- A cylindrical arrangement of short, close-packed stainless steel clad rods of plutonium metal (97.6 at.% ²³⁹Pu), reflected on all sides by thick copper reflector (IPPE, Obninsk, 1960).
- The isotopes in these benchmark models are C-nat, Si-{28–30}, Ti-{46–50}, Cr-{50,52–54}, Mn-55, Fe-{54,56–58}, Ni-{58,60–62,64}, Cu-{63,65}, Ga-nat, U-{235,238}, Pu-{238,239,240,241}.

2.4.2 Intermediate spectrum

pu-comp-inter-001 (1 case)

- A k_{∞} experiment at the HECTOR reactor (Winfrith, UK, 1960s): a graphite moderated plutonium oxide core (5% ²⁴⁰Pu). The benchmark model is an infinite medium with a material composition appropriate to the interpolated boron/²³⁹Pu ratio.
- The isotopes in these benchmark models are H-1, B-{10,11}, C-nat, O-16, Ca-

{40,42–44,46,48}, U-{235,238}, Pu-{239,240,241,242}.

Thermal scattering data for graphite is used.

pu-met-inter-002 (1 case)

- A cylindrical assembly containing plutonium, carbon and stainless steel, reflected by stainless steel and iron (ANL, ZPR-6 assembly 10, 1981–1982).
- The plutonium enrichment was 95.3% ^{239}Pu .
- The isotopes in these benchmark models are C-nat, Al-27, Si-{28–30}, Cr-{50,52–54}, Co-nat, Mn-55, Fe-{54,56–58}, Ni-{58,60–62,64}, Cu-{63,65}, Mo-{92,94–98,100}, Pu-{238–242}, Am-241.

2.4.3 Thermal spectrum

pu-sol-therm-001 (6 cases)

- Water reflected 11.5 inch diameter spheres of plutonium nitrate solution (Pacific Northwest Laboratories, 1960s). The plutonium concentration was varied.
- The plutonium enrichment was 95% ^{239}Pu .
- The isotopes in these benchmark models are H-1, N-14, O-16, Cr-{50,52–54}, Mn-55, Fe-{54,56–58}, Ni-{58,60–62,64}, Pu-{238,239,240,241,242}. Thermal scattering data for H in H_2O is used.

pu-sol-therm-002 (7 cases)

- Water reflected 12 inch diameter spheres of plutonium nitrate solution (1950s). The plutonium concentration was varied.
- The plutonium enrichment was 96.9% ^{239}Pu .
- The isotopes in these benchmark models are H-1, N-14, O-16, Cr-{50,52–54}, Fe-{54,56–58}, Ni-{58,60–62,64}, Pu-{239,240}. Thermal scattering data for H in H_2O is used.

pu-sol-therm-003 (8 cases)

- Water reflected 13 inch diameter spheres of plutonium nitrate solution (1950s). The plutonium concentration was varied.
- The plutonium enrichment was 98.3% ^{239}Pu (cases 1 and 2) and 96.9% ^{239}Pu (cases 3–7).
- The isotopes in these benchmark models are H-1, N-14, O-16, Al-27, Si-{28–30}, Cr-{50,52–54}, Mn-55, Fe-{54,56–58}, Ni-{58,60–62,64}, Cu-{63,65}, Pu-{239,240}. Thermal scattering data for H in H_2O is used.

pu-sol-therm-004 (13 cases)

- Water reflected 14 inch diameter spheres of plutonium nitrate solution (1950s). The plutonium concentration was varied.
- The plutonium enrichment was 99.5% ^{239}Pu (cases 1–4), 98.25% ^{239}Pu (case 5), and 96.9% ^{239}Pu (cases 6–13).
- The isotopes in these benchmark models are H-1, N-14, O-16, Cr-{50,52–54}, Fe-{54,56–58}, Ni-{58,60–62,64}, Pu-{239,240}. Thermal scattering data for H in H_2O is used.

pu-sol-therm-005 (9 cases)

- Water reflected 14 inch diameter spheres of plutonium nitrate solution (1950s). The plutonium concentration was varied.
- The plutonium enrichment was 96.0% ^{239}Pu (cases 1–7), and 95.6% ^{239}Pu (cases 8 and 9).
- The isotopes in these benchmark models are H-1, N-14, O-16, Cr-{50,52–54}, Fe-

{54,56–58}, Ni-{58,60–62,64}, Pu-{239,240}. Thermal scattering data for H in H₂O is used.

pu-sol-therm-006 (3 cases)

- Water reflected 15 inch diameter spheres of plutonium nitrate solution (1950s). The plutonium concentration was varied.
- The plutonium enrichment was 96.9% ²³⁹Pu.
- The isotopes in these benchmark models are H-1, N-14, O-16, Cr-{50,52–54}, Fe-{54,56–58}, Ni-{58,60–62,64}, Pu-{239,240}. Thermal scattering data for H in H₂O is used.

pu-sol-therm-007 (8 cases)

- Water reflected 11.5 inch diameter spheres partly filled with plutonium nitrate solution (Pacific Northwest Laboratories, 1960s). The plutonium concentration was varied.
- The plutonium enrichment was 95% ²³⁹Pu.
- The isotopes in these benchmark models are H-1, N-14, O-16, Cr-{50,52–54}, Mn-55, Fe-{54,56–58}, Ni-{58,60–62,64}, Pu-{238,239,240,241,242}. Thermal scattering data for H in H₂O is used.

pu-sol-therm-008 (29 cases)

- Concrete reflected 14 inch diameter spheres of plutonium nitrate solution (Pacific Northwest Laboratories, 1961–2). The geometry and the thickness of the concrete reflector was varied. Some cases had an extra shell of stainless steel outside the solution tank, inside the reflector. Some others an extra shell of cadmium at that place.
- The plutonium enrichment was 95% ²³⁹Pu.
- The isotopes in these benchmark models are H-1, N-14, O-16, Na-23, Mg-{24–26}, Al-27, Si-{28–30}, K-{39–41}, Ca-{40,42–44,46,48}, Cr-{50,52–54}, Mn-55, Fe-{54,56–58}, Ni-{58,60–62,64}, Cd-{106,108,110–114,116}, Pu-{238,239,240,241,242}. Thermal scattering data for H in H₂O is used.

pu-sol-therm-012 (22 cases)

- Plutonium nitrate solution in a large tank, with and without water reflector (Valduc, 1974). The tank was a right parallelepiped of dimension 130 × 130 × 100 cm³. The water reflector was either on six sides (cases 2–5), on five sides (cases 6–13), or on no sides (cases 14–23). The plutonium concentration was varied.
- The plutonium enrichment was 74% ²³⁹Pu, and 19% ²⁴⁰Pu.
- The isotopes in these benchmark models are H-1, B-10, C-nat, N-14, O-16, Al-27, Si-{28–30}, Cl-{35,37}, Ca-{40,42–44,46,48}, Cr-{50,52–54}, Fe-{54,56–58}, Ni-{58,60–62,64}, Pu-{239,240,241,242}, Am-241. Thermal scattering data for H in H₂O and for H in CH₂ is used.

2.4.4 Mixed spectrum

pu-met-mixed-001 (6 cases)

- Heterogeneous configurations of plutonium, silicon dioxide, and polyethylene (IPPE, Obninsk, 1999–2000). The cores were configured to cover a broad range in neutron spectra.
- The isotopes in these benchmark models are H-1, Li-{6,7}, B-{10,11}, C-nat, N-14, O-16, Na-23, Mg-{24–26}, Al-27, Si-{28–30}, S-32, K-{39,40,41}, Ca-{40,42–44,46,48}, Ti-{46–50}, V-nat, Cr-{50,52–54}, Mn-55, Fe-{54,56–58}, Ni-{58,60–62,64}, Cu-{63,65}, Ga-nat, Mo-{92,94–98,100}, Cd-{106,108,110–114,116}, Pb-{206–208}, U-{235,238}, Pu-

{239,240,241}, Am-241.

Thermal scattering data for H in H₂O is used.

2.5 MIX benchmarks

2.5.1 Fast spectrum

mix-met-fast-011 (4 cases)

- Cylindrical assemblies of mixed fissile plutonium and uranium metal, reflected by graphite (ANL, ZPPR-21 phases B–E, 1990). The ratio of plutonium to uranium was varied.
- The isotopes in these benchmark models are H-1, Li-{6,7}, B-{10,11}, C-nat, N-14, O-16, Na-23, Al-27, Si-{28–30}, Cr-{50,52–54}, Mn-55, Fe-{54,56–58}, Co-nat, Ni-{58,60–62,64}, Cu-{63,65}, Zr-{90–92,94,96}, Mo-{92,94–98,100}, U-{234,235,236,238}, Pu-{238,239,240,241,242}, Am-241.

2.5.2 Intermediate spectrum

No calculations for benchmarks in this category were performed.

2.5.3 Thermal spectrum

mix-comp-therm-012 (33 cases)

- Rectangular parallelepipeds of homogeneous plutonium uranium mixed oxide polystyrene (Pacific Northwest Laboratories, 1970-1972). The cores were either unreflected (cases 20–22 and 31–33) or plexiglas reflected (cases 1–19 and 23–30). The amount of plutonium in the MOX, and the plutonium vector were varied.
- The isotopes in these benchmark models are H-1, C-nat, O-16, U-{235,238}, Pu-{238,239,240,241,242}, Am-241. Thermal scattering data for H in CH₂ is used.

Kritz (2 cases)

- Core 2:19, consisting of light water moderated and reflected square lattices with mixed oxide fuel rods (Studsvik, Sweden, 1970s) [6]. Criticality was obtained at room temperature and at 235.9°C, by adjusting the boron content of the water and by adjusting the water height. The only differences between the cold and the hot case are the densities, the water level, and some slight dimensional changes of the core components.
- The plutonium enrichment was 91% ²³⁹Pu.
- The isotopes in these benchmark models are H-1, B-{10,11}, N-14, O-16, Cr-{50,52–54}, Fe-{54,56–58}, Ni-{58,60–62,64}, Zr-{90–92,94,96}, Sn-{112,114–120,122,124}, U-{235,238}, Pu-{239,240,241,242}, Am-241. Thermal scattering data for H in H₂O is used.

mix-sol-therm-001 (3 cases)

- Critical experiments with mixed plutonium and uranium nitrate solutions in a large cylindrical geometry (PNL, 1980s). The concentration of the solution and the U/Pu ratio was varied.
- The isotopes in these benchmark models are H-1, Li-6, B-10, N-14, O-16, Cr-{50,52–54}, Mn-55, Fe-{54,56–58}, Ni-{58,60–62,64}, Cd-{106,108,110–114,116}, Gd-{152,154–158,160}, U-{234,235,236,238}, Pu-{238,239,240,241,242}, Am-241. Thermal scattering data for H in H₂O is used.

2.6 U233 benchmarks

2.6.1 Fast spectrum

u233-met-fast-001 (1 case, 'Skidoo', 'Jezebel-233')

- A bare sphere of highly enriched uranium-233 metal (LANL, 1961).
- The uranium enrichment was 98% ²³³U.
- The isotopes in these benchmark models are U-{233,234,235,238}.

u233-met-fast-005 (2 cases)

- Highly enriched uranium-233 spheres, reflected by beryllium (LANL, 1958). The mass of the uranium-233 core was 10 kg (case 1) and 7.6 kg (case 2).
- The uranium enrichment was 98% ²³³U.
- The isotopes in these benchmark models are Be-9, O-16, U-{233,234,238}.

u233-met-fast-006 (1 case, 'Flattop-23')

- A highly enriched uranium-233 sphere, reflected by normal uranium (LANL, 1964).
- The uranium enrichment was 98% ²³³U.
- The isotopes in these benchmark models are U-{233,234,235,238}.

2.6.2 Intermediate spectrum

No calculations for benchmarks in this category were performed.

2.6.3 Thermal spectrum

u233-comp-therm-001 (8 cases)

- Cores of ²³⁵UO₂-ZrO₂ and cores of ²³³UO₂-ZrO₂, with blankets of either ²³³UO₂ or ThO₂ (BAPL, 1960s). The moderator was light water. Five assemblies were rectangular (cases 1-5) and three hexagonal (cases 6-8).
- The uranium enrichment was 97% ²³³U for cases 2, 3, 4, 7, and 8, and 93% ²³⁵U for cases 1, 5, and 6.
- The isotopes in these benchmark models are H-1, B-10, C-nat, O-16, Cr-{50,52-54}, Mn-55, Fe-{54,56-58}, Ni-{58,60-62,64}, Zr-{90-92,94,96}, Sn-{112,114-120,122,124}, Gd-{152,154-158,160}, Th-232, U-{233,234,235,238}. Thermal scattering data for H in H₂O and for H in CH₂ is used.

u233-sol-001 (5 cases)

- Unreflected spheres of uranium-233 nitrate solutions (ORNL, 1950s). The amount of boron poison and the uranium concentration was varied.
- The uranium enrichment was 98% ²³³U.
- The isotopes in these benchmark models are H-1, B-{10,11}, N-14, O-16, Al-27, Si-{28-30}, Mn-55, Fe-{54,56-58}, Cu-{63,65}, Th-232, U-{233,234,235,238}. Thermal scattering data for H in H₂O is used.

2.7 Occurrence of elements

In Table 2.1 are listed those elements that are present in a material of a benchmark series, either with more than 1 wt% or with more than 1e-4 atoms per barn-cm. Elements that do not show up in the table are either not at all present in the benchmark models, or only in minor fractions.

H in H ₂ O		(59 benchmark series)
D in D ₂ O	lmt01, hst04	
Be	hcm03	
Be in BeO	hcm03	
C in graphite	lct60, proteus, ict03, hci04, hmm05, pci01, pmm01	
H in ZrH	ict03, hcm03	
H in CH ₂		(26 benchmark series)
H		(75 benchmark series)
Li	mmf11	
Be	hcm03, hst38, hmf05, hmf057, u3mf05	
B		(13 benchmark series)
C		(58 benchmark series)
N		(33 benchmark series)
O		(72 benchmark series)
F	hst04, hst09, hst10, hst39, hmf07, lst01	
Na	lst18, hmm05, hmt18, hst02, hst38, pmm01, pst08, mcf01	
Mg		(30 benchmark series)
Al		(53 benchmark series)
Si		(59 benchmark series)
P	hst02	
S	hst02, lct02, lct05, lct09, lct10, lst18	
Cl	pst12	
K	lst18, hmt18, hmm05, hst02, pmm01, pst08	
Ca		(15 benchmark series)
Ti		(14 benchmark series)
Cr		(59 benchmark series)
Mn		(54 benchmark series)
Fe		(77 benchmark series)
Ni		(62 benchmark series)
Co	lct51	
Cu		(18 benchmark series)
Ga	pmf01, pmf02, pmf05, pmf06, pmf08, pmf12, pmf13, pmm01	
Zr	lct09, lct16, lct60, ict03, hci05, hcm03, pmf05, kritz, mmf11, u3ct01	
Nb	lct60, imf07, hcm03	
Mo	ict03, hmt16, hst42, hci05, hcm03, hmf05	
Cd	lct09, lct16, ict02, hst38, hmt06, hmm05, pst08, pmm01	
Sn	lct09, kritz, u3ct01	
Gd	ict02, hmt10, hmt16	
W	imf14, hmf60, hmf67, hcm03, pmf05	
Pb	lct10, lct17, hst38, hmf27, hmf57, hmf64	
Th	lct60, ici01, pmf08, u3ct01	
U		(87 benchmark series)
Pu		(24 benchmark series)

Table 2.1 A list of elements and the benchmark series in which these elements are present in *a* material, either with more than 1 wt% or with more than 1e-4 atoms per barn-cm.

3. Results of validation calculations

In this Section we report all the k_{eff} results of the calculations. In the following subsections, the results are given in graphical and tabular form. The columns contain the following items.

1. The benchmark value for k_{eff} , and its uncertainty in pcm between brackets. These values were obtained from Refs [2, 3, 4, 5, 6].
2. Results from calculations based on JEFF-3.0
3. The results of the present work, based on JEFF-3.1.
4. The values for the third column divided by the first column (including uncertainty).
5. The benchmark name

3.1 HEU results

3.1.1 Fast spectrum

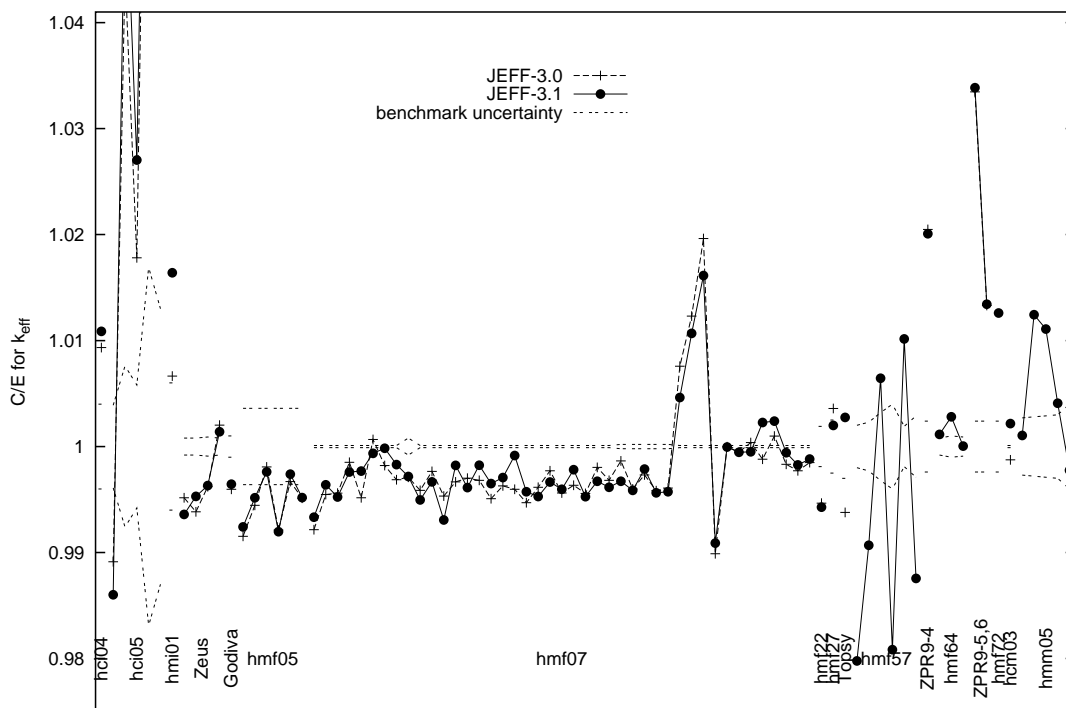


Figure 3.1 Results for the HEU benchmarks with a fast or intermediate spectrum

benchmark	JEFF-3.0	JEFF-3.1	C/E (JEFF-3.1)	name
1.00000(100)	0.99596(40)	0.99644(19)	0.99644(102)	heu-met-fast-001_bare-sphere
1.00000(360)	0.99153(69)	0.99242(72)	0.99242(367)	heu-met-fast-005_case-1
1.00070(360)	0.99515(60)	0.99586(70)	0.99516(367)	heu-met-fast-005_case-2
0.99960(360)	0.99767(80)	0.99721(79)	0.99761(369)	heu-met-fast-005_case-3
0.99890(360)	0.99103(69)	0.99087(87)	0.99196(371)	heu-met-fast-005_case-4
0.99800(360)	0.99470(80)	0.99540(78)	0.99739(369)	heu-met-fast-005_case-5

continued on next page

benchmark	JEFF-3.0	JEFF-3.1	C/E (JEFF-3.1)	name
0.99870(360)	0.99384(70)	0.99389(71)	0.99518(367)	heu-met-fast-005_case-6
0.99710(10)	0.98927(66)	0.99045(64)	0.99333(65)	heu-met-fast-007_case-1
0.99860(10)	0.99408(63)	0.99500(71)	0.99639(72)	heu-met-fast-007_case-2
1.00120(10)	0.99680(74)	0.99643(74)	0.99524(75)	heu-met-fast-007_case-3
0.99700(10)	0.99551(74)	0.99460(66)	0.99759(67)	heu-met-fast-007_case-4
1.00000(10)	0.99517(70)	0.99768(70)	0.99768(71)	heu-met-fast-007_case-5
1.00280(10)	1.00346(74)	1.00215(70)	0.99935(71)	heu-met-fast-007_case-6
0.99960(10)	0.99781(84)	0.99944(75)	0.99984(76)	heu-met-fast-007_case-7
0.99920(10)	0.99607(79)	0.99750(73)	0.99830(74)	heu-met-fast-007_case-8
1.00170(80)	0.99880(74)	0.99888(76)	0.99718(110)	heu-met-fast-007_case-9
1.00000(10)	0.99587(90)	0.99497(79)	0.99497(80)	heu-met-fast-007_case-10
0.99820(10)	0.99586(89)	0.99487(87)	0.99666(88)	heu-met-fast-007_case-11
0.99510(10)	0.99045(76)	0.98820(90)	0.99307(92)	heu-met-fast-007_case-12
1.00090(10)	0.99756(91)	0.99912(89)	0.99822(90)	heu-met-fast-007_case-13
0.99830(10)	0.99532(87)	0.99444(92)	0.99613(93)	heu-met-fast-007_case-14
0.99780(10)	0.99462(89)	0.99604(95)	0.99824(96)	heu-met-fast-007_case-15
0.99880(10)	0.99389(85)	0.99530(94)	0.99650(95)	heu-met-fast-007_case-16
0.99720(10)	0.99349(90)	0.99429(90)	0.99708(91)	heu-met-fast-007_case-17
0.99910(10)	0.99507(96)	0.99825(98)	0.99915(99)	heu-met-fast-007_case-18
0.99830(10)	0.99301(64)	0.99405(68)	0.99574(69)	heu-met-fast-007_case-19
0.99810(10)	0.99426(79)	0.99339(67)	0.99528(68)	heu-met-fast-007_case-20
0.99870(10)	0.99641(70)	0.99535(79)	0.99665(80)	heu-met-fast-007_case-21
0.99940(10)	0.99502(74)	0.99537(73)	0.99597(74)	heu-met-fast-007_case-22
0.99930(10)	0.99564(70)	0.99711(85)	0.99781(86)	heu-met-fast-007_case-23
1.00010(10)	0.99567(74)	0.99537(72)	0.99527(73)	heu-met-fast-007_case-24
0.99900(10)	0.99703(80)	0.99572(79)	0.99672(80)	heu-met-fast-007_case-25
0.99970(10)	0.99651(85)	0.99586(97)	0.99616(98)	heu-met-fast-007_case-26
0.99650(20)	0.99515(69)	0.99323(76)	0.99672(79)	heu-met-fast-007_case-27
0.99870(20)	0.99471(75)	0.99457(75)	0.99586(78)	heu-met-fast-007_case-28
0.99780(20)	0.99513(72)	0.99567(83)	0.99787(86)	heu-met-fast-007_case-29
0.99810(20)	0.99395(86)	0.99374(83)	0.99563(86)	heu-met-fast-007_case-30
1.00130(20)	0.99737(86)	0.99702(82)	0.99573(85)	heu-met-fast-007_case-31
0.99590(10)	1.00345(61)	1.00051(62)	1.00463(63)	heu-met-fast-007_case-32
0.99950(10)	1.01180(78)	1.01017(62)	1.01068(62)	heu-met-fast-007_case-33
0.99770(10)	1.01727(68)	1.01380(75)	1.01614(75)	heu-met-fast-007_case-34
1.00110(10)	0.99098(88)	0.99198(82)	0.99089(83)	heu-met-fast-007_case-35
0.99990(10)	0.99988(78)	0.99986(89)	0.99996(90)	heu-met-fast-007_case-36
0.99880(10)	0.99828(95)	0.99826(92)	0.99946(93)	heu-met-fast-007_case-37
1.00000(10)	1.00037(99)	0.99950(93)	0.99950(94)	heu-met-fast-007_case-38
1.00180(10)	1.00060(81)	1.00407(78)	1.00227(78)	heu-met-fast-007_case-39

continued on next page

benchmark	JEFF-3.0	JEFF-3.1	C/E (JEFF-3.1)	name
1.00130(10)	1.00229(88)	1.00370(88)	1.00240(88)	heu-met-fast-007_case-40
0.99940(10)	0.99773(81)	0.99881(108)	0.99941(109)	heu-met-fast-007_case-41
1.00160(10)	0.99931(88)	0.99987(78)	0.99827(79)	heu-met-fast-007_case-42
0.99980(10)	0.99828(93)	0.99862(88)	0.99882(89)	heu-met-fast-007_case-43
1.00000(190)	0.99466(45)	0.99428(42)	0.99428(195)	heu-met-fast-022
1.00000(250)	1.00359(40)	1.00199(40)	1.00199(253)	heu-met-fast-027
1.00000(300)	0.99379(43)	1.00275(51)	1.00275(304)	heu-met-fast-028
1.00000(200)		0.97977(76)	0.97977(215)	heu-met-fast-057_case-1
1.00000(230)		0.99069(65)	0.99069(239)	heu-met-fast-057_case-2
1.00000(320)		1.00645(69)	1.00645(327)	heu-met-fast-057_case-3
1.00000(400)		0.98084(59)	0.98084(404)	heu-met-fast-057_case-4
1.00000(190)		1.01016(63)	1.01016(200)	heu-met-fast-057_case-5
1.00000(290)		0.98755(71)	0.98755(299)	heu-met-fast-057_case-6
0.99550(240)		1.01549(50)	1.02008(246)	heu-met-fast-060
0.99960(80)		1.00075(69)	1.00115(106)	heu-met-fast-064_case-1
0.99960(100)		1.00240(79)	1.00280(127)	heu-met-fast-064_case-2
0.99960(90)		0.99964(73)	1.00004(116)	heu-met-fast-064_case-3
0.99590(240)		1.02962(55)	1.03386(247)	heu-met-fast-067_case-1
0.99380(240)		1.00714(58)	1.01342(248)	heu-met-fast-067_case-2
0.99910(240)		1.01169(74)	1.01260(251)	heu-met-fast-072_case-1

Table 3.1 The results for HEU benchmarks with a fast spectrum

3.1.2 Intermediate spectrum

benchmark	JEFF-3.0	JEFF-3.1	C/E (JEFF-3.1)	name
1.00000(400)	1.00934(52)	1.01087(48)	1.01087(403)	heu-comp-inter-004
1.03200(400)	1.02078(39)	1.01756(33)	0.98601(389)	heu-comp-inter-005_case-1
1.05000(800)	1.09699(44)	1.10783(44)	1.05508(763)	heu-comp-inter-005_case-2
1.03000(600)	1.04833(39)	1.05784(42)	1.02703(584)	heu-comp-inter-005_case-3
1.06400(1800)	1.15813(46)	1.15926(48)	1.08953(1692)	heu-comp-inter-005_case-4
0.99700(1300)	0.91850(42)	0.93460(39)	0.93741(1305)	heu-comp-inter-005_case-5
1.00100(600)	1.00766(46)	1.01742(78)	1.01640(604)	heu-met-inter-001_case-1
0.99770(80)	0.99287(83)	0.99130(78)	0.99359(112)	heu-met-inter-006_case-1
1.00010(80)	0.99394(90)	0.99540(84)	0.99530(116)	heu-met-inter-006_case-2
1.00150(90)	0.99771(87)	0.99780(75)	0.99631(117)	heu-met-inter-006_case-3
1.00160(80)	1.00362(80)	1.00299(76)	1.00139(110)	heu-met-inter-006_case-4

Table 3.2 The results for HEU benchmarks with an intermediate spectrum

3.1.3 Thermal spectrum

benchmark	JEFF-3.0	JEFF-3.1	C/E (JEFF-3.1)	name
1.00100(600)	1.00672(88)	1.00636(84)	1.00535(605)	heu-met-therm-001_simple
1.00100(600)	1.01575(81)	1.00881(90)	1.00780(606)	heu-met-therm-001_detail
1.00000(100)	1.00116(79)	1.00060(78)	1.00060(127)	heu-met-therm-003_case-1

continued on next page

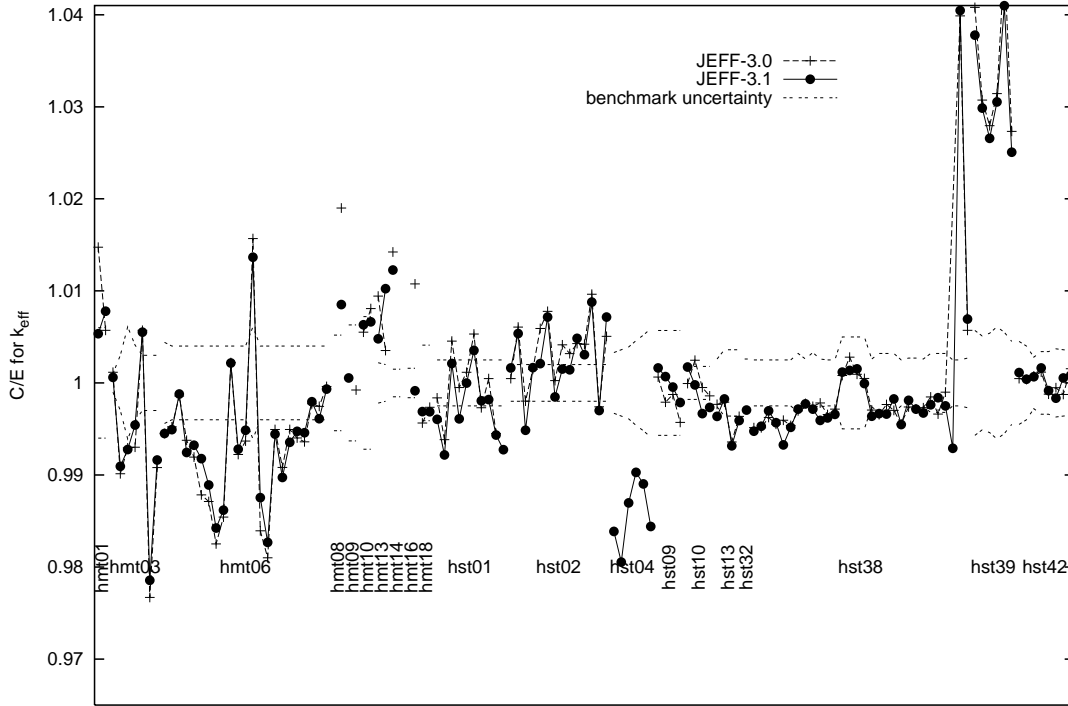


Figure 3.2 Results for the HEU benchmarks with a thermal spectrum

benchmark	JEFF-3.0	JEFF-3.1	C/E (JEFF-3.1)	name
0.99100(300)	0.98122(79)	0.98201(82)	0.99093(314)	heu-met-therm-003_case-2
0.98260(600)	0.97567(91)	0.97550(79)	0.99277(616)	heu-met-therm-003_case-3
0.98760(400)	0.98071(78)	0.98309(92)	0.99543(416)	heu-met-therm-003_case-4
0.99300(300)	0.99867(90)	0.99847(91)	1.00551(316)	heu-met-therm-003_case-5
0.98890(300)	0.96585(94)	0.96769(85)	0.97855(316)	heu-met-therm-003_case-6
0.99190(300)	0.98277(85)	0.98360(87)	0.99163(315)	heu-met-therm-003_case-7
1.00000(440)	0.99450(100)	0.99451(94)	0.99451(450)	heu-met-therm-006_case-1
1.00000(400)	0.99522(90)	0.99492(92)	0.99492(411)	heu-met-therm-006_case-2
1.00000(400)	0.99858(80)	0.99879(92)	0.99879(410)	heu-met-therm-006_case-3
1.00000(400)	0.99376(89)	0.99245(90)	0.99245(410)	heu-met-therm-006_case-4
1.00000(400)	0.99194(89)	0.99324(85)	0.99324(409)	heu-met-therm-006_case-5
1.00000(400)	0.98783(79)	0.99177(83)	0.99177(409)	heu-met-therm-006_case-6
1.00000(400)	0.98712(79)	0.98891(75)	0.98891(407)	heu-met-therm-006_case-7
1.00000(400)	0.98251(79)	0.98424(72)	0.98424(407)	heu-met-therm-006_case-8
1.00000(400)	0.98543(69)	0.98618(77)	0.98618(408)	heu-met-therm-006_case-9
1.00000(400)	1.00221(90)	1.00216(72)	1.00216(406)	heu-met-therm-006_case-10
1.00000(400)	0.99223(89)	0.99279(86)	0.99279(409)	heu-met-therm-006_case-11
1.00000(400)	0.99368(80)	0.99486(78)	0.99486(408)	heu-met-therm-006_case-12
1.00000(610)	1.01568(102)	1.01365(89)	1.01365(616)	heu-met-therm-006_case-13
1.00000(400)	0.98394(89)	0.98754(80)	0.98754(408)	heu-met-therm-006_case-14

continued on next page

benchmark	JEFF-3.0	JEFF-3.1	C/E (JEFF-3.1)	name
1.00000(400)	0.98100(78)	0.98268(88)	0.98268(410)	heu-met-therm-006_case-15
1.00000(400)	0.99494(80)	0.99444(68)	0.99444(406)	heu-met-therm-006_case-16
1.00000(400)	0.99082(89)	0.98973(94)	0.98973(411)	heu-met-therm-006_case-17
1.00000(400)	0.99494(90)	0.99355(92)	0.99355(411)	heu-met-therm-006_case-18
1.00000(400)	0.99402(70)	0.99474(77)	0.99474(407)	heu-met-therm-006_case-19
1.00000(400)	0.99360(80)	0.99459(87)	0.99459(409)	heu-met-therm-006_case-20
1.00000(400)	0.99774(90)	0.99796(77)	0.99796(407)	heu-met-therm-006_case-21
1.00000(400)	0.99746(90)	0.99612(87)	0.99612(409)	heu-met-therm-006_case-22
1.00000(400)	0.99961(90)	0.99933(90)	0.99933(410)	heu-met-therm-006_case-23
1.00090(520)	1.00995(85)	1.00942(90)	1.00851(527)	heu-met-therm-008_detail
1.00320(630)	1.00243(92)	1.00373(82)	1.00053(633)	heu-met-therm-009_simple
1.00300(720)	1.01110(78)	1.00933(87)	1.00631(723)	heu-met-therm-010_7.5mil
1.00260(720)	1.00813(87)	1.00926(92)	1.00664(724)	heu-met-therm-010_15mil
1.00210(220)	1.00563(78)	1.00691(75)	1.00480(232)	heu-met-therm-013_625in
0.99830(200)	1.00771(81)	1.00851(91)	1.01023(220)	heu-met-therm-013_15mil
0.99390(150)	1.00804(99)	1.00609(103)	1.01226(182)	heu-met-therm-014_simple
1.00170(160)	0.99850(101)	1.00084(90)	0.99914(183)	heu-met-therm-016_detail
1.00380(410)	1.00115(83)	1.00067(91)	0.99688(418)	heu-met-therm-018_simple
1.00380(410)	0.99943(88)	1.00065(84)	0.99686(417)	heu-met-therm-018_detail
1.00040(600)	0.99877(118)	0.99645(107)	0.99605(609)	heu-sol-therm-001_case-1
1.00210(720)	0.99592(112)	0.99426(117)	0.99218(728)	heu-sol-therm-001_case-2
1.00030(350)	1.00484(128)	1.00241(114)	1.00211(368)	heu-sol-therm-001_case-3
1.00080(530)	1.00030(123)	0.99690(106)	0.99610(540)	heu-sol-therm-001_case-4
1.00010(490)	1.00125(100)	1.00008(84)	0.99998(497)	heu-sol-therm-001_case-5
1.00020(460)	1.00552(90)	1.00374(100)	1.00354(471)	heu-sol-therm-001_case-6
1.00080(400)	0.99810(110)	0.99886(104)	0.99806(413)	heu-sol-therm-001_case-7
0.99980(380)	1.00027(121)	0.99799(113)	0.99819(397)	heu-sol-therm-001_case-8
1.00080(540)	0.99530(119)	0.99513(107)	0.99433(550)	heu-sol-therm-001_case-9
0.99930(540)		0.99205(99)	0.99274(550)	heu-sol-therm-001_case-10
1.00250(580)	1.00297(110)	1.00412(118)	1.00162(590)	heu-sol-therm-002_case-1
1.00280(580)	1.00888(101)	1.00819(117)	1.00537(590)	heu-sol-therm-002_case-2
1.00330(680)	1.00132(100)	0.99814(127)	0.99486(690)	heu-sol-therm-002_case-3
1.00340(690)	1.00489(111)	1.00507(103)	1.00166(695)	heu-sol-therm-002_case-4
1.00180(440)	1.00772(121)	1.00389(92)	1.00209(449)	heu-sol-therm-002_case-5
1.00230(410)	1.01010(111)	1.00948(108)	1.00716(423)	heu-sol-therm-002_case-6
1.00250(500)	1.00275(120)	1.00097(103)	0.99847(509)	heu-sol-therm-002_case-7
1.00300(550)	1.00715(101)	1.00451(106)	1.00151(558)	heu-sol-therm-002_case-8
1.00120(460)	1.00438(90)	1.00263(92)	1.00143(469)	heu-sol-therm-002_case-9
1.00240(500)	1.00669(91)	1.00726(94)	1.00485(507)	heu-sol-therm-002_case-10
1.00170(380)	1.00592(90)	1.00478(101)	1.00307(392)	heu-sol-therm-002_case-11

continued on next page

benchmark	JEFF-3.0	JEFF-3.1	C/E (JEFF-3.1)	name
1.00270(500)	1.01237(101)	1.01150(107)	1.00878(510)	heu-sol-therm-002_case-12
1.00250(550)	0.99990(120)	0.99949(105)	0.99700(559)	heu-sol-therm-002_case-13
1.00310(660)	1.00818(101)	1.01028(117)	1.00716(668)	heu-sol-therm-002_case-14
1.00000(330)		0.98387(97)	0.98387(344)	heu-sol-therm-004_case-1
1.00000(360)		0.98053(111)	0.98053(377)	heu-sol-therm-004_case-2
1.00000(390)		0.98696(103)	0.98696(404)	heu-sol-therm-004_case-3
1.00000(460)		0.99029(108)	0.99029(473)	heu-sol-therm-004_case-4
1.00000(520)		0.98902(121)	0.98902(534)	heu-sol-therm-004_case-5
1.00000(590)		0.98441(114)	0.98441(601)	heu-sol-therm-004_case-6
0.99900(430)	0.99963(111)	1.00063(100)	1.00163(442)	heu-sol-therm-009_case-1
1.00000(390)	0.99790(108)	1.00068(96)	1.00068(402)	heu-sol-therm-009_case-2
1.00000(360)	0.99874(97)	0.99955(107)	0.99955(376)	heu-sol-therm-009_case-3
0.99860(350)	0.99432(94)	0.99647(101)	0.99787(365)	heu-sol-therm-009_case-4
1.00000(290)	0.99994(88)	1.00173(98)	1.00173(306)	heu-sol-therm-010_case-1
1.00000(290)	1.00247(91)	0.99978(100)	0.99978(307)	heu-sol-therm-010_case-2
1.00000(290)	0.99949(89)	0.99666(99)	0.99666(307)	heu-sol-therm-010_case-3
0.99920(290)	0.99780(85)	0.99653(104)	0.99733(308)	heu-sol-therm-010_case-4
1.00120(260)	0.99888(60)	0.99757(59)	0.99637(266)	heu-sol-therm-013_case-1
1.00070(360)	0.99861(60)	0.99896(57)	0.99826(364)	heu-sol-therm-013_case-2
1.00090(360)	0.99448(70)	0.99406(58)	0.99317(364)	heu-sol-therm-013_case-3
1.00030(360)	0.99666(70)	0.99622(68)	0.99592(366)	heu-sol-therm-013_case-4
1.00150(260)		0.99855(37)	0.99705(262)	heu-sol-therm-032_case-1
1.00000(250)	0.99514(50)	0.99475(52)	0.99475(255)	heu-sol-therm-038_case-1
1.00000(250)	0.99513(45)	0.99530(51)	0.99530(255)	heu-sol-therm-038_case-2
1.00000(250)	0.99625(48)	0.99696(52)	0.99696(255)	heu-sol-therm-038_case-3
1.00000(250)	0.99551(50)	0.99568(56)	0.99568(256)	heu-sol-therm-038_case-4
1.00000(250)	0.99595(60)	0.99326(61)	0.99326(257)	heu-sol-therm-038_case-5
1.00000(250)	0.99538(55)	0.99518(55)	0.99518(256)	heu-sol-therm-038_case-6
1.00000(320)	0.99697(53)	0.99716(52)	0.99716(324)	heu-sol-therm-038_case-7
1.00000(260)	0.99777(54)	0.99772(47)	0.99772(264)	heu-sol-therm-038_case-8
1.00000(330)	0.99746(48)	0.99715(53)	0.99715(334)	heu-sol-therm-038_case-9
1.00000(260)	0.99782(59)	0.99593(52)	0.99593(265)	heu-sol-therm-038_case-10
1.00000(250)	0.99656(48)	0.99620(56)	0.99620(256)	heu-sol-therm-038_case-11
1.00000(250)	0.99715(59)	0.99658(63)	0.99658(258)	heu-sol-therm-038_case-12
1.00000(500)	1.00081(56)	1.00117(52)	1.00117(503)	heu-sol-therm-038_case-13
1.00000(500)	1.00280(50)	1.00136(61)	1.00136(504)	heu-sol-therm-038_case-14
1.00000(500)	1.00094(50)	1.00153(48)	1.00153(502)	heu-sol-therm-038_case-15
1.00000(500)	1.00049(54)	0.99994(51)	0.99994(503)	heu-sol-therm-038_case-16
1.00000(260)	0.99705(58)	0.99638(57)	0.99638(266)	heu-sol-therm-038_case-17
1.00000(320)	0.99655(56)	0.99667(56)	0.99667(325)	heu-sol-therm-038_case-18

continued on next page

benchmark	JEFF-3.0	JEFF-3.1	C/E (JEFF-3.1)	name
1.00000(320)	0.99766(64)	0.99662(54)	0.99662(325)	heu-sol-therm-038_case-19
1.00000(320)	0.99702(54)	0.99826(56)	0.99826(325)	heu-sol-therm-038_case-20
1.00000(250)	0.99553(47)	0.99547(50)	0.99547(255)	heu-sol-therm-038_case-21
1.00000(270)	0.99739(52)	0.99811(52)	0.99811(275)	heu-sol-therm-038_case-22
1.00000(270)	0.99718(48)	0.99715(57)	0.99715(276)	heu-sol-therm-038_case-23
1.00000(260)	0.99730(54)	0.99673(46)	0.99673(264)	heu-sol-therm-038_case-24
1.00000(320)	0.99848(49)	0.99763(44)	0.99763(323)	heu-sol-therm-038_case-25
1.00000(320)	0.99661(49)	0.99839(50)	0.99839(324)	heu-sol-therm-038_case-26
1.00000(320)	0.99900(50)	0.99751(53)	0.99751(324)	heu-sol-therm-038_case-27
1.00000(250)		0.99290(58)	0.99290(257)	heu-sol-therm-038_case-28
1.00000(250)	1.03988(55)	1.04047(50)	1.04047(255)	heu-sol-therm-038_case-29
1.00000(270)	1.00572(52)	1.00694(52)	1.00694(275)	heu-sol-therm-038_case-30
1.00000(570)	1.04080(97)	1.03778(100)	1.03778(578)	heu-sol-therm-039_case-1
1.00000(510)	1.03073(93)	1.02986(101)	1.02986(519)	heu-sol-therm-039_case-2
1.00120(540)	1.02917(106)	1.02780(94)	1.02657(547)	heu-sol-therm-039_case-3
1.00180(610)	1.03329(92)	1.03237(97)	1.03052(616)	heu-sol-therm-039_case-4
1.00180(550)	1.04789(94)	1.04286(99)	1.04099(557)	heu-sol-therm-039_case-5
1.00250(450)	1.02990(90)	1.02762(99)	1.02506(459)	heu-sol-therm-039_case-6
0.99570(390)	0.99617(48)	0.99683(47)	1.00113(395)	heu-sol-therm-042_case-1
0.99650(360)	0.99687(53)	0.99690(39)	1.00040(363)	heu-sol-therm-042_case-2
0.99940(280)	1.00016(41)	1.00007(41)	1.00067(283)	heu-sol-therm-042_case-3
1.00000(340)	1.00117(36)	1.00163(40)	1.00163(342)	heu-sol-therm-042_case-4
1.00000(340)	0.99877(29)	0.99916(28)	0.99916(341)	heu-sol-therm-042_case-5
1.00000(370)	0.99948(32)	0.99834(35)	0.99834(372)	heu-sol-therm-042_case-6
1.00000(360)	0.99874(28)	1.00054(23)	1.00054(361)	heu-sol-therm-042_case-7
1.00000(350)	1.00154(24)	1.00082(22)	1.00082(351)	heu-sol-therm-042_case-8

Table 3.3 The results for HEU benchmarks with a thermal spectrum

3.1.4 Mixed spectrum

benchmark	JEFF-3.0	JEFF-3.1	C/E (JEFF-3.1)	name
1.00000(10)	0.99874(77)	1.00217(75)	1.00217(76)	heu-comp-mixed-003_case-5
1.00070(270)		1.00175(88)	1.00105(284)	heu-met-mixed-005_case-1
1.00030(280)		1.01274(85)	1.01244(292)	heu-met-mixed-005_case-2
1.00120(290)		1.01230(90)	1.01109(303)	heu-met-mixed-005_case-3
1.00160(300)		1.00569(81)	1.00408(310)	heu-met-mixed-005_case-4
1.00050(400)		0.99826(86)	0.99776(409)	heu-met-mixed-005_case-5

3.2 IEU results

3.2.1 Fast spectrum

benchmark	JEFF-3.0	JEFF-3.1	C/E (JEFF-3.1)	name
0.99880(90)	0.99636(67)	0.99678(60)	0.99798(108)	ieu-met-fast-001_case-1

continued on next page

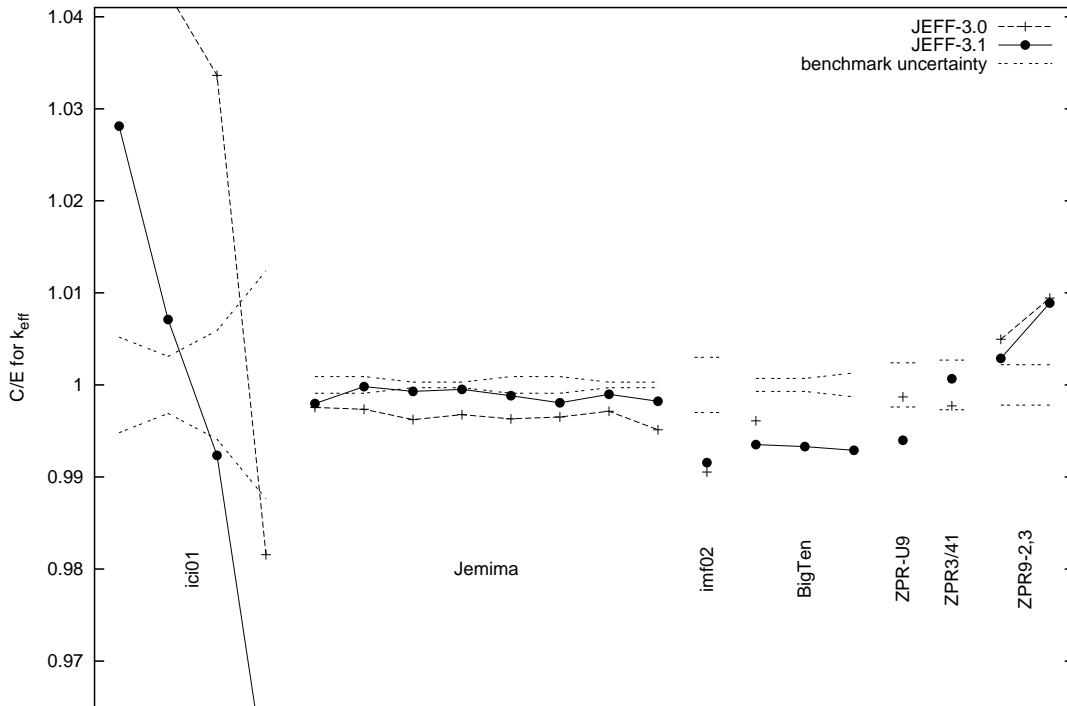


Figure 3.3 Results for the IEU benchmarks with a fast or intermediate spectrum

benchmark	JEFF-3.0	JEFF-3.1	C/E (JEFF-3.1)	name
0.99880(90)	0.99615(62)	0.99861(64)	0.99981(111)	ieu-met-fast-001_case-2
0.99900(30)	0.99523(71)	0.99830(63)	0.99930(70)	ieu-met-fast-001_case-3
0.99900(30)	0.99576(60)	0.99851(70)	0.99951(76)	ieu-met-fast-001_case-4
0.99890(90)	0.99521(72)	0.99773(55)	0.99883(106)	ieu-met-fast-001_case-1i
0.99970(90)	0.99622(67)	0.99775(63)	0.99805(110)	ieu-met-fast-001_case-2i
0.99930(30)	0.99644(59)	0.99828(63)	0.99898(70)	ieu-met-fast-001_case-3i
1.00020(30)	0.99532(70)	0.99843(59)	0.99823(66)	ieu-met-fast-001_case-4i
1.00000(300)	0.99053(59)	0.99156(29)	0.99156(301)	ieu-met-fast-002_case-1
1.00450(70)	1.00058(28)	0.99798(28)	0.99351(75)	ieu-met-fast-007_detail
1.00450(70)		0.99777(27)	0.99330(75)	ieu-met-fast-007_simple
0.99480(130)		0.98774(25)	0.99290(133)	ieu-met-fast-007_twozone
0.99540(240)	0.99411(31)	0.98942(42)	0.99399(245)	ieu-met-fast-010_case-1
1.00070(270)	0.99842(60)	1.00137(63)	1.00067(277)	ieu-met-fast-012_case-1
0.99580(220)	1.00074(27)	0.99868(53)	1.00289(227)	ieu-met-fast-014_case-1
0.99270(220)	1.00206(26)	1.00153(57)	1.00889(229)	ieu-met-fast-014_case-2

Table 3.4 The results for IEU benchmarks with a fast spectrum

3.2.2 Intermediate spectrum

benchmark	JEFF-3.0	JEFF-3.1	C/E (JEFF-3.1)	name
0.96900(500)	1.01364(29)	0.99624(35)	1.02811(517)	ieu-comp-inter-001_case-1
0.98000(300)	1.02175(41)	0.98696(42)	1.00710(309)	ieu-comp-inter-001_case-2

continued on next page

benchmark	JEFF-3.0	JEFF-3.1	C/E (JEFF-3.1)	name
1.01400(600)	1.04810(56)	1.00623(51)	0.99234(594)	ieu-comp-inter-001_case-3
0.96400(1200)	0.94622(60)	0.92252(64)	0.95697(1247)	ieu-comp-inter-001_case-4

Table 3.5 The results for IEU benchmarks with an intermediate spectrum

3.2.3 Thermal spectrum

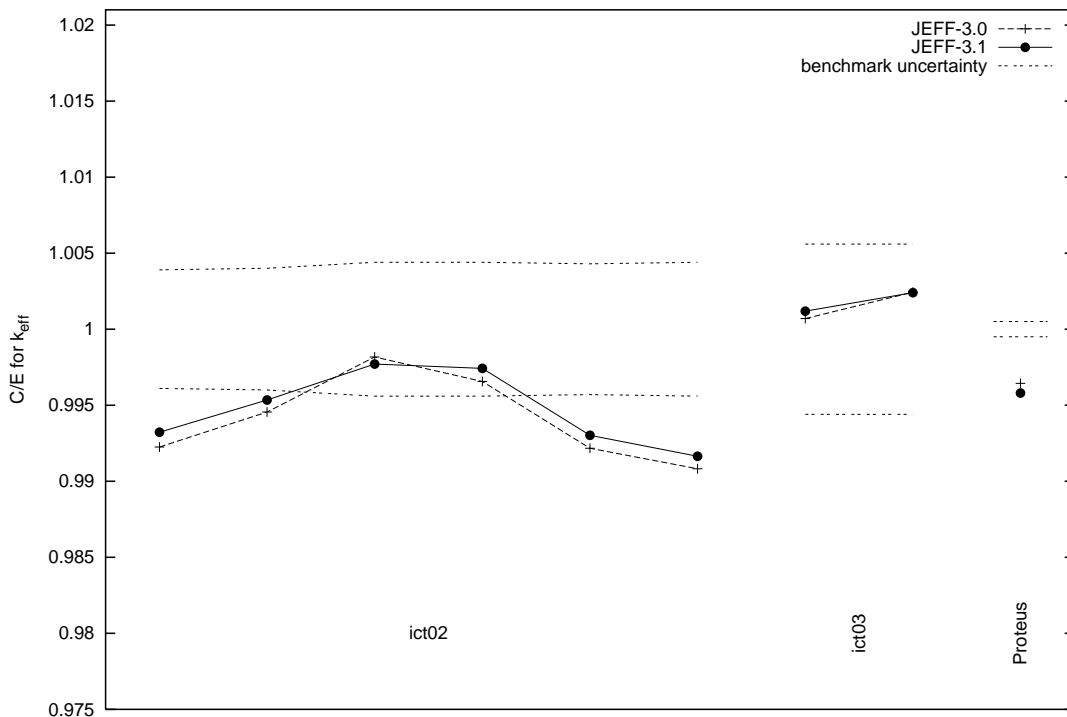


Figure 3.4 Results for the IEU benchmarks with a thermal spectrum

benchmark	JEFF-3.0	JEFF-3.1	C/E (JEFF-3.1)	name
1.00140(390)	0.99364(80)	0.99461(83)	0.99322(398)	ieu-comp-therm-002_case-1
1.00190(400)	0.99644(70)	0.99723(26)	0.99534(400)	ieu-comp-therm-002_case-2
1.00170(440)	0.99987(80)	0.99941(82)	0.99771(447)	ieu-comp-therm-002_case-3
1.00190(440)	0.99845(90)	0.99932(76)	0.99742(446)	ieu-comp-therm-002_case-4
1.00140(430)	0.99356(80)	0.99441(78)	0.99302(437)	ieu-comp-therm-002_case-5
1.00160(440)	0.99241(99)	0.99323(77)	0.99164(446)	ieu-comp-therm-002_case-6
1.00060(560)	1.00130(85)	1.00178(85)	1.00118(566)	ieu-comp-therm-003_core-132
1.00460(560)	1.00704(83)	1.00701(87)	1.00240(564)	ieu-comp-therm-003_core-133
1.01120(50)	1.00760(90)	1.00695(26)	0.99580(56)	ieu-comp-therm-proteus

Table 3.6 The results for IEU benchmarks with a thermal spectrum

3.3 LEU results

3.3.1 Thermal spectrum

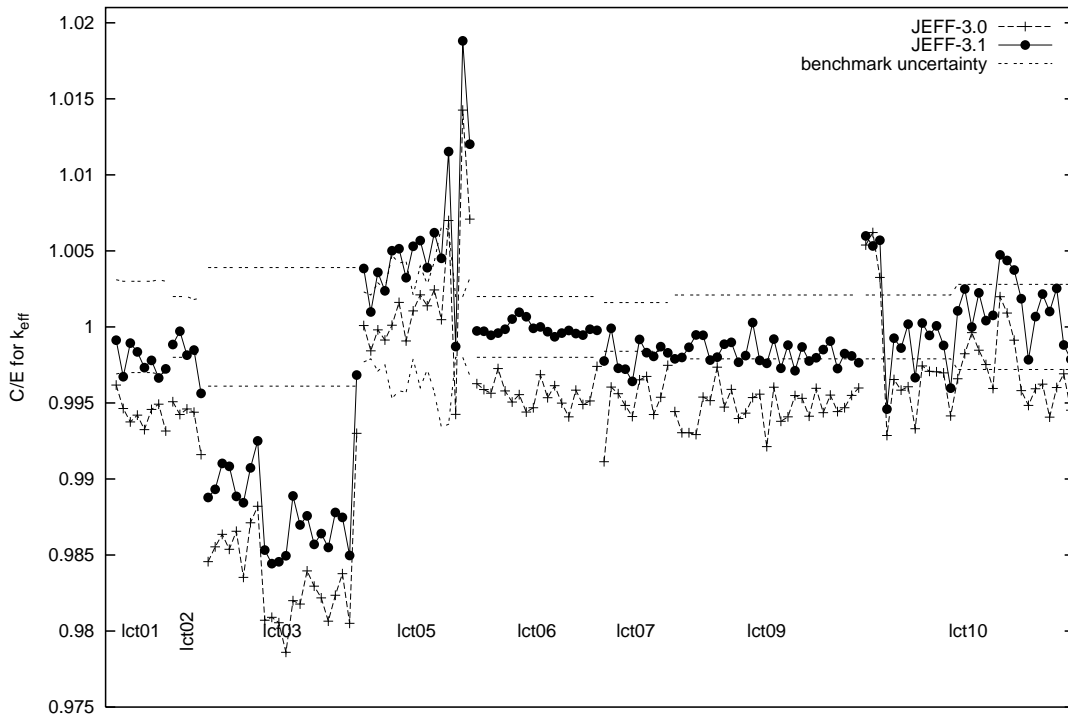


Figure 3.5 Results for the LEU benchmarks with a thermal spectrum

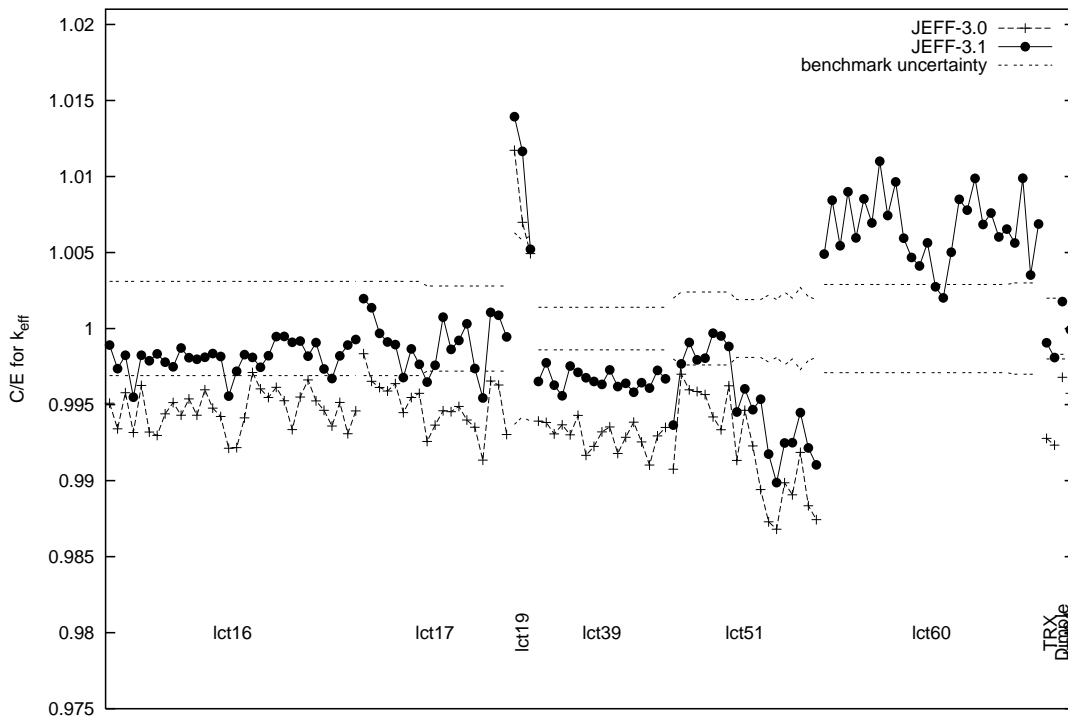


Figure 3.6 Results for the LEU benchmarks with a thermal spectrum (continued)

benchmark	JEFF-3.0	JEFF-3.1	C/E (JEFF-3.1)	name
1.00000(310)	0.99617(70)	0.99913(76)	0.99913(319)	leu-comp-therm-001_case-1

continued on next page

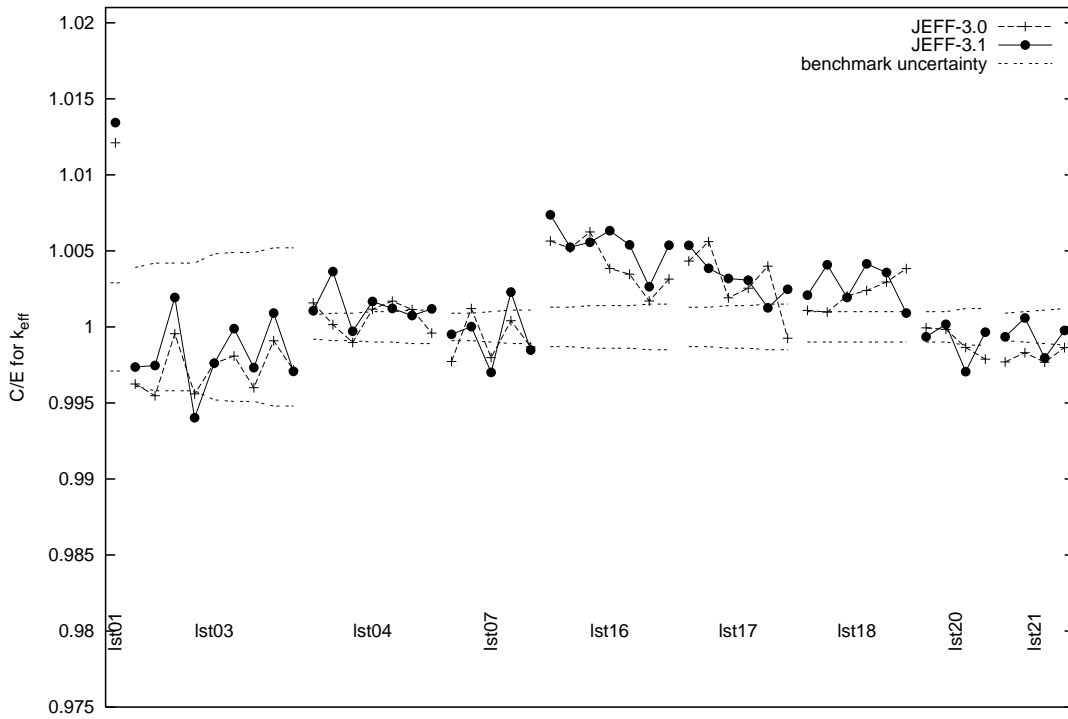


Figure 3.7 Results for the LEU benchmarks with a thermal spectrum (continued)

benchmark	JEFF-3.0	JEFF-3.1	C/E (JEFF-3.1)	name
0.99980(300)	0.99443(70)	0.99652(67)	0.99672(308)	leu-comp-therm-001_case-2
0.99980(300)	0.99355(70)	0.99873(64)	0.99893(307)	leu-comp-therm-001_case-3
0.99980(300)	0.99400(60)	0.99815(68)	0.99835(308)	leu-comp-therm-001_case-4
0.99980(300)	0.99304(70)	0.99712(62)	0.99732(306)	leu-comp-therm-001_case-5
0.99980(300)	0.99437(70)	0.99760(71)	0.99780(308)	leu-comp-therm-001_case-6
0.99980(310)	0.99472(70)	0.99644(67)	0.99664(317)	leu-comp-therm-001_case-7
0.99980(300)	0.99295(70)	0.99704(68)	0.99724(308)	leu-comp-therm-001_case-8
0.99970(200)	0.99478(90)	0.99854(88)	0.99884(219)	leu-comp-therm-002_case-1
0.99970(200)	0.99394(92)	0.99941(81)	0.99971(216)	leu-comp-therm-002_case-2
0.99970(200)	0.99430(82)	0.99784(83)	0.99814(217)	leu-comp-therm-002_case-3
0.99970(180)	0.99409(73)	0.99818(82)	0.99848(198)	leu-comp-therm-002_case-4
0.99970(190)	0.99130(80)	0.99533(78)	0.99563(206)	leu-comp-therm-002_case-5
1.00000(390)	0.98456(80)	0.98878(66)	0.98878(396)	leu-comp-therm-003_case-1
1.00000(390)	0.98554(74)	0.98932(83)	0.98932(399)	leu-comp-therm-003_case-2
1.00000(390)	0.98636(75)	0.99102(72)	0.99102(397)	leu-comp-therm-003_case-3
1.00000(390)	0.98537(77)	0.99083(73)	0.99083(397)	leu-comp-therm-003_case-4
1.00000(390)	0.98656(76)	0.98885(77)	0.98885(398)	leu-comp-therm-003_case-5
1.00000(390)	0.98353(73)	0.98844(78)	0.98844(398)	leu-comp-therm-003_case-6
1.00000(390)	0.98712(76)	0.99073(74)	0.99073(397)	leu-comp-therm-003_case-7
1.00000(390)	0.98820(71)	0.99250(79)	0.99250(398)	leu-comp-therm-003_case-8

continued on next page

benchmark	JEFF-3.0	JEFF-3.1	C/E (JEFF-3.1)	name
1.00000(390)	0.98071(74)	0.98532(70)	0.98532(396)	leu-comp-therm-003_case-9
1.00000(390)	0.98090(90)	0.98443(74)	0.98443(397)	leu-comp-therm-003_case-10
1.00000(390)	0.98055(74)	0.98455(83)	0.98455(399)	leu-comp-therm-003_case-11
1.00000(390)	0.97860(65)	0.98495(60)	0.98495(395)	leu-comp-therm-003_case-12
1.00000(390)	0.98200(74)	0.98888(71)	0.98888(397)	leu-comp-therm-003_case-13
1.00000(390)	0.98177(81)	0.98698(80)	0.98698(398)	leu-comp-therm-003_case-14
1.00000(390)	0.98395(63)	0.98758(76)	0.98758(398)	leu-comp-therm-003_case-15
1.00000(390)	0.98295(69)	0.98570(69)	0.98570(396)	leu-comp-therm-003_case-16
1.00000(390)	0.98218(77)	0.98641(80)	0.98641(398)	leu-comp-therm-003_case-17
1.00000(390)	0.98065(68)	0.98550(66)	0.98550(396)	leu-comp-therm-003_case-18
1.00000(390)	0.98235(78)	0.98780(74)	0.98780(397)	leu-comp-therm-003_case-19
1.00000(390)	0.98377(77)	0.98747(73)	0.98747(397)	leu-comp-therm-003_case-20
1.00000(390)	0.98051(76)	0.98497(67)	0.98497(396)	leu-comp-therm-003_case-21
1.00000(390)	0.99300(78)	0.99683(69)	0.99683(396)	leu-comp-therm-003_case-22
1.00000(230)	1.00009(25)	1.00384(87)	1.00384(246)	leu-comp-therm-005_case-1
1.00000(210)	0.99843(23)	1.00098(80)	1.00098(225)	leu-comp-therm-005_case-2
1.00000(290)	0.99981(24)	1.00359(74)	1.00359(299)	leu-comp-therm-005_case-3
1.00000(250)	0.99914(23)	1.00237(85)	1.00237(264)	leu-comp-therm-005_case-4
1.00000(470)	1.00011(26)	1.00501(71)	1.00501(475)	leu-comp-therm-005_case-5
1.00000(420)	1.00161(27)	1.00514(93)	1.00514(430)	leu-comp-therm-005_case-6
1.00000(430)	0.99908(27)	1.00323(85)	1.00323(438)	leu-comp-therm-005_case-7
1.00000(210)	1.00105(26)	1.00530(73)	1.00530(222)	leu-comp-therm-005_case-8
1.00000(400)	1.00211(23)	1.00568(85)	1.00568(409)	leu-comp-therm-005_case-9
1.00000(280)	1.00139(24)	1.00389(92)	1.00389(295)	leu-comp-therm-005_case-10
1.00000(430)	1.00243(24)	1.00619(88)	1.00619(439)	leu-comp-therm-005_case-11
1.00000(660)	1.00047(27)	1.00451(76)	1.00451(664)	leu-comp-therm-005_case-12
1.00000(640)	1.00700(25)	1.01153(78)	1.01153(645)	leu-comp-therm-005_case-13
1.00000(200)	0.99425(21)	0.99871(78)	0.99871(215)	leu-comp-therm-005_case-14
1.00000(200)	1.01426(24)	1.01881(80)	1.01881(215)	leu-comp-therm-005_case-15
1.00000(320)	1.00709(23)	1.01202(69)	1.01202(327)	leu-comp-therm-005_case-16
1.00000(200)	0.99627(75)	0.99973(23)	0.99973(201)	leu-comp-therm-006_case-1
1.00000(200)	0.99588(75)	0.99971(24)	0.99971(201)	leu-comp-therm-006_case-2
1.00000(200)	0.99564(78)	0.99945(24)	0.99945(201)	leu-comp-therm-006_case-3
1.00000(200)	0.99726(71)	0.99959(25)	0.99959(202)	leu-comp-therm-006_case-4
1.00000(200)	0.99579(68)	0.99985(24)	0.99985(201)	leu-comp-therm-006_case-5
1.00000(200)	0.99506(79)	1.00051(26)	1.00051(202)	leu-comp-therm-006_case-6
1.00000(200)	0.99555(75)	1.00096(23)	1.00096(201)	leu-comp-therm-006_case-7
1.00000(200)	0.99440(88)	1.00067(26)	1.00067(202)	leu-comp-therm-006_case-8
1.00000(200)	0.99468(82)	0.99991(23)	0.99991(201)	leu-comp-therm-006_case-9
1.00000(200)	0.99685(68)	1.00000(22)	1.00000(201)	leu-comp-therm-006_case-10

continued on next page

benchmark	JEFF-3.0	JEFF-3.1	C/E (JEFF-3.1)	name
1.00000(200)	0.99534(71)	0.99968(24)	0.99968(201)	leu-comp-therm-006_case-11
1.00000(200)	0.99613(74)	0.99935(22)	0.99935(201)	leu-comp-therm-006_case-12
1.00000(200)	0.99499(73)	0.99959(24)	0.99959(201)	leu-comp-therm-006_case-13
1.00000(200)	0.99409(74)	0.99976(25)	0.99976(202)	leu-comp-therm-006_case-14
1.00000(200)	0.99584(73)	0.99956(23)	0.99956(201)	leu-comp-therm-006_case-15
1.00000(200)	0.99490(70)	0.99946(20)	0.99946(201)	leu-comp-therm-006_case-16
1.00000(200)	0.99513(74)	0.99985(24)	0.99985(201)	leu-comp-therm-006_case-17
1.00000(200)	0.99740(73)	0.99977(22)	0.99977(201)	leu-comp-therm-006_case-18
1.00000(160)	0.99113(88)	0.99776(41)	0.99776(165)	leu-comp-therm-007_case-1
1.00000(160)	0.99604(94)	0.99991(42)	0.99991(165)	leu-comp-therm-007_case-2
1.00000(160)	0.99561(78)	0.99728(39)	0.99728(165)	leu-comp-therm-007_case-3
1.00000(160)	0.99484(66)	0.99722(33)	0.99722(163)	leu-comp-therm-007_case-4
1.00000(160)	0.99411(87)	0.99642(42)	0.99642(165)	leu-comp-therm-007_case-5
1.00000(160)	0.99652(88)	0.99918(45)	0.99918(166)	leu-comp-therm-007_case-6
1.00000(160)	0.99674(84)	0.99830(40)	0.99830(165)	leu-comp-therm-007_case-7
1.00000(160)	0.99424(87)	0.99806(45)	0.99806(166)	leu-comp-therm-007_case-8
1.00000(160)	0.99537(89)	0.99870(38)	0.99870(164)	leu-comp-therm-007_case-9
1.00000(160)	0.99747(81)	0.99829(42)	0.99829(165)	leu-comp-therm-007_case-10
1.00000(210)	0.99443(80)	0.99790(76)	0.99790(223)	leu-comp-therm-009_case-1
1.00000(210)	0.99304(79)	0.99799(71)	0.99799(222)	leu-comp-therm-009_case-2
1.00000(210)	0.99304(79)	0.99866(87)	0.99866(227)	leu-comp-therm-009_case-3
1.00000(210)	0.99292(79)	0.99947(70)	0.99947(221)	leu-comp-therm-009_case-4
1.00000(210)	0.99538(80)	0.99945(79)	0.99945(224)	leu-comp-therm-009_case-5
1.00000(210)	0.99515(80)	0.99782(81)	0.99782(225)	leu-comp-therm-009_case-6
1.00000(210)	0.99735(80)	0.99801(81)	0.99801(225)	leu-comp-therm-009_case-7
1.00000(210)	0.99472(80)	0.99886(83)	0.99886(226)	leu-comp-therm-009_case-8
1.00000(210)	0.99589(85)	0.99898(75)	0.99898(223)	leu-comp-therm-009_case-9
1.00000(210)	0.99397(90)	0.99768(88)	0.99768(228)	leu-comp-therm-009_case-10
1.00000(210)	0.99433(80)	0.99811(79)	0.99811(224)	leu-comp-therm-009_case-11
1.00000(210)	0.99535(70)	1.00028(84)	1.00028(226)	leu-comp-therm-009_case-12
1.00000(210)	0.99558(80)	0.99780(70)	0.99780(221)	leu-comp-therm-009_case-13
1.00000(210)	0.99213(79)	0.99760(77)	0.99760(224)	leu-comp-therm-009_case-14
1.00000(210)	0.99603(80)	0.99920(77)	0.99920(224)	leu-comp-therm-009_case-15
1.00000(210)	0.99379(89)	0.99728(78)	0.99728(224)	leu-comp-therm-009_case-16
1.00000(210)	0.99409(80)	0.99880(72)	0.99880(222)	leu-comp-therm-009_case-17
1.00000(210)	0.99548(70)	0.99712(74)	0.99712(223)	leu-comp-therm-009_case-18
1.00000(210)	0.99530(80)	0.99868(73)	0.99868(222)	leu-comp-therm-009_case-19
1.00000(210)	0.99413(90)	0.99776(84)	0.99776(226)	leu-comp-therm-009_case-20
1.00000(210)	0.99596(80)	0.99797(72)	0.99797(222)	leu-comp-therm-009_case-21
1.00000(210)	0.99436(80)	0.99851(76)	0.99851(223)	leu-comp-therm-009_case-22

continued on next page

benchmark	JEFF-3.0	JEFF-3.1	C/E (JEFF-3.1)	name
1.00000(210)	0.99552(70)	0.99906(84)	0.99906(226)	leu-comp-therm-009_case-23
1.00000(210)	0.99443(70)	0.99726(80)	0.99726(225)	leu-comp-therm-009_case-24
1.00000(210)	0.99468(70)	0.99824(73)	0.99824(222)	leu-comp-therm-009_case-25
1.00000(210)	0.99550(70)	0.99809(80)	0.99809(225)	leu-comp-therm-009_case-26
1.00000(210)	0.99598(70)	0.99764(78)	0.99764(224)	leu-comp-therm-009_case-27
1.00000(210)	1.00538(82)	1.00598(75)	1.00598(223)	leu-comp-therm-010_case-1
1.00000(210)	1.00620(84)	1.00532(73)	1.00532(222)	leu-comp-therm-010_case-2
1.00000(210)	1.00325(75)	1.00570(79)	1.00570(224)	leu-comp-therm-010_case-3
1.00000(210)	0.99286(85)	0.99459(77)	0.99459(224)	leu-comp-therm-010_case-4
1.00000(210)	0.99654(71)	0.99926(79)	0.99926(224)	leu-comp-therm-010_case-5
1.00000(210)	0.99584(70)	0.99861(72)	0.99861(222)	leu-comp-therm-010_case-6
1.00000(210)	0.99606(74)	1.00018(68)	1.00018(221)	leu-comp-therm-010_case-7
1.00000(210)	0.99330(72)	0.99666(81)	0.99666(225)	leu-comp-therm-010_case-8
1.00000(210)	0.99743(76)	1.00025(82)	1.00025(225)	leu-comp-therm-010_case-9
1.00000(210)	0.99708(75)	0.99944(80)	0.99944(225)	leu-comp-therm-010_case-10
1.00000(210)	0.99705(74)	1.00007(84)	1.00007(226)	leu-comp-therm-010_case-11
1.00000(210)	0.99698(79)	0.99878(76)	0.99878(223)	leu-comp-therm-010_case-12
1.00000(210)	0.99415(74)	0.99597(75)	0.99597(223)	leu-comp-therm-010_case-13
1.00000(280)	0.99659(88)	1.00105(84)	1.00105(292)	leu-comp-therm-010_case-14
1.00000(280)	0.99823(90)	1.00249(77)	1.00249(290)	leu-comp-therm-010_case-15
1.00000(280)	0.99962(86)	0.99999(71)	0.99999(289)	leu-comp-therm-010_case-16
1.00000(280)	0.99847(78)	1.00224(79)	1.00224(291)	leu-comp-therm-010_case-17
1.00000(280)	0.99752(79)	1.00041(84)	1.00041(292)	leu-comp-therm-010_case-18
1.00000(280)	0.99595(78)	1.00076(106)	1.00076(299)	leu-comp-therm-010_case-19
1.00000(280)	1.00199(79)	1.00473(90)	1.00473(294)	leu-comp-therm-010_case-20
1.00000(280)	1.00091(69)	1.00437(87)	1.00437(293)	leu-comp-therm-010_case-21
1.00000(280)	0.99913(80)	1.00374(74)	1.00374(290)	leu-comp-therm-010_case-22
1.00000(280)	0.99581(71)	1.00185(81)	1.00185(291)	leu-comp-therm-010_case-23
1.00000(280)	0.99484(67)	0.99784(92)	0.99784(295)	leu-comp-therm-010_case-24
1.00000(280)	0.99593(78)	1.00068(76)	1.00068(290)	leu-comp-therm-010_case-25
1.00000(280)	0.99624(75)	1.00216(86)	1.00216(293)	leu-comp-therm-010_case-26
1.00000(280)	0.99407(80)	1.00101(78)	1.00101(291)	leu-comp-therm-010_case-27
1.00000(280)	0.99601(83)	1.00253(79)	1.00253(291)	leu-comp-therm-010_case-28
1.00000(280)	0.99691(86)	0.99881(74)	0.99881(290)	leu-comp-therm-010_case-29
1.00000(280)	0.99452(76)	0.99787(83)	0.99787(292)	leu-comp-therm-010_case-30
1.00000(310)	0.99509(70)	0.99891(78)	0.99891(320)	leu-comp-therm-016_case-1
1.00000(310)	0.99341(60)	0.99736(70)	0.99736(318)	leu-comp-therm-016_case-2
1.00000(310)	0.99578(60)	0.99824(77)	0.99824(319)	leu-comp-therm-016_case-3
1.00000(310)	0.99316(60)	0.99548(85)	0.99548(322)	leu-comp-therm-016_case-4
1.00000(310)	0.99626(80)	0.99824(70)	0.99824(318)	leu-comp-therm-016_case-5

continued on next page

benchmark	JEFF-3.0	JEFF-3.1	C/E (JEFF-3.1)	name
1.00000(310)	0.99319(60)	0.99788(73)	0.99788(319)	leu-comp-therm-016_case-6
1.00000(310)	0.99297(70)	0.99833(71)	0.99833(318)	leu-comp-therm-016_case-7
1.00000(310)	0.99439(70)	0.99779(62)	0.99779(316)	leu-comp-therm-016_case-8
1.00000(310)	0.99513(60)	0.99748(68)	0.99748(317)	leu-comp-therm-016_case-9
1.00000(310)	0.99430(70)	0.99872(78)	0.99872(320)	leu-comp-therm-016_case-10
1.00000(310)	0.99537(80)	0.99808(63)	0.99808(316)	leu-comp-therm-016_case-11
1.00000(310)	0.99430(80)	0.99798(66)	0.99798(317)	leu-comp-therm-016_case-12
1.00000(310)	0.99597(60)	0.99811(73)	0.99811(319)	leu-comp-therm-016_case-13
1.00000(310)	0.99477(70)	0.99835(65)	0.99835(317)	leu-comp-therm-016_case-14
1.00000(310)	0.99422(60)	0.99816(64)	0.99816(317)	leu-comp-therm-016_case-15
1.00000(310)	0.99213(79)	0.99556(72)	0.99556(318)	leu-comp-therm-016_case-16
1.00000(310)	0.99217(70)	0.99719(71)	0.99719(318)	leu-comp-therm-016_case-17
1.00000(310)	0.99413(60)	0.99828(76)	0.99828(319)	leu-comp-therm-016_case-18
1.00000(310)	0.99711(70)	0.99810(68)	0.99810(317)	leu-comp-therm-016_case-19
1.00000(310)	0.99603(80)	0.99745(73)	0.99745(319)	leu-comp-therm-016_case-20
1.00000(310)	0.99546(80)	0.99821(75)	0.99821(319)	leu-comp-therm-016_case-21
1.00000(310)	0.99613(70)	0.99947(72)	0.99947(318)	leu-comp-therm-016_case-22
1.00000(310)	0.99525(80)	0.99948(78)	0.99948(320)	leu-comp-therm-016_case-23
1.00000(310)	0.99336(70)	0.99910(71)	0.99910(318)	leu-comp-therm-016_case-24
1.00000(310)	0.99550(70)	0.99918(71)	0.99918(318)	leu-comp-therm-016_case-25
1.00000(310)	0.99662(70)	0.99818(75)	0.99818(319)	leu-comp-therm-016_case-26
1.00000(310)	0.99524(70)	0.99907(69)	0.99907(318)	leu-comp-therm-016_case-27
1.00000(310)	0.99462(60)	0.99734(64)	0.99734(317)	leu-comp-therm-016_case-28
1.00000(310)	0.99359(70)	0.99671(66)	0.99671(317)	leu-comp-therm-016_case-29
1.00000(310)	0.99514(80)	0.99820(56)	0.99820(315)	leu-comp-therm-016_case-30
1.00000(310)	0.99308(79)	0.99891(64)	0.99891(317)	leu-comp-therm-016_case-31
1.00000(310)	0.99458(70)	0.99928(68)	0.99928(317)	leu-comp-therm-016_case-32
1.00000(310)	0.99834(70)	1.00197(65)	1.00197(317)	leu-comp-therm-017_case-1
1.00000(310)	0.99653(80)	1.00137(68)	1.00137(317)	leu-comp-therm-017_case-2
1.00000(310)	0.99612(60)	0.99968(81)	0.99968(320)	leu-comp-therm-017_case-3
1.00000(310)	0.99589(70)	0.99912(63)	0.99912(316)	leu-comp-therm-017_case-10
1.00000(310)	0.99638(80)	0.99894(73)	0.99894(318)	leu-comp-therm-017_case-11
1.00000(310)	0.99447(60)	0.99677(69)	0.99677(318)	leu-comp-therm-017_case-12
1.00000(310)	0.99546(60)	0.99866(68)	0.99866(317)	leu-comp-therm-017_case-13
1.00000(310)	0.99574(70)	0.99764(74)	0.99764(319)	leu-comp-therm-017_case-14
1.00000(280)	0.99257(70)	0.99648(64)	0.99648(287)	leu-comp-therm-017_case-15
1.00000(280)	0.99365(70)	0.99758(67)	0.99758(288)	leu-comp-therm-017_case-16
1.00000(280)	0.99459(80)	1.00075(61)	1.00075(287)	leu-comp-therm-017_case-17
1.00000(280)	0.99453(70)	0.99863(69)	0.99863(288)	leu-comp-therm-017_case-18
1.00000(280)	0.99488(70)	0.99922(83)	0.99922(292)	leu-comp-therm-017_case-19

continued on next page

benchmark	JEFF-3.0	JEFF-3.1	C/E (JEFF-3.1)	name
1.00000(280)	0.99398(70)	1.00031(83)	1.00031(292)	leu-comp-therm-017_case-20
1.00000(280)	0.99351(70)	0.99737(80)	0.99737(291)	leu-comp-therm-017_case-21
1.00000(280)	0.99135(79)	0.99543(71)	0.99543(289)	leu-comp-therm-017_case-22
1.00000(280)	0.99655(70)	1.00106(79)	1.00106(291)	leu-comp-therm-017_case-23
1.00000(280)	0.99629(70)	1.00087(65)	1.00087(287)	leu-comp-therm-017_case-24
1.00000(280)	0.99303(60)	0.99945(77)	0.99945(290)	leu-comp-therm-017_case-25
1.00000(630)	1.01172(81)	1.01393(72)	1.01393(634)	leu-comp-therm-019_case-1
1.00000(580)	1.00698(81)	1.01165(85)	1.01165(586)	leu-comp-therm-019_case-2
1.00000(610)	1.00493(50)	1.00521(66)	1.00521(614)	leu-comp-therm-019_case-3
1.00000(140)	0.99391(88)	0.99652(40)	0.99652(146)	leu-comp-therm-039_case-1
1.00000(140)	0.99382(90)	0.99775(48)	0.99775(148)	leu-comp-therm-039_case-2
1.00000(140)	0.99307(93)	0.99628(35)	0.99628(144)	leu-comp-therm-039_case-3
1.00000(140)	0.99367(82)	0.99558(37)	0.99558(145)	leu-comp-therm-039_case-4
1.00000(140)	0.99301(82)	0.99753(46)	0.99753(147)	leu-comp-therm-039_case-5
1.00000(140)	0.99429(86)	0.99712(46)	0.99712(147)	leu-comp-therm-039_case-6
1.00000(140)	0.99166(82)	0.99676(44)	0.99676(147)	leu-comp-therm-039_case-7
1.00000(140)	0.99225(80)	0.99652(40)	0.99652(146)	leu-comp-therm-039_case-8
1.00000(140)	0.99320(80)	0.99633(41)	0.99633(146)	leu-comp-therm-039_case-9
1.00000(140)	0.99353(80)	0.99728(43)	0.99728(146)	leu-comp-therm-039_case-10
1.00000(140)	0.99178(83)	0.99618(41)	0.99618(146)	leu-comp-therm-039_case-11
1.00000(140)	0.99285(83)	0.99640(47)	0.99640(148)	leu-comp-therm-039_case-12
1.00000(140)	0.99384(78)	0.99581(39)	0.99581(145)	leu-comp-therm-039_case-13
1.00000(140)	0.99254(86)	0.99644(42)	0.99644(146)	leu-comp-therm-039_case-14
1.00000(140)	0.99102(95)	0.99608(42)	0.99608(146)	leu-comp-therm-039_case-15
1.00000(140)	0.99294(92)	0.99725(42)	0.99725(146)	leu-comp-therm-039_case-16
1.00000(140)	0.99350(68)	0.99669(39)	0.99669(145)	leu-comp-therm-039_case-17
1.00100(200)	0.99174(69)	0.99464(84)	0.99365(217)	leu-comp-therm-051_case-1
1.00100(240)	0.99800(70)	0.99868(74)	0.99768(251)	leu-comp-therm-051_case-2
1.00100(240)	0.99697(80)	1.00009(69)	0.99909(249)	leu-comp-therm-051_case-3
1.00100(240)	0.99686(70)	0.99894(78)	0.99794(252)	leu-comp-therm-051_case-4
1.00100(240)	0.99666(80)	0.99905(78)	0.99805(252)	leu-comp-therm-051_case-5
1.00100(240)	0.99518(70)	1.00069(70)	0.99969(250)	leu-comp-therm-051_case-6
1.00100(240)	0.99434(70)	1.00051(69)	0.99951(249)	leu-comp-therm-051_case-7
1.00100(240)	0.99724(80)	0.99982(72)	0.99882(250)	leu-comp-therm-051_case-8
1.00100(190)	0.99232(70)	0.99550(79)	0.99451(206)	leu-comp-therm-051_case-9
1.00100(190)	0.99561(70)	0.99703(79)	0.99603(206)	leu-comp-therm-051_case-10
1.00100(190)	0.99327(70)	0.99565(71)	0.99466(203)	leu-comp-therm-051_case-11
1.00100(190)	0.99040(69)	0.99635(74)	0.99535(204)	leu-comp-therm-051_case-12
1.00100(220)	0.98828(79)	0.99273(72)	0.99174(231)	leu-comp-therm-051_case-13
1.00100(190)	0.98779(69)	0.99086(77)	0.98987(205)	leu-comp-therm-051_case-14

continued on next page

benchmark	JEFF-3.0	JEFF-3.1	C/E (JEFF-3.1)	name
1.00100(240)	0.99085(69)	0.99346(72)	0.99247(250)	leu-comp-therm-051_case-15
1.00100(200)	0.99006(79)	0.99348(78)	0.99249(215)	leu-comp-therm-051_case-16
1.00100(270)	0.99284(70)	0.99546(66)	0.99447(278)	leu-comp-therm-051_case-17
1.00100(210)	0.98934(69)	0.99314(71)	0.99215(222)	leu-comp-therm-051_case-18
1.00100(190)	0.98842(69)	0.99202(66)	0.99103(201)	leu-comp-therm-051_case-19
0.99900(260)		1.00390(59)	1.00490(267)	leu-comp-therm-060_case-1
0.99770(260)		1.00612(65)	1.00844(268)	leu-comp-therm-060_case-2
1.00010(260)		1.00554(73)	1.00544(270)	leu-comp-therm-060_case-3
1.00170(260)		1.01071(78)	1.00899(271)	leu-comp-therm-060_case-4
1.00090(260)		1.00687(64)	1.00596(267)	leu-comp-therm-060_case-5
0.98940(270)		0.99784(81)	1.00853(285)	leu-comp-therm-060_case-6
1.00280(260)		1.00976(61)	1.00694(266)	leu-comp-therm-060_case-7
1.00390(260)		1.01494(79)	1.01100(270)	leu-comp-therm-060_case-8
1.00430(260)		1.01176(61)	1.00743(266)	leu-comp-therm-060_case-9
1.00140(260)		1.01105(72)	1.00964(269)	leu-comp-therm-060_case-10
1.00010(260)		1.00604(68)	1.00594(269)	leu-comp-therm-060_case-11
1.00090(260)		1.00557(64)	1.00467(267)	leu-comp-therm-060_case-12
1.00100(260)		1.00512(76)	1.00412(271)	leu-comp-therm-060_case-13
1.00150(260)		1.00715(79)	1.00564(271)	leu-comp-therm-060_case-14
1.00120(260)		1.00395(68)	1.00275(268)	leu-comp-therm-060_case-15
1.00070(260)		1.00272(67)	1.00202(268)	leu-comp-therm-060_case-16
1.00120(260)		1.00623(70)	1.00502(269)	leu-comp-therm-060_case-17
1.00060(260)		1.00911(73)	1.00850(270)	leu-comp-therm-060_case-18
1.00070(260)		1.00850(71)	1.00779(269)	leu-comp-therm-060_case-19
1.00390(260)		1.01382(68)	1.00988(268)	leu-comp-therm-060_case-20
1.00030(260)		1.00714(65)	1.00684(268)	leu-comp-therm-060_case-21
1.00360(260)		1.01122(73)	1.00759(269)	leu-comp-therm-060_case-22
1.00170(260)		1.00773(58)	1.00602(266)	leu-comp-therm-060_case-23
1.00250(260)		1.00906(64)	1.00654(267)	leu-comp-therm-060_case-24
1.00160(260)		1.00724(62)	1.00563(267)	leu-comp-therm-060_case-25
0.99960(260)		1.00949(77)	1.00989(271)	leu-comp-therm-060_case-26
1.00000(200)	0.99278(17)	0.99906(60)	0.99906(209)	leu-comp-therm-trx_case-1_3d
1.00000(200)	0.99233(18)	0.99809(52)	0.99809(207)	leu-comp-therm-trx_case-2_3d
0.99830(170)	0.99510(50)	1.00007(50)	1.00177(177)	leu-comp-therm-dimple
0.99900(570)	0.99474(60)	0.99892(58)	0.99992(574)	leu-met-therm-001_case-1
0.99910(290)	1.01120(88)	1.01252(86)	1.01343(302)	leu-sol-therm-001
0.99970(390)	0.99595(81)	0.99706(65)	0.99736(396)	leu-sol-therm-003_case-1
0.99930(420)	0.99477(70)	0.99676(69)	0.99746(426)	leu-sol-therm-003_case-2
0.99950(420)	0.99905(69)	1.00143(76)	1.00193(427)	leu-sol-therm-003_case-3
0.99950(420)	0.99510(69)	0.99352(75)	0.99402(427)	leu-sol-therm-003_case-4

continued on next page

benchmark	JEFF-3.0	JEFF-3.1	C/E (JEFF-3.1)	name
0.99970(480)	0.99730(64)	0.99731(54)	0.99761(483)	leu-sol-therm-003_case-5
0.99990(490)	0.99798(54)	0.99979(63)	0.99989(494)	leu-sol-therm-003_case-6
0.99940(490)	0.99540(54)	0.99672(53)	0.99732(493)	leu-sol-therm-003_case-7
0.99930(520)	0.99839(49)	1.00021(47)	1.00091(522)	leu-sol-therm-003_case-8
0.99960(520)	0.99677(43)	0.99668(45)	0.99708(522)	leu-sol-therm-003_case-9
0.99940(80)	1.00098(68)	1.00046(76)	1.00106(110)	leu-sol-therm-004_case-001
0.99990(90)	1.00005(69)	1.00354(65)	1.00364(111)	leu-sol-therm-004_case-029
0.99990(90)	0.99887(58)	0.99961(70)	0.99971(114)	leu-sol-therm-004_case-033
0.99990(100)	1.00106(59)	1.00157(72)	1.00167(123)	leu-sol-therm-004_case-034
0.99990(100)	1.00159(67)	1.00111(59)	1.00121(116)	leu-sol-therm-004_case-046
0.99940(110)	1.00054(55)	1.00015(54)	1.00075(123)	leu-sol-therm-004_case-051
0.99960(110)	0.99919(65)	1.00078(62)	1.00118(126)	leu-sol-therm-004_case-054
0.99610(90)	0.99384(72)	0.99561(66)	0.99951(112)	leu-sol-therm-007_case-14
0.99730(90)	0.99850(63)	0.99732(79)	1.00002(120)	leu-sol-therm-007_case-30
0.99850(100)	0.99648(64)	0.99551(61)	0.99701(117)	leu-sol-therm-007_case-32
0.99880(110)	0.99920(56)	1.00109(67)	1.00229(129)	leu-sol-therm-007_case-36
0.99830(110)	0.99699(66)	0.99678(64)	0.99848(128)	leu-sol-therm-007_case-49
0.99960(130)	1.00525(84)	1.00697(99)	1.00737(163)	leu-sol-therm-016_case-105
0.99990(130)	1.00507(83)	1.00514(83)	1.00524(154)	leu-sol-therm-016_case-113
0.99940(140)	1.00564(68)	1.00497(81)	1.00557(162)	leu-sol-therm-016_case-125
0.99960(140)	1.00344(70)	1.00593(76)	1.00633(159)	leu-sol-therm-016_case-129
0.99950(140)	1.00297(71)	1.00489(69)	1.00539(156)	leu-sol-therm-016_case-131
0.99920(150)	1.00090(66)	1.00184(68)	1.00264(165)	leu-sol-therm-016_case-140
0.99940(150)	1.00254(68)	1.00477(79)	1.00537(169)	leu-sol-therm-016_case-196
0.99810(130)	1.00242(90)	1.00345(86)	1.00536(156)	leu-sol-therm-017_case-104
0.99860(130)	1.00420(78)	1.00244(78)	1.00385(152)	leu-sol-therm-017_case-122
0.99890(140)	1.00081(82)	1.00208(83)	1.00318(163)	leu-sol-therm-017_case-123
0.99920(140)	1.00174(73)	1.00227(79)	1.00307(161)	leu-sol-therm-017_case-126
0.99870(150)	1.00268(82)	0.99996(71)	1.00126(166)	leu-sol-therm-017_case-130
0.99960(150)	0.99886(68)	1.00207(66)	1.00247(164)	leu-sol-therm-017_case-147
0.99920(100)	1.00028(70)	1.00129(66)	1.00209(120)	leu-sol-therm-018_case-1
0.99960(100)	1.00057(70)	1.00368(64)	1.00408(119)	leu-sol-therm-018_case-2
0.99960(100)	1.00164(80)	1.00153(78)	1.00193(127)	leu-sol-therm-018_case-3
0.99970(100)	1.00209(70)	1.00385(71)	1.00415(123)	leu-sol-therm-018_case-4
0.99920(100)	1.00215(80)	1.00278(64)	1.00358(119)	leu-sol-therm-018_case-5
0.99960(100)	1.00343(70)	1.00051(76)	1.00091(126)	leu-sol-therm-018_case-6
0.99950(100)	0.99944(66)	0.99885(62)	0.99935(118)	leu-sol-therm-020_case-216
0.99960(100)	0.99944(56)	0.99977(62)	1.00017(118)	leu-sol-therm-020_case-217
0.99970(120)	0.99835(59)	0.99676(46)	0.99706(129)	leu-sol-therm-020_case-220
0.99980(120)	0.99768(52)	0.99945(46)	0.99965(129)	leu-sol-therm-020_case-226

continued on next page

benchmark	JEFF-3.0	JEFF-3.1	C/E (JEFF-3.1)	name
0.99830(90)	0.99600(64)	0.99765(65)	0.99935(111)	leu-sol-therm-021_case-215
0.99850(100)	0.99680(66)	0.99909(59)	1.00059(116)	leu-sol-therm-021_case-218
0.99890(110)	0.99658(58)	0.99686(47)	0.99796(120)	leu-sol-therm-021_case-221
0.99930(120)	0.99794(54)	0.99906(58)	0.99976(133)	leu-sol-therm-021_case-223

Table 3.7 The results for LEU benchmarks with a thermal spectrum

3.4 PU results

3.4.1 Fast spectrum

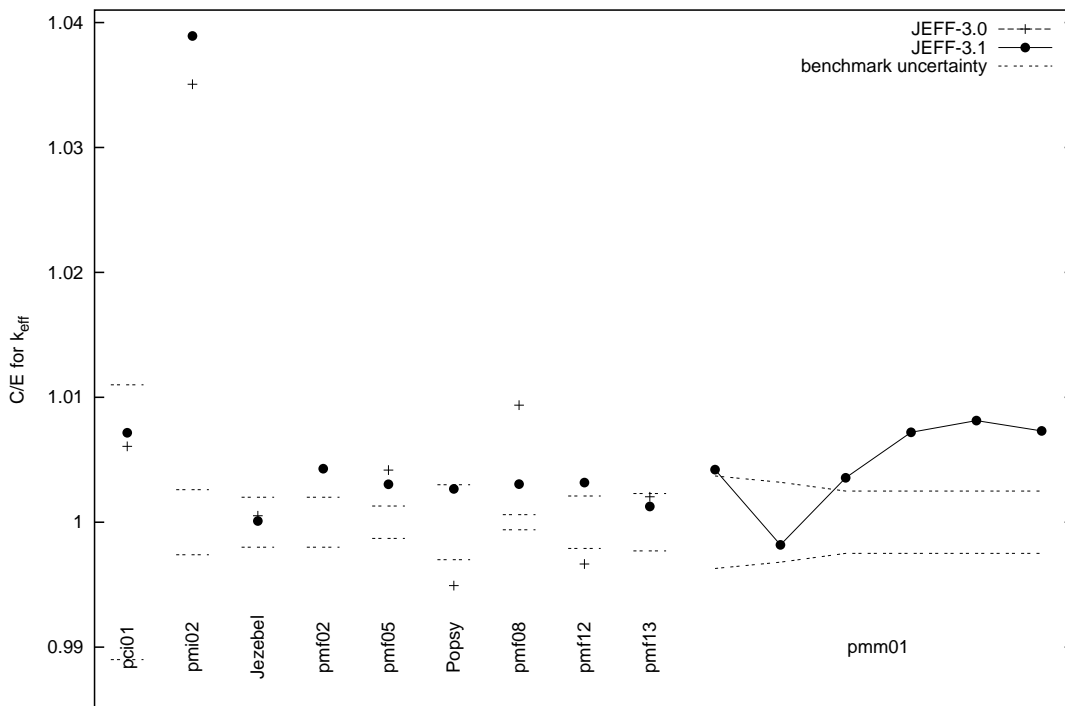


Figure 3.8 Results for the PU benchmarks with a fast, intermediate, or mixed spectrum

benchmark	JEFF-3.0	JEFF-3.1	C/E (JEFF-3.1)	name
1.00000(200)	1.00052(40)	1.00010(19)	1.00010(201)	pu-met-fast-001_bare-sphere
1.00000(200)		1.00428(67)	1.00428(211)	pu-met-fast-002
1.00000(130)	1.00417(73)	1.00304(70)	1.00304(148)	pu-met-fast-005
1.00000(300)	0.99492(44)	1.00267(43)	1.00267(303)	pu-met-fast-006
1.00000(60)	1.00937(45)	1.00305(35)	1.00305(69)	pu-met-fast-008_case-1
1.00090(210)	0.99756(71)	1.00407(67)	1.00317(220)	pu-met-fast-012
1.00340(230)	1.00545(72)	1.00466(80)	1.00126(243)	pu-met-fast-013

Table 3.8 The results for PU benchmarks with a fast spectrum

3.4.2 Intermediate spectrum

benchmark	JEFF-3.0	JEFF-3.1	C/E (JEFF-3.1)	name
1.00000(1100)	1.00608(57)	1.00716(44)	1.00716(1101)	pu-comp-inter-001
0.98690(260)	1.02150(47)	1.02532(73)	1.03893(273)	pu-met-inter-002_case-1

Table 3.9 The results for PU benchmarks with an intermediate spectrum

3.4.3 Thermal spectrum

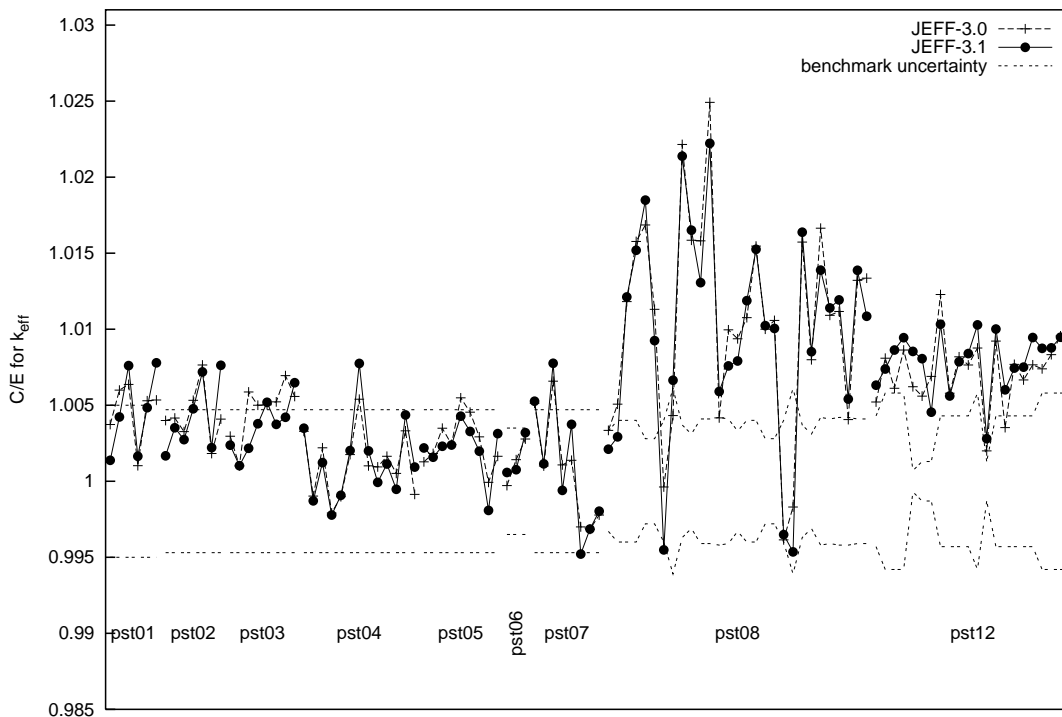


Figure 3.9 Results for the PU benchmarks with a thermal spectrum

benchmark	JEFF-3.0	JEFF-3.1	C/E (JEFF-3.1)	name
1.00000(500)	1.00373(95)	1.00138(95)	1.00138(509)	pu-sol-therm-001_case-1
1.00000(500)	1.00599(108)	1.00423(95)	1.00423(509)	pu-sol-therm-001_case-2
1.00000(500)	1.00637(102)	1.00760(87)	1.00760(507)	pu-sol-therm-001_case-3
1.00000(500)	1.00102(96)	1.00164(104)	1.00164(511)	pu-sol-therm-001_case-4
1.00000(500)	1.00529(94)	1.00484(106)	1.00484(511)	pu-sol-therm-001_case-5
1.00000(500)	1.00534(95)	1.00779(102)	1.00779(510)	pu-sol-therm-001_case-6
1.00000(470)	1.00399(87)	1.00167(97)	1.00167(480)	pu-sol-therm-002_case-1
1.00000(470)	1.00416(91)	1.00352(87)	1.00352(478)	pu-sol-therm-002_case-2
1.00000(470)	1.00326(90)	1.00274(95)	1.00274(479)	pu-sol-therm-002_case-3
1.00000(470)	1.00532(101)	1.00476(86)	1.00476(478)	pu-sol-therm-002_case-4
1.00000(470)	1.00765(91)	1.00719(92)	1.00719(479)	pu-sol-therm-002_case-5
1.00000(470)	1.00182(92)	1.00221(93)	1.00221(479)	pu-sol-therm-002_case-6
1.00000(470)	1.00409(106)	1.00762(97)	1.00762(480)	pu-sol-therm-002_case-7
1.00000(470)	1.00296(86)	1.00237(92)	1.00237(479)	pu-sol-therm-003_case-1

continued on next page

benchmark	JEFF-3.0	JEFF-3.1	C/E (JEFF-3.1)	name
1.00000(470)	1.00101(89)	1.00102(93)	1.00102(479)	pu-sol-therm-003_case-2
1.00000(470)	1.00587(80)	1.00217(91)	1.00217(479)	pu-sol-therm-003_case-3
1.00000(470)	1.00500(85)	1.00378(88)	1.00378(478)	pu-sol-therm-003_case-4
1.00000(470)	1.00503(90)	1.00519(103)	1.00519(481)	pu-sol-therm-003_case-5
1.00000(470)	1.00522(89)	1.00374(96)	1.00374(480)	pu-sol-therm-003_case-6
1.00000(470)	1.00695(91)	1.00421(87)	1.00421(478)	pu-sol-therm-003_case-7
1.00000(470)	1.00558(93)	1.00648(87)	1.00648(478)	pu-sol-therm-003_case-8
1.00000(470)	1.00328(89)	1.00349(74)	1.00349(476)	pu-sol-therm-004_case-1
1.00000(470)	0.99903(82)	0.99871(86)	0.99871(478)	pu-sol-therm-004_case-2
1.00000(470)	1.00220(85)	1.00123(70)	1.00123(475)	pu-sol-therm-004_case-3
1.00000(470)	0.99791(75)	0.99778(87)	0.99778(478)	pu-sol-therm-004_case-4
1.00000(470)	0.99898(82)	0.99908(88)	0.99908(478)	pu-sol-therm-004_case-5
1.00000(470)	1.00175(79)	1.00202(94)	1.00202(479)	pu-sol-therm-004_case-6
1.00000(470)	1.00539(87)	1.00775(84)	1.00775(477)	pu-sol-therm-004_case-7
1.00000(470)	1.00101(71)	1.00200(75)	1.00200(476)	pu-sol-therm-004_case-8
1.00000(470)	1.00094(85)	0.99993(90)	0.99993(479)	pu-sol-therm-004_case-9
1.00000(470)	1.00164(90)	1.00113(86)	1.00113(478)	pu-sol-therm-004_case-10
1.00000(470)	1.00052(90)	0.99947(91)	0.99947(479)	pu-sol-therm-004_case-11
1.00000(470)	1.00331(80)	1.00436(78)	1.00436(476)	pu-sol-therm-004_case-12
1.00000(470)	0.99914(84)	1.00093(77)	1.00093(476)	pu-sol-therm-004_case-13
1.00000(470)	1.00128(79)	1.00219(75)	1.00219(476)	pu-sol-therm-005_case-1
1.00000(470)	1.00182(83)	1.00158(81)	1.00158(477)	pu-sol-therm-005_case-2
1.00000(470)	1.00349(84)	1.00230(99)	1.00230(480)	pu-sol-therm-005_case-3
1.00000(470)	1.00242(89)	1.00238(93)	1.00238(479)	pu-sol-therm-005_case-4
1.00000(470)	1.00548(85)	1.00428(89)	1.00428(478)	pu-sol-therm-005_case-5
1.00000(470)	1.00454(101)	1.00327(85)	1.00327(478)	pu-sol-therm-005_case-6
1.00000(470)	1.00292(86)	1.00198(69)	1.00198(475)	pu-sol-therm-005_case-7
1.00000(470)	0.99993(84)	0.99808(84)	0.99808(477)	pu-sol-therm-005_case-8
1.00000(470)	1.00164(89)	1.00313(92)	1.00313(479)	pu-sol-therm-005_case-9
1.00000(350)	0.99971(89)	1.00058(81)	1.00058(359)	pu-sol-therm-006_case-1
1.00000(350)	1.00142(84)	1.00076(86)	1.00076(360)	pu-sol-therm-006_case-2
1.00000(350)	1.00278(74)	1.00319(75)	1.00319(358)	pu-sol-therm-006_case-3
1.00000(470)	1.00513(92)	1.00526(95)	1.00526(479)	pu-sol-therm-007_case-2
1.00000(470)	1.00100(97)	1.00114(90)	1.00114(479)	pu-sol-therm-007_case-3
1.00000(470)	1.00658(99)	1.00776(103)	1.00776(481)	pu-sol-therm-007_case-5
1.00000(470)	1.00107(104)	0.99940(91)	0.99940(479)	pu-sol-therm-007_case-6
1.00000(470)	1.00138(90)	1.00374(85)	1.00374(478)	pu-sol-therm-007_case-7
1.00000(470)	0.99700(101)	0.99521(94)	0.99521(479)	pu-sol-therm-007_case-8
1.00000(470)	0.99683(99)	0.99686(93)	0.99686(479)	pu-sol-therm-007_case-9
1.00000(470)	0.99778(107)	0.99803(89)	0.99803(478)	pu-sol-therm-007_case-10

continued on next page

benchmark	JEFF-3.0	JEFF-3.1	C/E (JEFF-3.1)	name
1.00000(330)	1.00335(91)	1.00211(95)	1.00211(343)	pu-sol-therm-008_case-1
1.00000(400)	1.00507(86)	1.00292(96)	1.00292(411)	pu-sol-therm-008_case-2
1.00000(400)	1.01181(100)	1.01212(88)	1.01212(409)	pu-sol-therm-008_case-3
1.00000(400)	1.01577(85)	1.01519(103)	1.01519(413)	pu-sol-therm-008_case-4
1.00000(280)	1.01685(82)	1.01849(81)	1.01849(291)	pu-sol-therm-008_case-5
1.00000(280)	1.01131(80)	1.00925(90)	1.00925(294)	pu-sol-therm-008_case-7
1.00000(400)	0.99962(86)	0.99549(89)	0.99549(410)	pu-sol-therm-008_case-8
1.00000(610)	1.00432(102)	1.00664(106)	1.00664(619)	pu-sol-therm-008_case-9
1.00000(370)	1.02215(90)	1.02138(85)	1.02138(379)	pu-sol-therm-008_case-10
1.00000(310)	1.01585(83)	1.01651(83)	1.01651(321)	pu-sol-therm-008_case-11
1.00000(410)	1.01581(101)	1.01306(111)	1.01306(424)	pu-sol-therm-008_case-12
1.00000(410)	1.02492(98)	1.02222(90)	1.02222(419)	pu-sol-therm-008_case-13
1.00000(420)	1.00417(93)	1.00590(100)	1.00590(432)	pu-sol-therm-008_case-14
1.00000(410)	1.00996(87)	1.00758(108)	1.00758(424)	pu-sol-therm-008_case-15
1.00000(330)	1.00937(97)	1.00791(72)	1.00791(338)	pu-sol-therm-008_case-16
1.00000(400)	1.01076(81)	1.01187(81)	1.01187(408)	pu-sol-therm-008_case-17
1.00000(400)	1.01546(95)	1.01525(99)	1.01525(412)	pu-sol-therm-008_case-18
1.00000(280)	1.01000(94)	1.01023(92)	1.01023(294)	pu-sol-therm-008_case-19
1.00000(280)	1.01058(92)	1.01005(82)	1.01005(292)	pu-sol-therm-008_case-20
1.00000(400)	0.99615(93)	0.99649(91)	0.99649(410)	pu-sol-therm-008_case-21
1.00000(610)	0.99831(97)	0.99535(113)	0.99535(620)	pu-sol-therm-008_case-22
1.00000(370)	1.01573(81)	1.01638(87)	1.01638(380)	pu-sol-therm-008_case-23
1.00000(310)	1.00799(90)	1.00852(88)	1.00852(322)	pu-sol-therm-008_case-24
1.00000(420)	1.01664(100)	1.01388(105)	1.01388(433)	pu-sol-therm-008_case-25
1.00000(410)	1.01091(102)	1.01140(104)	1.01140(423)	pu-sol-therm-008_case-26
1.00000(420)	1.01116(95)	1.01192(114)	1.01192(435)	pu-sol-therm-008_case-27
1.00000(420)	1.00406(105)	1.00540(90)	1.00540(429)	pu-sol-therm-008_case-28
1.00000(410)	1.01321(110)	1.01387(71)	1.01387(416)	pu-sol-therm-008_case-29
1.00000(410)	1.01335(86)	1.01085(97)	1.01085(421)	pu-sol-therm-008_case-30
1.00000(430)	1.00521(63)	1.00632(50)	1.00632(433)	pu-sol-therm-012_case-2
1.00000(580)	1.00809(60)	1.00738(56)	1.00738(583)	pu-sol-therm-012_case-3
1.00000(580)	1.00611(52)	1.00863(51)	1.00863(582)	pu-sol-therm-012_case-4
1.00000(580)	1.00863(49)	1.00944(54)	1.00944(582)	pu-sol-therm-012_case-5
1.00000(70)	1.00622(97)	1.00854(100)	1.00854(121)	pu-sol-therm-012_case-6
1.00000(130)	1.00560(94)	1.00806(100)	1.00806(164)	pu-sol-therm-012_case-7
1.00000(130)	1.00689(89)	1.00454(97)	1.00454(162)	pu-sol-therm-012_case-8
1.00000(430)	1.01228(87)	1.01032(83)	1.01032(438)	pu-sol-therm-012_case-9
1.00000(430)	1.00579(78)	1.00561(78)	1.00561(437)	pu-sol-therm-012_case-10
1.00000(430)	1.00818(74)	1.00786(72)	1.00786(436)	pu-sol-therm-012_case-11
1.00000(430)	1.00765(64)	1.00840(65)	1.00840(435)	pu-sol-therm-012_case-12

continued on next page

benchmark	JEFF-3.0	JEFF-3.1	C/E (JEFF-3.1)	name
1.00000(580)	1.00876(48)	1.01028(54)	1.01028(582)	pu-sol-therm-012_case-13
1.00000(130)	1.00200(100)	1.00280(85)	1.00280(155)	pu-sol-therm-012_case-14
1.00000(430)	1.00922(81)	1.01001(86)	1.01001(438)	pu-sol-therm-012_case-15
1.00000(430)	1.00353(70)	1.00601(75)	1.00601(436)	pu-sol-therm-012_case-16
1.00000(430)	1.00769(88)	1.00744(76)	1.00744(437)	pu-sol-therm-012_case-17
1.00000(430)	1.00666(69)	1.00750(60)	1.00750(434)	pu-sol-therm-012_case-18
1.00000(430)	1.00766(59)	1.00945(68)	1.00945(435)	pu-sol-therm-012_case-19
1.00000(580)	1.00739(55)	1.00874(51)	1.00874(582)	pu-sol-therm-012_case-20
1.00000(580)	1.00832(56)	1.00877(52)	1.00877(582)	pu-sol-therm-012_case-21
1.00000(580)	1.00956(49)	1.00947(41)	1.00947(581)	pu-sol-therm-012_case-22
1.00000(580)	1.00841(49)	1.00787(44)	1.00787(582)	pu-sol-therm-012_case-23

Table 3.10 The results for PU benchmarks with a thermal spectrum

3.4.4 Mixed spectrum

benchmark	JEFF-3.0	JEFF-3.1	C/E (JEFF-3.1)	name
1.00020(370)		1.00441(99)	1.00421(383)	pu-met-mixed-001_case-1
1.00020(320)		0.99839(83)	0.99819(331)	pu-met-mixed-001_case-2
1.00050(250)		1.00406(98)	1.00356(268)	pu-met-mixed-001_case-3
1.00000(250)		1.00720(91)	1.00720(266)	pu-met-mixed-001_case-4
1.00010(250)		1.00823(83)	1.00813(263)	pu-met-mixed-001_case-5
1.00030(250)		1.00761(87)	1.00731(264)	pu-met-mixed-001_case-6

3.5 MIX results

3.5.1 Fast spectrum

benchmark	JEFF-3.0	JEFF-3.1	C/E (JEFF-3.1)	name
0.98660(230)	0.98388(49)	0.98997(47)	1.00342(238)	mix-comp-fast-001
0.98970(230)	0.98783(48)	0.99002(70)	1.00032(243)	mix-met-fast-011_case-1
0.99980(230)	0.99274(44)	0.99539(46)	0.99559(235)	mix-met-fast-011_case-2
1.00180(240)	0.99749(49)	0.99852(47)	0.99673(244)	mix-met-fast-011_case-3
1.00120(240)	0.99842(53)	1.00128(42)	1.00008(243)	mix-met-fast-011_case-4

Table 3.11 The results for MIX benchmarks with a fast spectrum

3.5.2 Thermal spectrum

benchmark	JEFF-3.0	JEFF-3.1	C/E (JEFF-3.1)	name
1.00520(670)	0.97599(51)	0.97597(53)	0.97092(669)	mix-comp-therm-012_case-1
1.00520(670)	0.97668(58)	0.97812(60)	0.97306(669)	mix-comp-therm-012_case-2
1.00520(670)	0.97475(65)	0.97389(52)	0.96885(669)	mix-comp-therm-012_case-3
1.00520(670)	0.97976(50)	0.97874(51)	0.97368(669)	mix-comp-therm-012_case-4
1.00520(670)	0.97589(53)	0.97640(62)	0.97135(670)	mix-comp-therm-012_case-5
1.00520(750)	0.98124(59)	0.98007(60)	0.97500(749)	mix-comp-therm-012_case-6

continued on next page

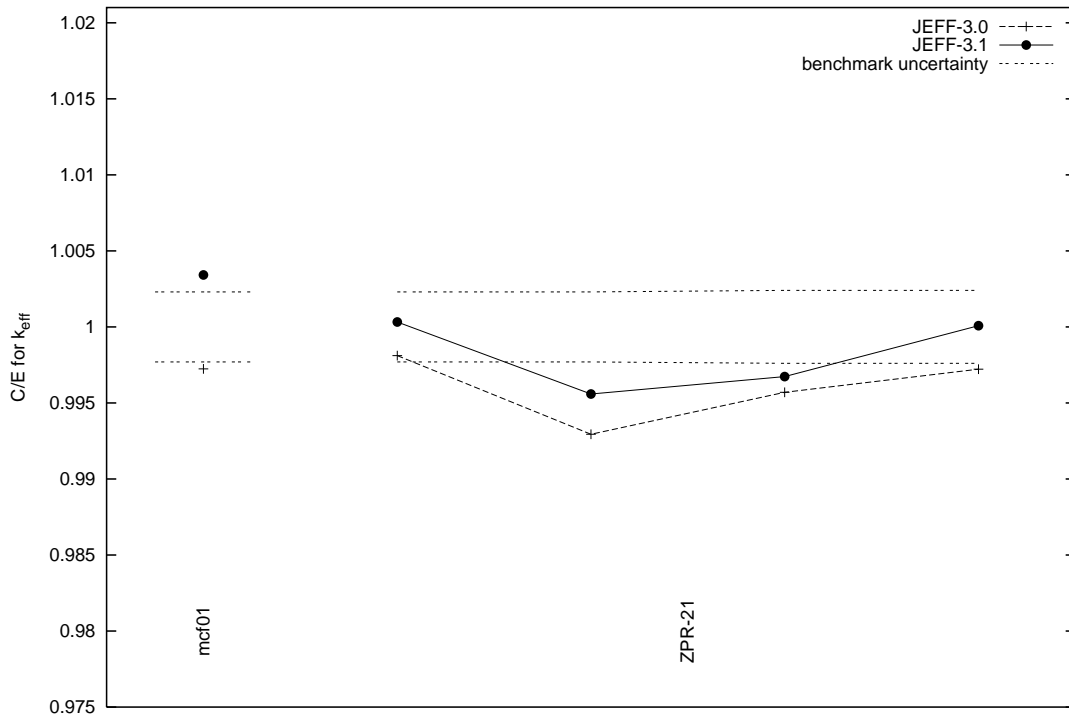


Figure 3.10 Results for the MIX benchmarks with a fast spectrum

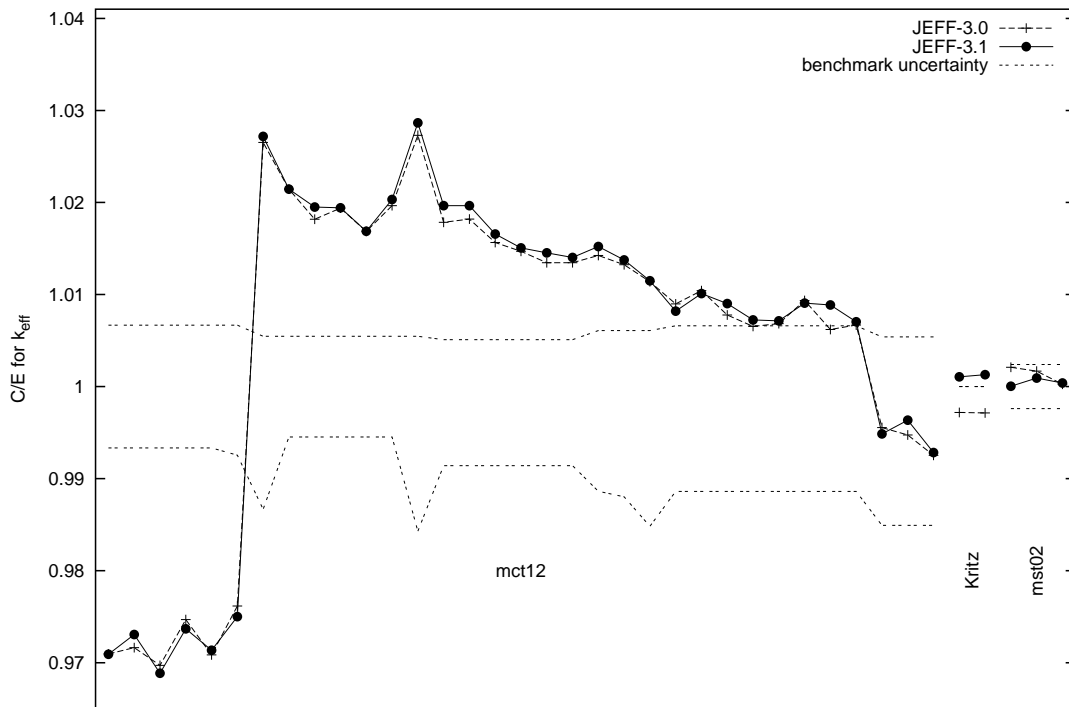


Figure 3.11 Results for the MIX benchmarks with a thermal spectrum

benchmark	JEFF-3.0	JEFF-3.1	C/E (JEFF-3.1)	name
1.00530(1340)	1.03196(51)	1.03261(53)	1.02717(1334)	mix-comp-therm-012_case-7

continued on next page

benchmark	JEFF-3.0	JEFF-3.1	C/E (JEFF-3.1)	name
1.00530(550)	1.02686(56)	1.02685(49)	1.02144(549)	mix-comp-therm-012_case-8
1.00530(550)	1.02358(55)	1.02491(46)	1.01951(549)	mix-comp-therm-012_case-9
1.00530(550)	1.02479(54)	1.02482(58)	1.01942(550)	mix-comp-therm-012_case-10
1.00530(550)	1.02224(55)	1.02227(51)	1.01688(549)	mix-comp-therm-012_case-11
1.00530(550)	1.02506(50)	1.02574(56)	1.02033(550)	mix-comp-therm-012_case-12
1.00530(1580)	1.03273(55)	1.03410(52)	1.02865(1572)	mix-comp-therm-012_case-13
1.00120(860)	1.01907(52)	1.02087(67)	1.01965(861)	mix-comp-therm-012_case-14
1.00120(860)	1.01942(62)	1.02087(65)	1.01965(861)	mix-comp-therm-012_case-15
1.00120(860)	1.01687(56)	1.01779(53)	1.01657(861)	mix-comp-therm-012_case-16
1.00120(860)	1.01591(63)	1.01628(57)	1.01506(861)	mix-comp-therm-012_case-17
1.00120(860)	1.01467(62)	1.01575(58)	1.01453(861)	mix-comp-therm-012_case-18
1.00120(860)	1.01467(57)	1.01524(56)	1.01402(861)	mix-comp-therm-012_case-19
1.00140(1140)	1.01567(55)	1.01664(70)	1.01522(1140)	mix-comp-therm-012_case-20
1.00140(1200)	1.01466(71)	1.01517(68)	1.01375(1200)	mix-comp-therm-012_case-21
1.00140(1520)	1.01281(63)	1.01292(67)	1.01150(1519)	mix-comp-therm-012_case-22
1.00070(1140)	1.00969(56)	1.00890(64)	1.00819(1141)	mix-comp-therm-012_case-23
1.00070(1140)	1.01113(68)	1.01082(64)	1.01011(1141)	mix-comp-therm-012_case-24
1.00070(1140)	1.00849(64)	1.00973(61)	1.00902(1141)	mix-comp-therm-012_case-25
1.00070(1140)	1.00724(57)	1.00795(55)	1.00724(1141)	mix-comp-therm-012_case-26
1.00070(1140)	1.00754(64)	1.00784(48)	1.00714(1140)	mix-comp-therm-012_case-27
1.00070(1140)	1.01006(66)	1.00978(60)	1.00907(1141)	mix-comp-therm-012_case-28
1.00070(1140)	1.00690(68)	1.00958(64)	1.00887(1141)	mix-comp-therm-012_case-29
1.00070(1140)	1.00738(62)	1.00773(52)	1.00703(1140)	mix-comp-therm-012_case-30
1.00170(1510)	0.99723(78)	0.99655(68)	0.99486(1509)	mix-comp-therm-012_case-31
1.00170(1510)	0.99643(61)	0.99804(64)	0.99635(1509)	mix-comp-therm-012_case-32
1.00170(1510)	0.99421(73)	0.99452(66)	0.99283(1509)	mix-comp-therm-012_case-33
1.00000(0)	0.99718(22)	1.00105(22)	1.00105(22)	mix-comp-therm-kritz_core-2.19cold
1.00000(0)	0.99713(7)	1.00129(22)	1.00129(22)	mix-comp-therm-kritz_core-2.19hot
1.00000(240)	1.00209(58)	1.00003(47)	1.00003(245)	mix-sol-therm-002_exp-58
1.00000(240)	1.00167(61)	1.00092(53)	1.00092(246)	mix-sol-therm-002_exp-59
1.00000(240)	1.00026(45)	1.00038(49)	1.00038(245)	mix-sol-therm-002_exp-61

Table 3.12 The results for MIX benchmarks with a thermal spectrum. † The benchmark value and its uncertainty is still under investigation for Kritz.

3.6 U233 results

3.6.1 Fast spectrum

benchmark	JEFF-3.0	JEFF-3.1	C/E (JEFF-3.1)	name
1.00000(100)	1.01359(38)	1.00445(37)	1.00445(107)	u233-met-fast-001
1.00000(90)	1.00895(41)	1.00099(36)	1.00099(97)	u233-met-fast-005_case-1
1.00000(60)	1.00710(49)	1.00033(48)	1.00033(77)	u233-met-fast-005_case-2
1.00000(140)	1.00391(53)	1.00608(44)	1.00608(147)	u233-met-fast-006

Table 3.13 The results for U233 benchmarks with a fast spectrum

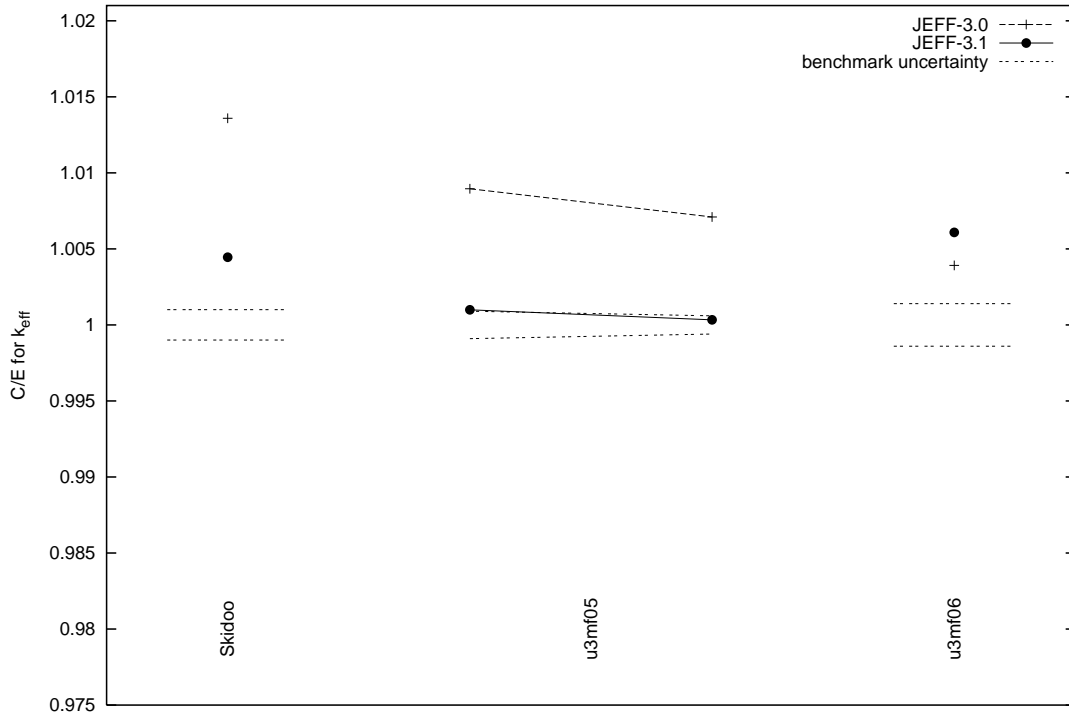


Figure 3.12 Results for the U233 benchmarks with a fast spectrum

3.6.2 Thermal spectrum

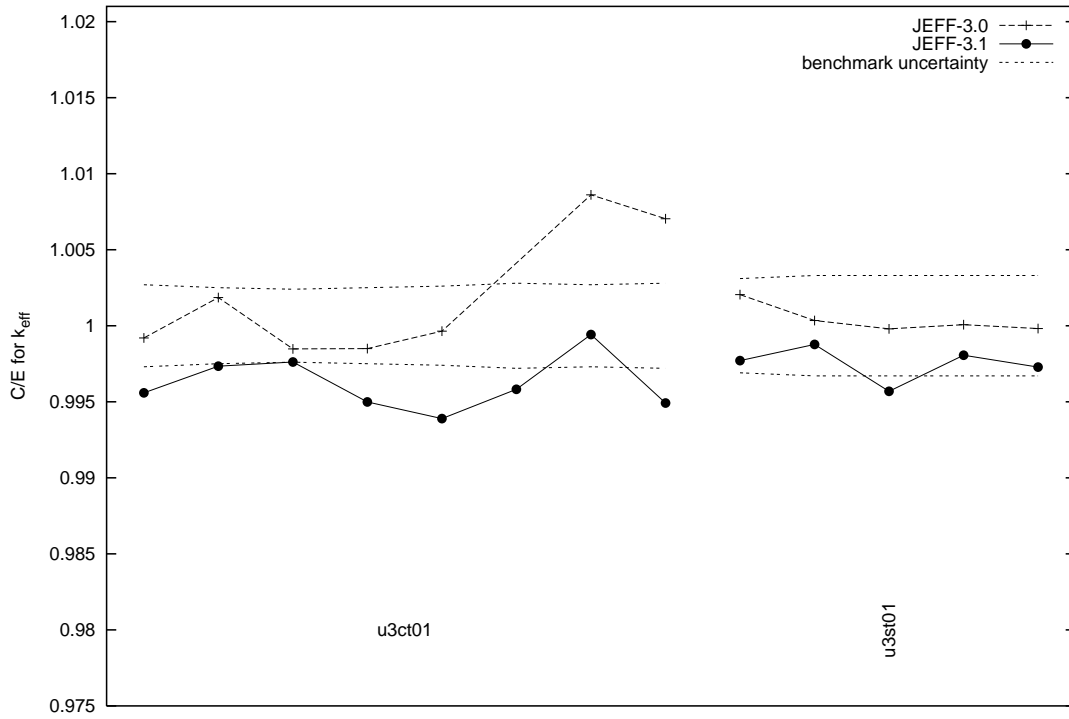


Figure 3.13 Results for the U233 benchmarks with a thermal spectrum

benchmark	JEFF-3.0	JEFF-3.1	C/E (JEFF-3.1)	name
1.00060(270)	0.99980(123)	0.99619(98)	0.99559(287)	u233-comp-therm-001_case-1
1.00150(250)	1.00335(106)	0.99884(99)	0.99734(269)	u233-comp-therm-001_case-2
1.00000(240)	0.99848(112)	0.99761(112)	0.99761(265)	u233-comp-therm-001_case-3
1.00070(250)	0.99920(85)	0.99569(80)	0.99499(262)	u233-comp-therm-001_case-4
1.00150(260)	1.00114(76)	0.99538(89)	0.99389(275)	u233-comp-therm-001_case-5
1.00150(280)		0.99731(102)	0.99582(298)	u233-comp-therm-001_case-6
0.99950(270)	1.00811(112)	0.99892(102)	0.99942(289)	u233-comp-therm-001_case-7
1.00040(280)	1.00744(112)	0.99532(90)	0.99492(294)	u233-comp-therm-001_case-8
1.00000(310)	1.00205(61)	0.99771(53)	0.99771(315)	u233-sol-therm-001_case-1
1.00050(330)	1.00084(62)	0.99927(80)	0.99877(339)	u233-sol-therm-001_case-2
1.00060(330)	1.00039(63)	0.99629(58)	0.99569(335)	u233-sol-therm-001_case-3
0.99980(330)	0.99987(59)	0.99786(69)	0.99806(337)	u233-sol-therm-001_case-4
0.99990(330)	0.99972(62)	0.99718(60)	0.99728(335)	u233-sol-therm-001_case-5

Table 3.14 The results for U233 benchmarks with a thermal spectrum

3.7 Summary

In the previous subsections, results for many benchmarks were presented. The number of benchmarks in each of the ICSBEP main categories is summarized in Table 3.15.

	COMP				MET				SOL	total
	therm	inter	fast	mixed	therm	inter	fast	mixed	therm	
LEU	257	/	/	/	1	/	/	/	49	307
IEU	9	4	/	/	/	/	16	/		29
HEU	/	6	/	/	42	5	66	5	87	211
MIX	35	/	1	1	/	/	4		3	44
PU	/	1	/	/	/	1	7	6	105	120
U233	8	/	/	/	/	/	4		5	17
total	309	11	1	1	43	6	97	11	249	728

Table 3.15 The number of benchmarks per main ICSBEP category for thermal/intermediate/fast neutron spectrum.

For a specific situation, it can be useful to compute averages of those benchmark cases that are most applicable to that situation. Here, however, we only give average values for $C/E - 1$ for the main ICSBEP categories, see Table 3.16.

Closer inspection of individual benchmarks will reveal deviations from the average. For various of these cases it may well be that the nuclear data library can, at a later date, still be improved further to yield better results. A detailed discussion of these problems, and the possibilities to solve them, is beyond the scope of the present paper.

	COMP				MET				SOL
	therm	inter	fast	mixed	therm	inter	fast	mixed	therm
LEU	-98	/	/	/	-7	/	/	/	145
IEU	-359	-376	/	/	/	/	-197	/	
HEU	/	1915	/	217	-308	60	-116	528	66
MIX	512	/	336	/	/	/	-182	/	44
PU	/	716	/	/	/	3842	251	476	568
U233	-380	/	/	/	/	/	296	/	-249

Table 3.16 The average values for $C/E - 1$ (in pcm) per main ICSBEP benchmark category.

References

- [1] J.F. Briesmeister (Ed.), *MCNP - A General Monte Carlo N-Particle Transport Code, Version 4C*, Technical Report LA-13709-M, Los Alamos National Laboratory, USA (2000)
J.S. Hendricks, *MCNP4C3*, Report X-5:RN(U)-JSH-01-17, Los Alamos National Laboratory, USA (2001)
- [2] J. Blair Briggs (ed.), *International Handbook of Evaluated Criticality Safety Benchmark Experiments*, NEA/NSC/DOC(95)03/I, Nuclear Energy Agency, Paris (September 2004 Edition)
- [3] T. Williams, M. Rosselet, and W. Scherer (Eds.), *Critical Experiments and Reactor Physics Calculations for Low-Enriched High Temperature Gas Cooled Reactors*, IAEA Tecdoc 1249 (advance electronic version, 2001)
- [4] A. D. Knipe, *Specifications of the Dimple S01 Benchmark Assemblies*, Report AEA TSD 0375 (JEF/DOC-504), AEA Technology (1994)
- [5] J. Hardy, D. Klein and J. J. Volpe, *A study of physics parameters in several H₂O-moderated lattices of slightly enriched and natural uranium*, Nuc. Sci. Eng. **40** (1970) 101;
Cross section evaluation working group (CSEWG), *Benchmark Specifications*, ENDF-202 (1986)
- [6] I. Remec, J. C. Gehin, and R. J. Ellis, *KRITZ-2:19 experiment on regular H₂O/fuel pin lattices with mixed oxide fuel at temperatures up to 245°C, A Study (Draft) by the OECD/NEA Working Party on Scientific Issues of Reactor Systems (WPRS)*, To be published as part of the International Reactor Physics Benchmark Project.
- [7] S.C. van der Marck, A. Hogenbirk, and R. Klein Meulekamp, *New temperature interpolation in MCNP*, Proc. M&C-2005, Avignon (France), 2005